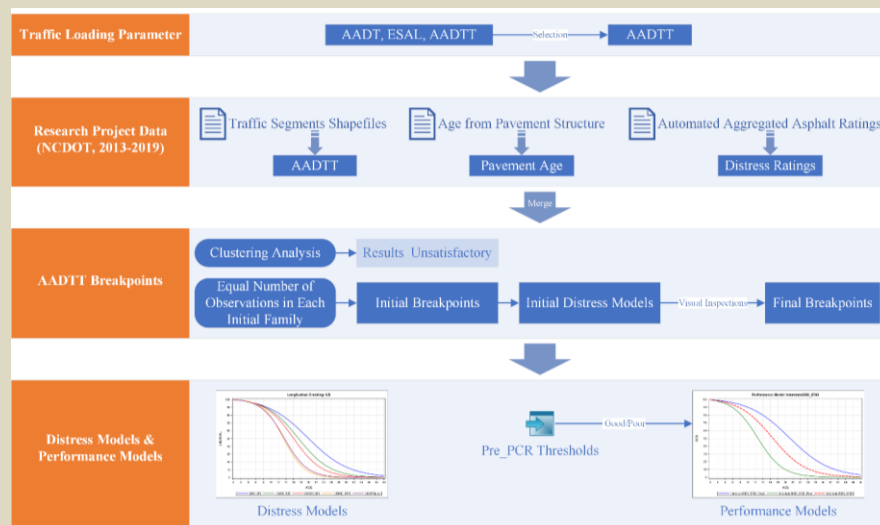




RESEARCH & DEVELOPMENT

Development of Pavement Performance Models using New Breakpoints and Pretreatment Conditions



Flow Chart for the Research Project

Don Chen, Ph.D., LEED A.P.

Thomas Nicholas II, Ph.D., P.E.

**Dept. of Engineering Technology and Construction Management
University of North Carolina at Charlotte, Charlotte, NC 28223**

NCDOT Project 2020-014

FHWA/NC/2020-014

December 2021

Development of Pavement Performance Models using New Breakpoints and Pretreatment Conditions

Final Report

(Report No. RP 2020-14)

To North Carolina Department of Transportation
(Research Project No. RP 2020-14)

Submitted by

Don Chen, Ph.D., LEED A.P.
Professor

Department of Engineering Technology and Construction Management
University of North Carolina at Charlotte, Charlotte, NC 28223-0001
Phone: (704) 687-5036; Fax: (704) 687-6653; E-mail: dchen9@uncc.edu

Thomas Nicholas II, Ph.D.
Associate Professor
Department of Engineering Technology and Construction Management
University of North Carolina at Charlotte, Charlotte, NC 28223-0001

**Department of Engineering Technology and Construction Management
University of North Carolina at Charlotte
Charlotte, NC**

December 2021

| | | | |
|---|--|--|-----------|
| 1. Report No. FHWA/NC/2020-14 | 2. Government Accession No. | 3. Recipient's Catalog No. | |
| 4. Title and Subtitle Development of Pavement Performance Models using New Breakpoints and Pretreatment Conditions | | 5. Report Date December 2021 | |
| | | 6. Performing Organization Code | |
| 7. Author(s) Don Chen, Thomas Nicholas II, | | 8. Performing Organization Report No. | |
| 9. Performing Organization Name and Address Smith 274, Dept. of Engineering Technology and Construction Management University of North Carolina at Charlotte Charlotte, NC 28223-0001 | | 10. Work Unit No. (TRAIS) | |
| | | 11. Contract or Grant No. | |
| 12. Sponsoring Agency Name and Address North Carolina Department of Transportation Research and Analysis Group 1 South Wilmington Street Raleigh, North Carolina 27601 | | 13. Type of Report and Period Covered Final Report August 2019 – December 2021 | |
| | | 14. Sponsoring Agency Code RP 2021-14 | |
| Supplementary Notes: | | | |
| 16. Abstract Previous studies indicated that two factors, traffic loading parameter and pre-treatment pavement condition, can have significantly impact on pavement performance and should be considered when developing pavement performance models. This study was conducted to use these two factors to develop new pavement performance models for the NCDOT Pavement Management System (PMS). A new traffic load indicator, AADTT, was selected and then its breakpoints were determined. These breakpoints, together with thresholds of pre-treatment pavement conditions, were used to define new pavement families; the corresponding distress and performance models were also developed. In addition, a pilot study was conducted to use ESAL as an alternative traffic loading parameter to develop distress and performance models for Interstate routes. These new models are expected to be more accurate and robust in predicting pavement deterioration trends because of the inclusion of additional pertinent factors; once the existing somewhat obsolete performance models developed using AADT are replaced by these new models, the performance of the NCDOT PMS will be improved and more informed maintenance and rehabilitation decisions can be made. | | | |
| 17. Key Words AADTT, pre-treatment conditions, distress model, performance model, sigmoidal curve | | 18. Distribution Statement | |
| 19. Security Classif. (of this report) Unclassified | 20. Security Classif. (of this page) Unclassified | 21. No. of Pages 99 | 22. Price |

DISCLAIMER

The contents of this report reflect the views of the author(s) and not necessarily the views of the University. The author(s) are responsible for the facts and the accuracy of the data presented herein. The contents do not necessarily reflect the official views or policies of either the North Carolina Department of Transportation or the Federal Highway Administration at the time of publication. This report does not constitute a standard, specification, or regulation.

ACKNOWLEDGMENTS

This research was sponsored by the North Carolina Department of Transportation. The authors gratefully acknowledge the support and assistance from the following individuals:

Research Project Steering and Implementation Committee: Camille Coombes (Chair), Mustan Kadibhai (Research Engineer), Matt Whitley, Clark Morrison, James Phillips, Neil Mastin, Shihai Zhang, and Todd Whittington.

Transportation Planning Division: Kent Taylor, Traffic Data Resource Engineer, for providing truck data.

The authors also would like to thank the following UNC Charlotte graduate students for their participation in this study: Tamim Adnan and Taraneh Kamyab.

EXECUTIVE SUMMARY

This study was conducted to develop new pavement distress and performance models that will help NCDOT accurately predict pavement performance and maintain all state-owned roadways in a cost-effective manner. To this end, a more appropriate traffic loading parameter, Annual Average Daily Truck Traffic (AADTT), was selected and its breakpoints were determined to group roadways in North Carolina into new pavement families, then distress models and performance models (*Roadway_Good* and *Roadway_Poor*) were developed. Lastly, these newly developed models were compared with the ones developed previously using Annual Average Daily Traffic (AADT) as the traffic loading parameter, and findings and conclusions were provided, as follows:

- Data availability. Research data needed for this research project, e.g., AADTT, Pavement Age, Pavement Distress Ratings, etc., have been frequently updated and made available to the research team by NCDOT engineers. These raw data are either published on a website that can be accessed publicly or provided to researchers upon request on a timely basis.
- Development of pavement families. Clustering analysis and the equal number of observations method were used to determine the AADTT breakpoints, which were then used to group roadways into new pavement families. It was observed that clustering analysis used in this project did not provide sufficient accuracy because its resolution of is not sufficient to capture intermediate AADTT values as final breakpoints.
- Distress models. A comparison of distress model curves developed using AADT (referring to as AADT distress curves) with the model curves developed in this project using AADTT (referring to as AADTT distress curves) indicates the following:
 - Load Related Distresses (LDRs): Alligator Cracking AADTT distress curves are flatter than those of AADT model curves. Wheel Path Patching, Non-wheel Path Patching, and Rutting AADTT distress curves are quite flat. One possible reason is that these three types of distresses are not severe in asphalt pavements in North Carolina. The possible reason for the flatter curvature is that the data collection vendor has recently changed. It is reasonable to assume that algorithms used to process raw images are different, which can lead to distress ratings that are different than the ones provided by the previous vendor. If this is the case, it is necessary to conduct a detailed comparison between AADT distress curves and AADTT distress curves, and then update the NCDOT PMS Decision Trees accordingly.

- Non-Load Related Distresses (NDRs): Transverse Cracking and Longitudinal Cracking curves are quite consistent, other than transverse cracking curves for Interstate roadways.
- Performance models. The curvature of performance models developed using AADTT breakpoints (referring to as the AADTT performance models) is as expected. A comparison of AADT and AADTT performance curves indicates that in general, AADTT curves are flatter, which might be the result of a different vendor's processing algorithms. A further comparison of AADT performance curves and AADTT Roadway_Poor performance curves indicates that they share the same deterioration trends.
- A pilot study was conducted to use Equivalent Single Axle Load (ESAL) as an alternative traffic loading parameter. Due to the time constraint, only Interstate routes were analyzed, and corresponding distress and performance models were developed. In this pilot study, ESAL values were calculated using a simplified equation. The resulting distress model curves lay between the AADT curves and AADTT curves, indicating that ESAL distress curves reflect NCDOT preventive maintenance practices closer than AADTT curves.

The following recommendations are provided for future research endeavors:

- Comparing to clustering analysis, the same number of observations per family method is more appropriate to be used to create pavement families, mainly because pavement distress data is variable in nature. The latter method is sufficiently accurate to capture reasonable intermediate AADTT values as family breakpoints.
- A subsequent research project is recommended to quantify the differences between AADT and AADTT distress and performance curves. Current Decision Trees in the NCDOT PMS are using the critical thresholds derived from previously developed AADT models. With the use of a new data collection vendor and the newly developed AADTT models, current Decision Trees should be updated to achieve PMS' maximum level of performance.
- Two sub-distress models, *Roadway_Good* and *Roadway_Poor*, should be developed for each distress type. The corresponding sub-performance models were developed in this research project, and these model curves provide additionally useful information such as the ranges of PCR values at a given age. The similar procedure can be implemented to distress models to provide the ranges of distress index values, which can be used to fine tune the NCDOT PMS' Decision Trees.
- ESAL should be further studied as the alternative traffic loading parameter to develop

distress and performance models for US and NC routes, and a comparison of ESAL and AADTT model curves should be conducted to study the differences between these two traffic loading parameters, and the results can assist NCDOT with an enhanced ability to update the decision trees, and thus make informative pavement management decisions.

Table of Contents

| | |
|--|----|
| CHAPTER 1 INTRODUCTION AND OBJECTIVES | 1 |
| 1.1 Background..... | 1 |
| 1.2 Research Needs and Significance | 1 |
| 1.3 Research Objectives..... | 2 |
| 1.4 Report Organization..... | 2 |
| CHAPTER 2 LITERATURE REVIEW | 4 |
| 2.1 Traffic Loading Parameters | 4 |
| 2.2 Pre-treatment Pavement Conditions..... | 5 |
| 2.3 Grouping Roadway Families | 5 |
| CHAPTER 3 RESEARCH METHODOLOGY | 7 |
| 3.1 Traffic Loading Parameter | 7 |
| 3.2 Research Project Data | 9 |
| 3.2.1 Pavement Age Data..... | 9 |
| 3.2.2 Asphalt Pavement Distress Data..... | 10 |
| 3.2.3 Data Merging..... | 10 |
| 3.2.3 Distress Normalization | 11 |
| 3.2.3 Distress Index Calculation..... | 12 |
| 3.3 AADTT Breakpoints..... | 13 |
| 3.3.1 Initial AADTT Breakpoints | 13 |
| 3.3.2 Initial Distress Models..... | 16 |
| 3.4 Final Distress Models | 19 |
| 3.4 Final Performance Models | 21 |
| CHAPTER 4 A Pilot Study on ESAL | 24 |
| 4.1 Initial ESAL Breakpoints..... | 26 |
| 4.2 Initial Distress Models | 26 |
| 4.3 Final Distress Models | 27 |
| 4.4 Final Performance Models | 29 |
| CHAPTER 5 FINDINGS AND CONCLUSIONS | 31 |
| CHAPTER 6 RECOMMENDATIONS | 37 |
| CITED REFERENCES | 38 |
| Appendix A. Distress Model Curves | 41 |
| Appendix B. Performance Model Curves | 54 |
| Appendix C. AADT vs. AADTT Distress Model Curves | 61 |
| Appendix D. AADT vs. AADTT Performance Model Curves | 71 |

| | |
|--|-----------|
| Appendix E. AADT vs. AADTT Roadway_Poor Performance Model Curves | 74 |
| Appendix F. Distress Model Curves for Interstate Routes (ESAL) | 77 |
| Appendix G. Performance Model Curves for Interstate Routes (ESAL) | 82 |

LIST OF FIGURES

| | |
|--|----|
| Figure 1. Flow Chart for the Research Project | 7 |
| Figure 2. NCDOT Traffic Segments Shapefile..... | 8 |
| Figure 3. NCDOT Segments Output (2015)..... | 8 |
| Figure 4. NCDOT Pavement Age Data | 9 |
| Figure 5. Asphalt Pavement Distress Data | 10 |
| Figure 6. Distress Index Value Calculation Tool..... | 13 |
| Figure 7. Transverse Cracking vs. Age for Initial Interstate Families..... | 15 |
| Figure 8. Transverse Cracking vs. Age for Initial US Families..... | 15 |
| Figure 9. Transverse Cracking vs. Age for Initial NC Families | 16 |
| Figure 10. Initial Interstate Transverse Cracking model curves | 17 |
| Figure 11. Initial US Alligator Cracking model curves..... | 18 |
| Figure 12. Transverse Cracking Model curves for US Roadways..... | 19 |
| Figure 13. Performance Model Curves for Interstate0-3000 | 23 |
| Figure 14. Performance Model Curves for US520-850..... | 23 |
| Figure 15. AADTT Breakpoints for Interstate..... | 32 |
| Figure 16. AADTT Breakpoints for US | 32 |
| Figure 17. AADTT Breakpoints for NC | 33 |
| Figure 18. Comparison of Distress Model Curves..... | 34 |
| Figure 19. Performance Models: Combined, Good, and Poor..... | 35 |
| Figure 20. AADT Performance Models and AADTT Performance Models..... | 36 |
| Figure 21. AADT Performance Models and AADTT Roadway_Poor Performance Models | 36 |
| Figure A 1. Transverse Cracking: Interstate | 42 |
| Figure A 2. Transverse Cracking: US | 42 |
| Figure A 3. Transverse Cracking: NC | 43 |
| Figure A 4. Alligator Cracking: Interstate | 43 |
| Figure A 5. Alligator Cracking: US..... | 44 |
| Figure A 6. Alligator Cracking: NC | 44 |
| Figure A 7. Raveling: Interstate..... | 45 |
| Figure A 8. Raveling: US..... | 45 |
| Figure A 9. Raveling: NC | 46 |
| Figure A 10. Longitudinal Cracking: Interstate | 46 |
| Figure A 11. Longitudinal Cracking: US..... | 47 |
| Figure A 12. Longitudinal Cracking: NC | 47 |
| Figure A 13. Longitudinal Lane Joint Cracking: Interstate | 48 |
| Figure A 14. Longitudinal Lane Joint Cracking: US..... | 48 |
| Figure A 15. Longitudinal Lane Joint Cracking: NC | 49 |
| Figure A 16. Wheel Path Patching: Interstate..... | 49 |
| Figure A 17. Wheel Path Patching: US | 50 |
| Figure A 18. Wheel Path Patching: NC | 50 |
| Figure A 19. Non-Wheel Path Patching: Interstate | 51 |
| Figure A 20. Non-Wheel Path Patching: US | 51 |
| Figure A 21. Non-Wheel Path Patching: NC..... | 52 |
| Figure A 22. Rutting: Interstate | 52 |
| Figure A 23. Rutting: US | 53 |
| Figure A 24. Rutting: NC..... | 53 |

| | |
|--|----|
| Figure B 1. Performance Model: Interstate0_3000..... | 55 |
| Figure B 2. Performance Model: Interstate3000_5700..... | 55 |
| Figure B 3. Performance Model: Interstate5700plus..... | 56 |
| Figure B 4. Performance Model: US0_280 | 56 |
| Figure B 5. Performance Model: US280_520 | 57 |
| Figure B 6. Performance Model: US520_880 | 57 |
| Figure B 7. Performance Model: US880_1670 | 58 |
| Figure B 8. Performance Model: US1670plus..... | 58 |
| Figure B 9. Performance Model: NC0_250..... | 59 |
| Figure B 10. Performance Model: NC250_420..... | 59 |
| Figure B 11. Performance Model: NC420_850..... | 60 |
| Figure B 12. Performance Model: NC850plus | 60 |
| | |
| Figure C 1. Interstate: Alligator Cracking Models | 62 |
| Figure C 2. Interstate: Longitudinal Cracking Models | 62 |
| Figure C 3. Interstate: Non _ Wheel Path Practicing Models..... | 63 |
| Figure C 4. Interstate: Wheel Path Practicing Models..... | 63 |
| Figure C 5. Interstate: Rutting Models: Interstate: Rutting Models | 64 |
| Figure C 6. Interstate: Transverse Cracking Models | 64 |
| Figure C 7. NC: Alligator Cracking Models..... | 65 |
| Figure C 8. NC: Longitudinal Cracking Models | 65 |
| Figure C 9. NC: Non _ Wheel Path Patching Models | 66 |
| Figure C 10. NC: Wheel Path Patching Models | 66 |
| Figure C 11. NC: Rutting Models..... | 67 |
| Figure C 12. NC: Transverse Cracking Models..... | 67 |
| Figure C 13. US: Alligator Cracking Models | 68 |
| Figure C 14. US: Longitudinal Cracking Models..... | 68 |
| Figure C 15. US: Non _ Wheel Path Patching Models..... | 69 |
| Figure C 16. US: Wheel Path Patching Models..... | 69 |
| Figure C 17. US: Rutting Models | 70 |
| Figure C 18. US: Transverse Cracking Models | 70 |
| | |
| Figure D 1. Interstate: Performance Models..... | 72 |
| Figure D 2. US: Performance Models..... | 72 |
| Figure D 3. NC: Performance Models | 73 |
| | |
| Figure E 1. Interstate Performance Models: AADT vs. AADTT Roadway_Poor | 75 |
| Figure E 2. US Performance Models: AADT vs. AADTT Roadway_Poor | 75 |
| Figure E 3. NC Performance Models: AADT vs. AADTT Roadway_Poor..... | 76 |
| | |
| Figure F 1. Transverse Cracking: Interstate (ESAL) | 78 |
| Figure F 2. Alligator Cracking: Interstate (ESAL) | 78 |
| Figure F 3. Raveling: Interstate (ESAL)..... | 79 |
| Figure F 4. Longitudinal Cracking: Interstate (ESAL)..... | 79 |
| Figure F 5. Longitudinal Lane Joint Cracking: Interstate (ESAL) | 80 |
| Figure F 6. Wheel Path Patching: Interstate (ESAL)..... | 80 |
| Figure F 7. Non-Wheel Path Patching: Interstate (ESAL) | 81 |

| | |
|--|----|
| Figure F 8. Rutting: Interstate (ESAL) | 81 |
| Figure G 1. Performance Model: Interstate0_1500 (ESAL)..... | 83 |
| Figure G 2. Performance Model: Interstate1500_2300 (ESAL)..... | 83 |
| Figure G 3. Performance Model: Interstate2300_5200 (ESAL)..... | 84 |
| Figure G 4. Performance Model: Interstate5200_7700 (ESAL)..... | 84 |
| Figure G 5. Performance Model: Interstate7700plus (ESAL) | 85 |

LIST OF TABLES

| | |
|--|----|
| Table 1. Clustering Analysis Results | 14 |
| Table 2. Final AADTT Breakpoints | 20 |
| Table 3. Final Distress Models | 20 |
| Table 4. Pre_PCR Values | 21 |
| Table 5. Final Performance Models..... | 22 |
| Table 6. Final ESAL Breakpoint (Interstate Routes)..... | 27 |
| Table 7. Final Distress Models for Interstate Routes (ESAL)..... | 28 |
| Table 8. Final Performance Models for Interstate Routes (ESAL) | 29 |

CHAPTER 1 INTRODUCTION AND OBJECTIVES

1.1 Background

The principal goal of this study is to develop new pavement distress and performance models that will help NCDOT accurately predict pavement performance and maintain all state-owned roadways in a cost-effective manner. For Interstate, US, and NC highways, this goal is directly related to the need to identify a new traffic loading parameter that can better explain pavement performance, determine breakpoints of this parameter, use these breakpoints and pre-treatment pavement conditions to define roadway families, and perform nonlinear statistical analysis to develop distress and performance models.

Traffic loading is an important factor used in the pavement analysis and design process and is critical to estimate the possible damage of existing roadways. It is typically quantified by parameters such as Annual Average Daily Traffic (AADT), Equivalent Single Axle Load (ESAL), and Annual Average Daily Truck Traffic (AADTT). AADT is a composite parameter that comprises of light, medium, and heavy traffic volumes, whereas ESAL and AADTT mainly represents traffic volume of heavy vehicles.

In this study, pre-treatment pavement condition is determined by the Pavement Condition Rating (PCR) value before pavement needs to be treated, i.e., the Pre_PCR value. Once treated, pavements with higher Pre_PCR values are expected to have longer service lives than those of with lower Pre_PCR values. Accurate prediction of pavement performance for both cases is essential for NCDOT engineers to make cost-effective pavement management decisions.

1.2 Research Needs and Significance

In the NCDOT PMS, AADT is used as the traffic loading parameter. Roadway sections are grouped into pavement families based on their AADT values, and then corresponding family performance models are developed. This method has limitations. Firstly, AADT breakpoints (e.g., 50k in the Interstate 0-50k family) are arbitrary. During recent NCDOT research projects [1] [2] [3], it has been observed that several roadway family curves are close to each other. This indicates that these roadway families should be combined into one family. In other words, the breakpoints of these

families need to be adjusted. Secondly, PCR is largely determined by load-related distresses which are caused mainly by heavy traffic volumes. This necessitates the need for a different traffic loading parameter other than AADT, as AADT is not a good traffic loading indicator for heavy traffic.

Pre-treatment pavement condition has not been adopted in the NCDOT PMS because this information is not available until the completion of a recent NCDOT research project [4]. From that research project, thresholds of pretreatment pavement conditions, represented by the averages of Pre_PCR values of Interstate, US, and NC roadways, were determined. These thresholds were used to classify a pavement's pretreatment pavement condition as Good or Poor in this study, and then pavement families were further divided into two sub-families, i.e., Good and Poor, and corresponding performance models were developed. Compared to existing roadway family models, these new models are expected to be more accurate and robust because of the inclusion of additional pertinent pre-treatment pavement condition information, and once implemented, they can lead to improved performance of the NCDOT's PMS.

1.3 Research Objectives

To select breakpoints to define new pavement performance families and develop new pavement performance models, the following research objectives are proposed in this study:

- Selection of a new traffic load parameter
- Determination of new breakpoints and formation of new pavement families
- Development of pavement family models

1.4 Report Organization

An introduction to the research project, research needs, and objectives are presented in Chapter 1. A comprehensive literature review is provided in Chapter 2. The research methodology is described in Chapter 3. Chapter 4 summarizes the findings of a pilot study using ESAL as the alternative traffic loading parameter. Chapter 5 focuses on findings and conclusions. Chapter 6 provides recommendations for future research.

Appendix A includes plots of distress model curves. Appendix B presents performance model curves. Comparison plots of AADT and AADTT distress model curves are included in Appendix C, and comparison plots of AADT and AADTT performance model curves are included in Appendix D. Appendix E includes AADT and AADTT *Roadway_Poor* performance model curves. Distress model curves developed using ESAL for Interstate routes are included in Appendix F, and corresponding performance curves developed using ESAL for Interstate routes are included in Appendix G.

CHAPTER 2 LITERATURE REVIEW

2.1 Traffic Loading Parameters

Traffic loading parameters have been studied by many researchers and their findings are summarized below.

Madanat et al. [5] investigated impact of several predictors on the performance (in terms of IRI) of asphalt pavements and overlays. The most relevant predictors are the IRI value in the previous year, the ESAL value in the subject year, and the cumulative ESAL value (from the most recent treatment to the previous year). Serigos et al. [6] indicated that higher ESAL values significantly reduced preventive maintenance treatment's effective life. In this study, the sum of all annual ESAL values of a pavement section, weighted by a time factor, was used to reflect traffic values during the life of the treatment. The missing annual number of ESALs was replaced with the average of the set of annual ESALs for the corresponding roadway section. In another study [7], three traffic load levels (Low, Medium, and Heavy), in terms of predicted 20 years of ESALs, were used as factors to develop pavement prediction models for the TXDOT PMS. It was concluded that the new system "can serve as an effective tool in support for decision makers, pavement engineers, budget planners, and administrators."

In 2006 [8], Federal Highway Administration (FHWA) elaborated on how AADTT can be an impactful traffic indicator in pavement design, analysis and management systems. In 2018 Raheel et al. [9] quantified the impact of heavy traffic on pavement performance and concluded that the truck volume caused 47% more damage in asphalt pavement than other types of traffic volumes. Llopis-Castelló et al. [10] evaluated pavement distresses and conditions using AADT, AADTT, ESAL, and KESAL (ESAL in thousands). They recommended that AADTT and KESAL, rather than AADT, to be considered as prevalent traffic factors for pavement distress analysis. Onayev et al. [11] concluded that cumulative equivalent single axial load (CESAL) can be replaced by AADTT which can better describe the impact of heavy traffic loading on pavement deterioration in cracking predictability model. In another study, Yamany and Abraham [12] developed pavement performance models using probabilistic function to predict pavement condition. Cumulative

AADTT used to develop the models were retrieved from LTPP database. The results were satisfactory as they showed an 87% accuracy in terms of performance prediction.

2.2 Pre-treatment Pavement Conditions

Previous studies concluded that pre-treatment pavement conditions directly affect pavement performance after pavements are treated.

A study of asphalt pavements sections in Tennessee [13] indicated that pre-treatment pavement conditions can significantly impact effectiveness and cost-effectiveness of pavement preventive maintenance treatments. In 2016, effectiveness analyses of flexible pavement treatments using LTPP SPS-3 data [14] indicated that long-term roughness change and rutting can be significantly affected by pre-treatment surface condition, and that treatments applied to pavement sections that had poor pre-treatment conditions are more likely to develop severer rutting than the corresponding control sections. A study presented at the 2018 NCAT Test Track Conference [15] and several other studies [16] [17] [18] concluded that pavements' post-treatment performance is highly dependent on pavements' pre-treatment condition.

2.3 Grouping Roadway Families

Grouping roadways into families and managing these families using corresponding family performance models has proven to be an effective pavement management practice. Various family grouping methods have been studied by researchers elsewhere in the United States and internationally.

Shahin et al. [19] provided guidance on how pavement sections can be grouped into families based on pavement types, application aspects and other factors. In another study [20], IRI, PSI (Pavement Serviceability Index), PCR (Pavement Condition Rating) and AADT thresholds were used to group roadways into families to allow consistent implementation of family-based treatment strategies.

Statistical methods such as the clustering approach have been used to group roadway families. In a relevant study [21], AADT collected by Automatic Traffic Recorder Stations (ATRs) was used as input to a clustering approach to identify roadway attributes and traffic patterns, then corresponding roadway families were created. This study, however, has two limitations: firstly, traffic data collected by ATRs differed from year to year and was too variable to be considered logical; secondly, it was challenging to obtain reasonable roadway families. In 2001, Rossi et al. [22] used several clustering methods to group roadways using AADT collected from 50 ATR sites in the Province of Venice. They concluded that the performance of clustering methods used in this study was depending on data sets and traffic patterns.

CHAPTER 3 RESEARCH METHODOLOGY

This chapter describes the procedures used to develop pavement performance models using the newly selected traffic loading parameter and its breakpoints, as well as pre-treatment conditions of Interstate, US, and NC roadways. The main steps are included in the flow chart below (Figure 1).

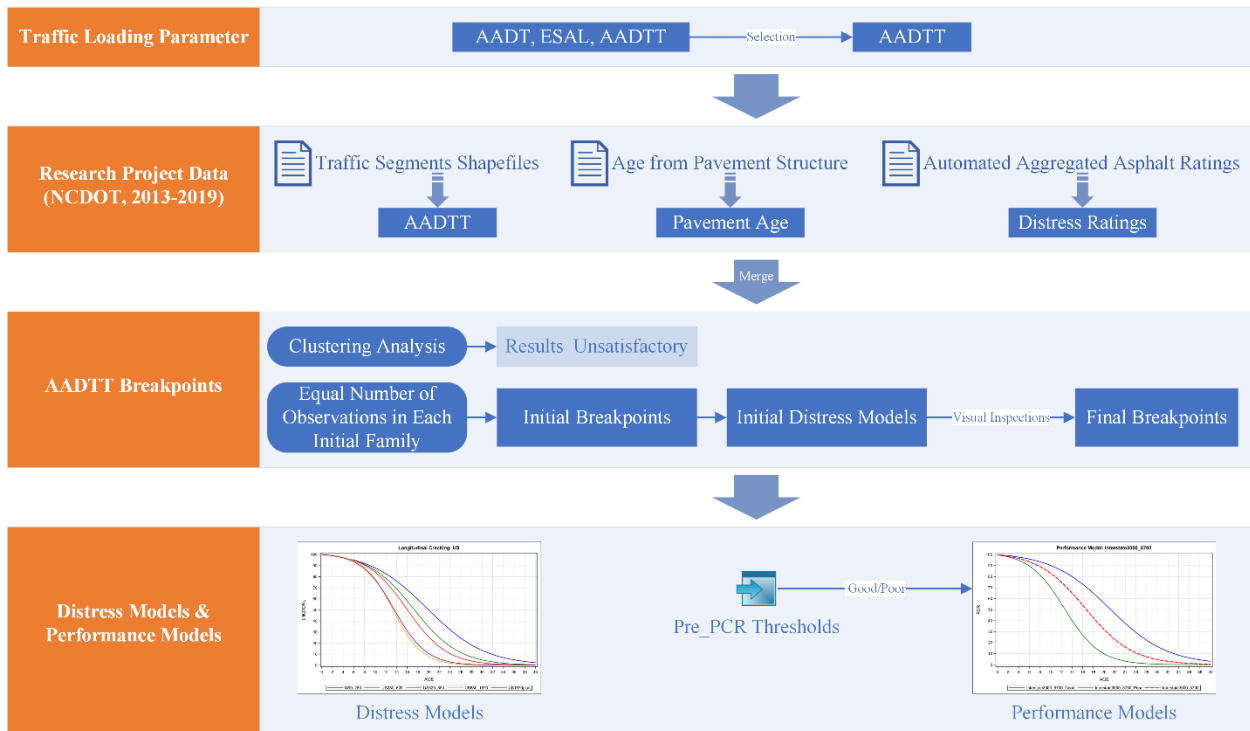


Figure 1. Flow Chart for the Research Project

3.1 Traffic Loading Parameter

As indicated by the literature review, both ESAL and AADTT are better traffic loading parameters than AADT. In this study, AADTT was selected to be the traffic loading parameter because NCDOT has collected AADTT data since 2013, whereas ESAL for each roadway section is not readily available. From NCDOT’s “Traffic Survey GIS Data Products & Documents” webpage [23], Traffic Segments Shapefiles from 2013 to 2019 (highlighted in Figure 2) were downloaded and then imported into ArcGIS to generate Excel spreadsheet outputs. An excerpt of the generated Excel spreadsheets is shown in Figure 3.

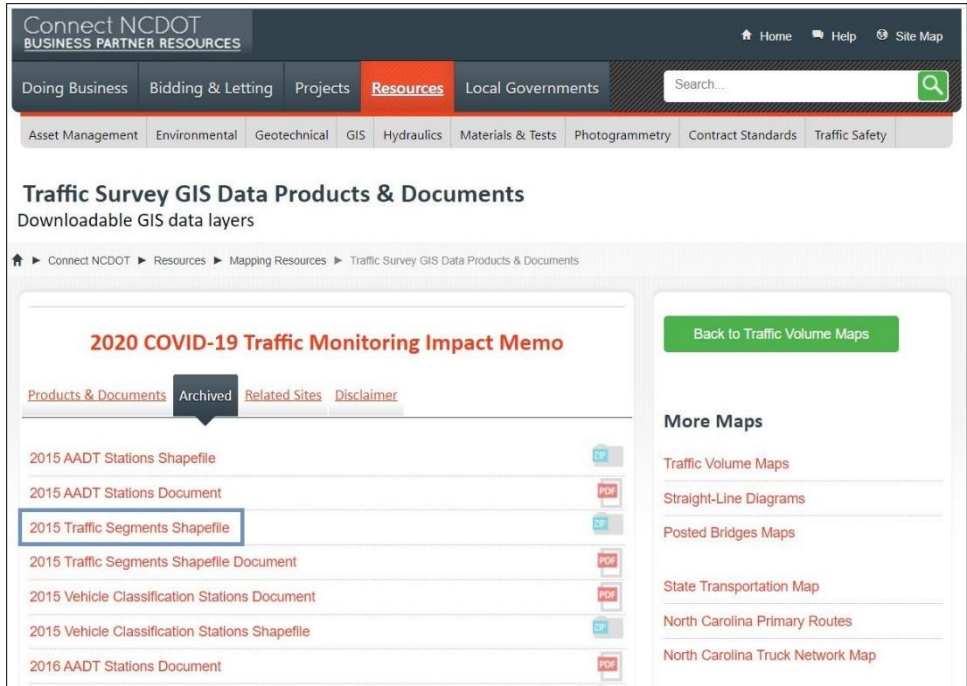


Figure 2. NCDOT Traffic Segments Shapefile

| FID | Rte_ID | BegMP1 | EndMP1 | AADT2015 | SU_PCT | MU_PCT | SU_AADT | MU_AADT | AADTT2015 | SOURCE |
|-----|------------|--------|--------|----------|-------------|-------------|---------|---------|-----------|--------|
| 0 | 1000002610 | 0 | 0.567 | 22000 | 0.028317218 | 0.03920533 | 650 | 900 | 1550 | MAINT |
| 1 | 1000002610 | 25.114 | 28.244 | 72000 | 0.03670694 | 0.072655041 | 2750 | 5440 | 8190 | MAINT |
| 2 | 1000002610 | 18.744 | 20.495 | 81000 | 0.03670694 | 0.072655041 | 3150 | 6230 | 9380 | MAINT |
| 3 | 1000002610 | 20.495 | 25.114 | 78000 | 0.03670694 | 0.072655041 | 3020 | 5970 | 8990 | MAINT |
| 4 | 1000002610 | 28.574 | 29.167 | 52000 | 0.031624567 | 0.094039567 | 1850 | 5490 | 7340 | MAINT |
| 5 | 1000002644 | 0 | 0.01 | 72000 | 0.03670694 | 0.072655041 | 2750 | 5440 | 8190 | MAINT |
| 6 | 1000002644 | 0.01 | 3.288 | 52000 | 0.031624567 | 0.094039567 | 1850 | 5490 | 7340 | MAINT |
| 7 | 1000002644 | 3.288 | 9.014 | 53000 | 0.031624567 | 0.094039567 | 1710 | 5100 | 6810 | MAINT |
| 8 | 1000002644 | 9.014 | 12.571 | 51000 | 0.027627065 | 0.09602649 | 1420 | 4930 | 6350 | MAINT |
| 9 | 1000002644 | 13.656 | 17.46 | 35000 | 0.022393642 | 0.094389902 | 810 | 3400 | 4210 | MAINT |
| 10 | 1000002644 | 12.571 | 13.656 | 48000 | 0.027627065 | 0.09602649 | 1310 | 4560 | 5870 | MAINT |
| 11 | 1000002656 | 10.776 | 12.606 | 22000 | 0.028317218 | 0.03920533 | 650 | 900 | 1550 | MAINT |
| 12 | 1000002656 | 9.066 | 10.776 | 19000 | 0.028317218 | 0.03920533 | 570 | 790 | 1360 | MAINT |
| 13 | 1000002656 | 0 | 3.351 | 8800 | 0.031330949 | 0.112125324 | 300 | 1080 | 1380 | MAINT |
| 14 | 1000002656 | 3.351 | 9.066 | 10000 | 0.031330949 | 0.112125324 | 340 | 1230 | 1570 | MAINT |
| 15 | 1000002674 | 0 | 1.305 | 35000 | 0.022393642 | 0.094389902 | 810 | 3400 | 4210 | MAINT |
| 16 | 1000002674 | 1.305 | 7.818 | 34000 | 0.022393642 | 0.094389902 | 790 | 3310 | 4100 | MAINT |
| 17 | 1000002674 | 7.818 | 13.121 | 27000 | 0.025171887 | 0.126928953 | 730 | 3670 | 4400 | MAINT |
| 18 | 1000004000 | 1.335 | 2.316 | 119000 | 0.023403194 | 0.061194126 | 2610 | 6810 | 9420 | MAINT |
| 19 | 1000004000 | 4.026 | 6.166 | 123000 | 0.023403194 | 0.061194126 | 2710 | 7080 | 9790 | MAINT |
| 20 | 1000004000 | 2.316 | 4.026 | 124000 | 0.023403194 | 0.061194126 | 2750 | 7180 | 9930 | MAINT |
| 21 | 1000004000 | 7.926 | 8.886 | 117000 | 0.023403194 | 0.061194126 | 2600 | 6790 | 9390 | MAINT |
| 22 | 1000004000 | 6.166 | 7.926 | 120000 | 0.023403194 | 0.061194126 | 2680 | 7020 | 9700 | MAINT |

Figure 3. NCDOT Segments Output (2015)

In Figure 3, **AADTT2015** is estimated annual average daily total trucks for 2015. AADTT is one of the most important data in this study. As described in subsequent sections, it is used to determine breakpoints which are thresholds for grouping roadway families. In addition, the following are the index variables that are used later to merge with other raw data obtained from NCDOT:

- **Rte_Id**: GIS 10 digit unique route identifier

- **BegMP1:** Route milepost at the beginning of the reference
- **EndMP1:** Route milepost at the end of the reference

3.2 Research Project Data

3.2.1 Pavement Age Data

Pavement age, as the independent variable, is an essential component of pavement distress models and performance models. Pavement age data was obtained from the NCDOT Pavement Management Section. In this study, pavement age is defined as:

$$Age = EFF_YEAR - YEAR_LAST_REHAB \quad (1)$$

where:

EFF_YEAR: year the roadway section was surveyed

YEAR_LAST_REHAB: year the roadway section was last rehabilitated

An excerpt of the pavement age data file is shown in Figure 4. The following are the index variables that are used later to merge with other raw data obtained from NCDOT:

- **COUNTY:** unique county number identifier
- **ROUTE1:** unique route number identifier
- **OFFSET_FROM:** Route milepost at the beginning of the reference
- **OFFSET_TO:** Route milepost at the end of the reference

| COUNTY | ROUTE1 | OFFSET_FROM | OFFSET_TO | LENGTH | EFF_YEAR | YEAR_LAST_REHAB | YEAR_CONSTR | TOTAL_THICK |
|--------|----------|-------------|-----------|--------|----------|-----------------|-------------|-------------|
| 96 | 10000795 | 1.997 | 2.042 | 0.045 | 2015 | 2010 | 2005 | 19.5 |
| 96 | 10000795 | 2.042 | 9.994 | 7.952 | 2015 | 2010 | 2005 | 26.5 |
| 96 | 10000795 | 9.994 | 11.047 | 1.053 | 2015 | 2010 | 2005 | 26.5 |
| 96 | 10000795 | 11.047 | 13.351 | 2.304 | 2015 | 2010 | 2005 | 26.5 |
| 96 | 10000795 | 1.997 | 2.042 | 0.045 | 2015 | 2010 | 2005 | 19.5 |
| 96 | 10000795 | 2.042 | 9.994 | 7.952 | 2015 | 2010 | 2005 | 26.5 |
| 96 | 10000795 | 9.994 | 11.047 | 1.053 | 2015 | 2010 | 2005 | 26.5 |
| 96 | 10000795 | 11.047 | 13.351 | 2.304 | 2015 | 2010 | 2005 | 26.5 |
| 96 | 10000795 | 13.351 | 13.551 | 0.2 | 2015 | 2005 | 2005 | 23 |
| 96 | 10400795 | 0 | 2.492 | 2.492 | 2015 | 2010 | 2005 | 26.5 |
| 96 | 10400795 | 2.492 | 3.556 | 1.064 | 2015 | 2010 | 2005 | 26.5 |
| 96 | 10400795 | 3.556 | 11.501 | 7.945 | 2015 | 2010 | 2005 | 26.5 |
| 96 | 10400795 | 11.501 | 11.544 | 0.043 | 2015 | 2010 | 2005 | 19.5 |
| 96 | 10400795 | 0 | 2.492 | 2.492 | 2015 | 2010 | 2005 | 26.5 |
| 96 | 10400795 | 2.492 | 3.556 | 1.064 | 2015 | 2010 | 2005 | 26.5 |
| 96 | 10400795 | 3.556 | 11.501 | 7.945 | 2015 | 2010 | 2005 | 26.5 |
| 96 | 10400795 | 11.501 | 11.544 | 0.043 | 2015 | 2010 | 2005 | 19.5 |
| 96 | 10400795 | 11.544 | 12.763 | 1.219 | 2015 | 2005 | 2005 | 16 |
| 96 | 10400795 | 12.763 | 13.537 | 0.774 | 2015 | 2005 | 2005 | 16.5 |
| 96 | 37000581 | 0 | 0.62 | 0.62 | 2015 | 2005 | 2005 | 16.5 |
| 96 | 37400581 | 0 | 0.641 | 0.641 | 2015 | 2005 | 2005 | 16.5 |

Figure 4. NCDOT Pavement Age Data

3.2.2 Asphalt Pavement Distress Data

Asphalt pavement distress data was also obtained from the NCDOT Pavement Management Section. As shown in the excerpt below (Figure 5), this data includes distress ratings, e.g., TRNSVRS_LOW_LF, which represents Low severity Transverse Cracking ratings measured in LF. In addition, the following index variables that are used later to merge with other raw data obtained from NCDOT are included:

- **ROUTE1**: unique route number identifier
- **COUNTY**: unique county number identifier
- **OFFSET_FROM**: Route milepost at the beginning of the reference
- **OFFSET_TO**: Route milepost at the end of the reference

| ROUTE1 | COUNTY | OFFSET_FROM | OFFSET_TO | TRNSVRS_LOW_LF | TRNSVRS_MDRT_LF | TRNSVRS_HGH_LF |
|----------|--------|-------------|-----------|----------------|-----------------|----------------|
| 10000074 | 86 | 4.565 | 6.565 | 624 | 221 | 63 |
| 10000074 | 86 | 6.565 | 8.565 | 731 | 304 | 43 |
| 10000074 | 86 | 8.565 | 10.565 | 198 | 81 | 16 |
| 10000074 | 86 | 10.565 | 12.565 | 282 | 150 | 67 |
| 10000074 | 86 | 12.565 | 14.565 | 232 | 50 | 39 |
| 10000074 | 86 | 14.565 | 16.565 | 367 | 107 | 53 |
| 10000074 | 86 | 16.565 | 17.413 | 228 | 243 | 57 |
| 10000077 | 86 | 0 | 0.938 | 401 | 111 | 178 |
| 10000077 | 86 | 4.493 | 6.493 | 596 | 246 | 74 |
| 10000077 | 86 | 6.493 | 8.493 | 803 | 385 | 91 |
| 10000077 | 86 | 12.493 | 14.493 | 2969 | 315 | 106 |
| 10000077 | 86 | 14.493 | 16.493 | 2635 | 197 | 58 |
| 10000077 | 99 | 0 | 2 | 55 | 0 | 3 |
| 10000077 | 99 | 2 | 3.132 | 61 | 40 | 39 |
| 10000077 | 99 | 9.654 | 11.654 | 2099 | 417 | 270 |
| 10000077 | 99 | 11.654 | 13.757 | 860 | 431 | 514 |
| 10400077 | 86 | 6.359 | 8.359 | 3766 | 685 | 150 |
| 10400077 | 86 | 8.359 | 10.359 | 3104 | 579 | 276 |
| 10400077 | 86 | 14.359 | 16.359 | 564 | 213 | 138 |
| 10400077 | 86 | 16.359 | 18.359 | 582 | 278 | 146 |
| 10400077 | 86 | 22.359 | 22.881 | 368 | 102 | 55 |

Figure 5. Asphalt Pavement Distress Data

3.2.3 Data Merging

The abovementioned three types of data were merged using the same shared unique index variables. The merged data file includes 59,430 individual roadway sections.

The following spatial conditions were used when merging data i and data i+1:

- if $MP_FROM_i \geq MP_TO_i+1$ then DELETE

- if $MP_TO_i \leq MP_FROM_i+1$ then DELETE
- if $MP_FROM_i \geq MP_FROM_i+1$ and $MP_TO_i \leq MP_TO_i+1$ then KEEP
- if $MP_FROM_i+1 \leq MP_FROM_i \leq MP_TO_i+1$ and $MP_TO_i \geq MP_TO_i+1$ then KEEP
- if $MP_FROM_i+1 \leq MP_TO_i \leq MP_TO_i+1$ and $MP_FROM_i \leq MP_FROM_i+1$ then KEEP
- if $MP_FROM_i \leq MP_FROM_i+1$ and $MP_TO_i \geq MP_TO_i+1$ then KEEP

where:

- MP_FROM: Route milepost at the beginning of the reference
- MP_TO: Route milepost at the end of the reference
- i: Research data, $i = 1, 2, 3$.

3.2.3 Distress Normalization

Pavement distress ratings (Figure 5) need to be normalized so they are unitless and become percentages over section length or area. Normalized distress ratings are later used to calculate distress index values. Normalization equations are:

Transverse Cracking and Reflection Transverse Cracking

$$TRNSVRS_LOW = (TRNSVRS_LOW_LF + REFLCT_TRNSVRS_LOW_LF)/(LENGTH \times 5280) \quad (2)$$

$$TRNSVRS_MDRT = (TRNSVRS_MDRT_LF + REFLCT_TRNSVRS_MDRT_LF)/(LENGTH \times 5280) \quad (3)$$

$$TRNSVRS_HGH = (TRNSVRS_HGH_LF + REFLCT_TRNSVRS_HGH_LF)/(LENGTH \times 5280) \quad (4)$$

Alligator Cracking

$$ALGTR_LOW = ALGTR_LOW_SF/(LENGTH \times 5280 \times 7) \times 100 \quad (5)$$

$$ALGTR_MDRT = ALGTR_MDRT_SF/(LENGTH \times 5280 \times 7) \times 100 \quad (6)$$

$$ALGTR_HGH = ALGTR_HGH_SF/(LENGTH \times 5280 \times 7) \times 100 \quad (7)$$

Raveling

$$RVL_LOW = RVL_LOW_SF/(LENGTH \times 5280 \times LANE_WIDTH) \times 100 \quad (8)$$

$$RVL_MDRT = RVL_MDRT_SF/(LENGTH \times 5280 \times LANE_WIDTH) \times 100 \quad (9)$$

$$RVL_HGH = RVL_HGH_SF/(LENGTH \times 5280 \times LANE_WIDTH) \times 100 \quad (10)$$

Longitudinal Cracking

$$LNGTDNL_LOW = LNGTDNL_LOW_LF / (LENGTH \times 5280) \quad (11)$$

$$LNGTDNL_HGH = LNGTDNL_HGH_LF / (LENGTH \times 5280) \quad (12)$$

Longitudinal Lane Joint Cracking

$$LNGTDNL_LANE_JNT_LOW = LNGTDNL_LANE_JNT_LOW_LF / (LENGTH \times 5280) \quad (13)$$

$$LNGTDNL_LANE_JNT_HGH = LNGTDNL_LANE_JNT_HGH_LF / (LENGTH \times 5280) \quad (14)$$

Patching Area - Wheel Path

$$WP_PTCH = WP_PTCH_SF / (LENGTH \times 7 \times 5280) \times 100 \quad (15)$$

Patching Area – Non-Wheel Path

$$NWP_PTCH = NWP_PTCH_SF / (LENGTH \times 5280 \times (LANE_WIDTH - 7 + 0.0001)) \times 100 \quad (16)$$

Rutting

$$MAX_RUT = 100 - 100 \times (MAX_RUT_AVG)^2 \quad (17)$$

$$\text{if } MAX_RUT_AVG < 0.05 \text{ then } MAX_RUT = 100 \quad (18)$$

It was decided to combine Transverse Cracking and Reflection Transverse Cracking due to their similarities in terms of pavement management practices. In Equation (16), 0.0001 is added to avoid a zero denominator.

3.2.3 Distress Index Calculation

Pavement distress index values are calculated using the Excel spreadsheet tool developed by NCDOT (Figure 6). In this spreadsheet, normalized distress ratings are entered into the orange cells as low_sev_in, med_sev_in, or high_sev_in. Based on a previous study [24], 99th percentiles of normalized distress ratings are entered into the tool as Maximum Allowable Extent (MAE) values, i.e., low_sev_mae_in, med_sev_mae_in, and high_sev_mae_in; Threshold Amounts for distress that has three severity levels (L/M/H) are 60, 30, and 0; 60 and 0 for distress that has two severity levels (L/H); and 0 for distress that has one severity level (L). After entering these

parameters and normalized distress ratings, the distress index value is calculated and shown at the bottom of the spreadsheet tool.

| | | | |
|---|-----------|--|----|
| f_mae(a.ALGTR_LOW_PCT,a.ALGTR_MDRT_PCT, a.ALGTR_HGH_PCT,null,100, 80, 50,75,40,0,0,0,0) | | | |
| INPUTS | | | |
| OUTPUT | | | |
| Distress Values passed into the function. Distresses with less than three severities should pass null to low then med in that order. Function return MAE index with 100 as good 0 as bad | | | |
| low_sev_in | 0 | | |
| med_sev_in | 20 | *OK* - Sum distress total is 100 or less | |
| high_sev_in | 40 | | |
| The normalizing factor will normalize absolute distress amounts null indicates no normalization required | | | |
| normalizing_in | null | | |
| MAE Amounts (Low Med and High) are the Extent amounts that maximize deduction for that severity | | | |
| low_sev_mae_in | 100 | | |
| med_sev_mae_in | 80 | | |
| high_sev_mae_in | 50 | | |
| Threshold Amounts are lowest possible score for that severity when it occurs alone | | | |
| low_sev_threshold_in | 75 | | |
| med_sev_threshold_in | 40 | | |
| high_sev_threshold_in | 0 | | |
| Begin deduct scores are the extent value when point deductions begin for each severity level | | | |
| low_sev_begin | 0 | distr_low | 0 |
| med_sev_begin | 0 | distr_med | 20 |
| high_sev_begin | 0 | distr_high | 40 |
| d1 | 0 | | |
| d2 | 15 | d2c | 15 |
| d3 | 80 | d3c | 83 |
| Alligator Cracking Index Value | 17 | | |

Figure 6. Distress Index Value Calculation Tool

3.3 AADTT Breakpoints

3.3.1 Initial AADTT Breakpoints

AADTT breakpoints are AADTT threshold values that are used to group roadways into pavement families. Two methods were used to determine initial breakpoints: (1) clustering analysis and (2) equal number of observations in each initial family.

(1) Clustering Analysis

In clustering analysis, distress index values were standardized, then the hierarchical clustering technique was used to determine number of clusters. The results indicated that Interstate should have 3 clusters, with 4,470 and 8,820 as AADTT breakpoints; US should have 4 clusters, with 830, 1,860, and 3,440 as AADTT breakpoints; and NC should have 4 clusters, with 390, 900, and 1,790

as AADTT breakpoints. Initial results are included in Table 1. Based on resulting AADTT breakpoints, either 3 or 4 families were created for Interstate, US, and NC roadways. *Error! Reference source not found.* It was observed that the sizes of families are not balanced. For example, Family #1 of Interstate, US, and NC roadways comprises 46.9%, 61.1%, and 62.7% of the total number of roadway sections in each respective roadway classification. Therefore, it is logical to assume that the first AADTT breakpoint of each classification is too large to capture some reasonable intermediate breakpoints, which necessitates further breakdown of the sizes of roadway families. This leads to the next method.

Table 1. Clustering Analysis Results

| | | Family #1 | Family #2 | Family #3 | Family #4 |
|------------|--------------------|-------------|-----------------|-----------------|-----------|
| Interstate | AADTT Breakpoints | (0 - 4,740) | (4,740 - 8,820) | > 8,820 | |
| | Number of Sections | 1,837 | 1,531 | 547 | |
| | Percentage | 46.9% | 39.1% | 14.0% | |
| US | AADTT Breakpoints | (0 - 830) | (830 - 1,860) | (1,860 - 3,440) | > 3,440 |
| | Number of Sections | 14,140 | 5,718 | 2,656 | 634 |
| | Percentage | 61.1% | 24.7% | 11.5% | 2.7% |
| NC | AADTT Breakpoints | (0 - 390) | (390 - 900) | (900 - 1,790) | > 1,790 |
| | Number of Sections | 20,306 | 8,491 | 2,993 | 577 |
| | Percentage | 62.7% | 26.2% | 9.2% | 1.8% |

(2) Equal Number of Observations in Each Initial Family

After studying the total numbers of roadway sections of Interstate, US, and NC, it was decided to develop 7 initial Interstate families of 500 roadway sections, 10 initial US families of 2,000 sections, and 10 initial NC families of 3,000 sections. It is expected that this breakdown allows the identification of all reasonable AADTT breakpoints. Corresponding initial AADTT breakpoints are:

- Interstate: **2,000, 3,000, 4,200, 5,700, 6,700, 8,000**
- US: **160, 280, 400, 520, 660, 880, 1,200, 1,670, 2,460**
- NC: **80, 140, 190, 250, 320, 420, 570, 850, 1,900**

Scatterplots of Transverse Cracking index vs. Age for Interstate, US, and NC are shown in Figure 7, Figure 8, and Figure 9. As indicated by these figures, outliers need to be removed before these raw data can be used to develop distress and performance models.

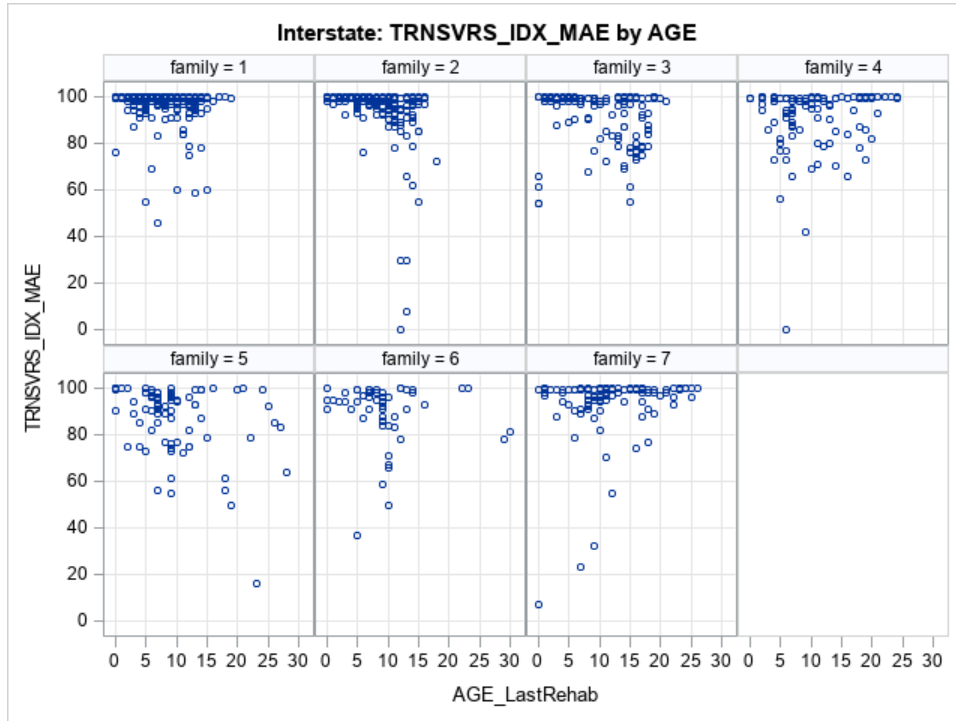


Figure 7. Transverse Cracking vs. Age for Initial Interstate Families

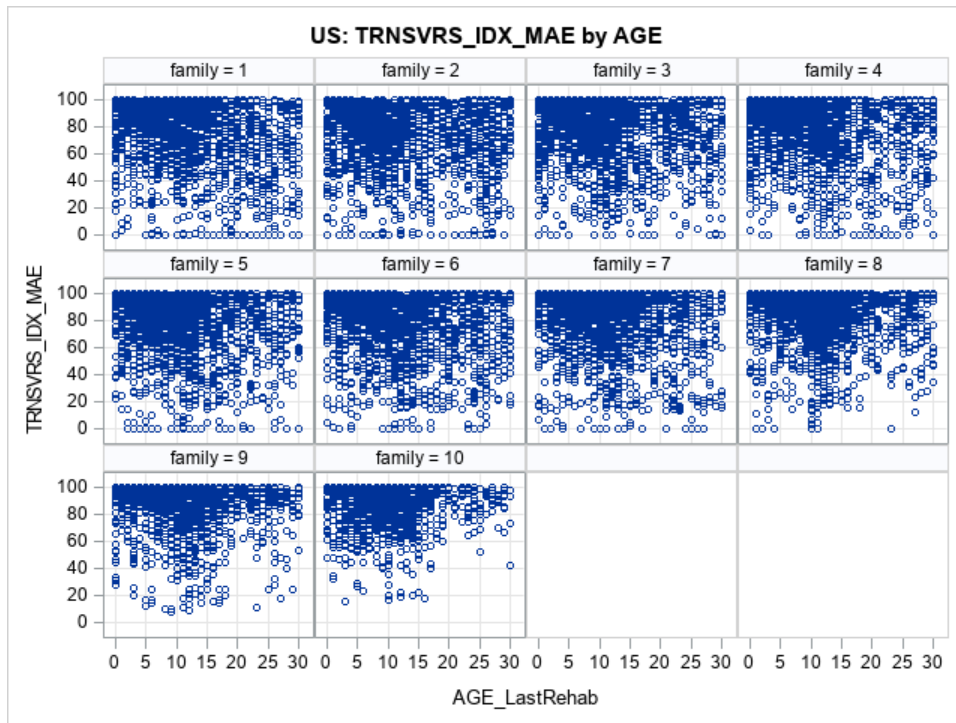


Figure 8. Transverse Cracking vs. Age for Initial US Families

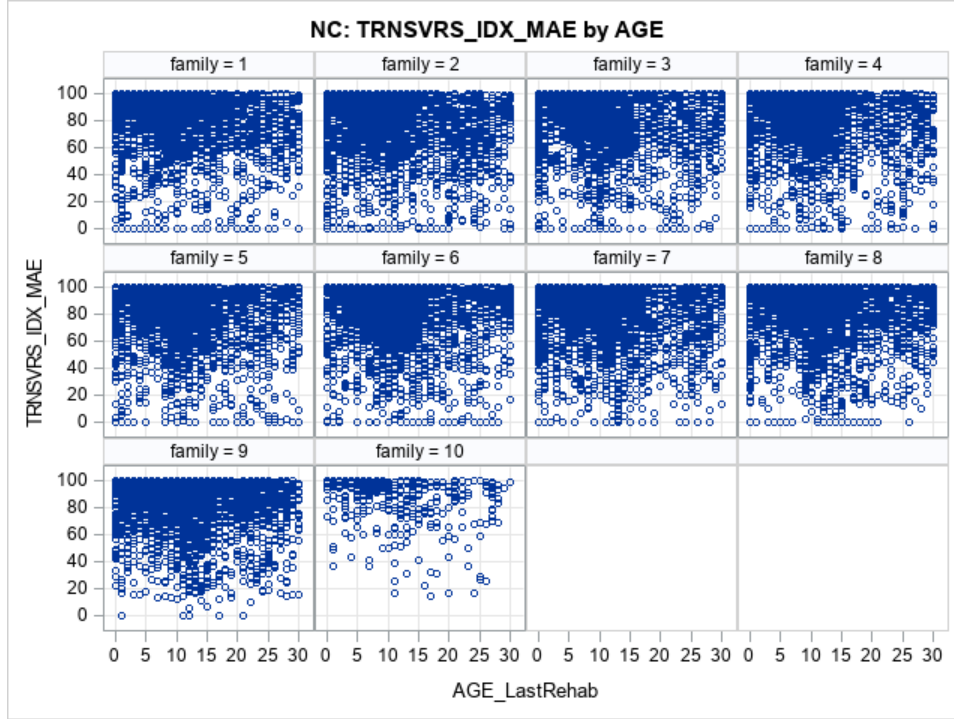


Figure 9. Transverse Cracking vs. Age for Initial NC Families

3.3.2 Initial Distress Models

Outliers in the raw distress data needs to be cleaned before distress models can be developed. Interquartile range (IQR) of each distress at each age was calculated and the following equations were used to remove outliers:

$$IQR = Q_1 - Q_3 \quad (19)$$

$$Bottom\ Boundary = Q_1 - 1.5 * IQR \quad (20)$$

$$Upper\ Boundary = Q_3 + 1.5 * IQR \quad (21)$$

where:

Q_1 : The 25th percentile

Q_3 : The 75th percentile

Individual observations at each age beyond the corresponding bottom and upper boundaries were considered as outliers and remove. Additionally, the following steps were used to further remove outliers:

- if AGE = 0 and DISTRESS INDEX VALUE < 100 then DELETE
- if AGE = 1 and DISTRESS INDEX VALUE < 95 then DELETE
- if AGE = 2 and DISTRESS INDEX VALUE < 90 then DELETE
- if AGE = 3 and DISTRESS INDEX VALUE < 85 then DELETE

Initial distress models, i.e., Distress Index Value vs. Age, were then developed using the following sigmoidal equation [1] [2] [3] for Transverse Cracking, Alligator Cracking, Raveling, Longitudinal Cracking, Longitudinal Lane Joint Cracking, Wheel Path Patching, Non-wheel Path Patching, and Rutting:

$$\text{Distress_Index_Value} = a / (1 + e^{((-Pavement_Age + b)/c)}) \quad (22)$$

where a, b, and c are Model parameters.

Distress model curves belonging to each classification were plotted together and visual inspections were conducted to identify AADTT breakpoints by grouping model curves that are close to each other. Two examples, i.e., Interstate Transverse Cracking model curves (Figure 10) and US Alligator Cracking model curves (Figure 11), are shown below.

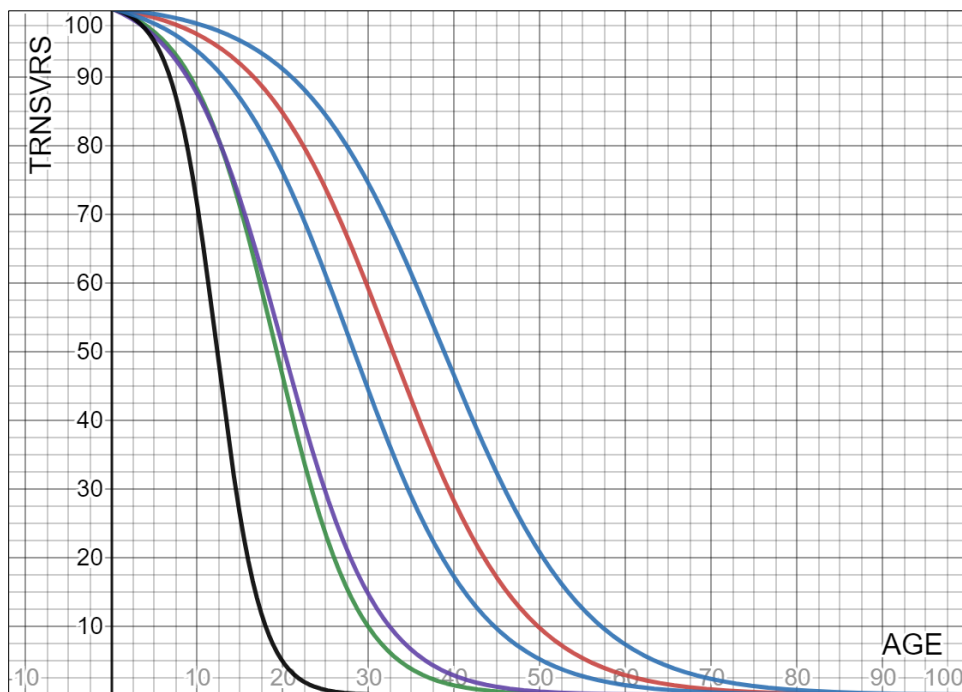


Figure 10. Initial Interstate Transverse Cracking model curves

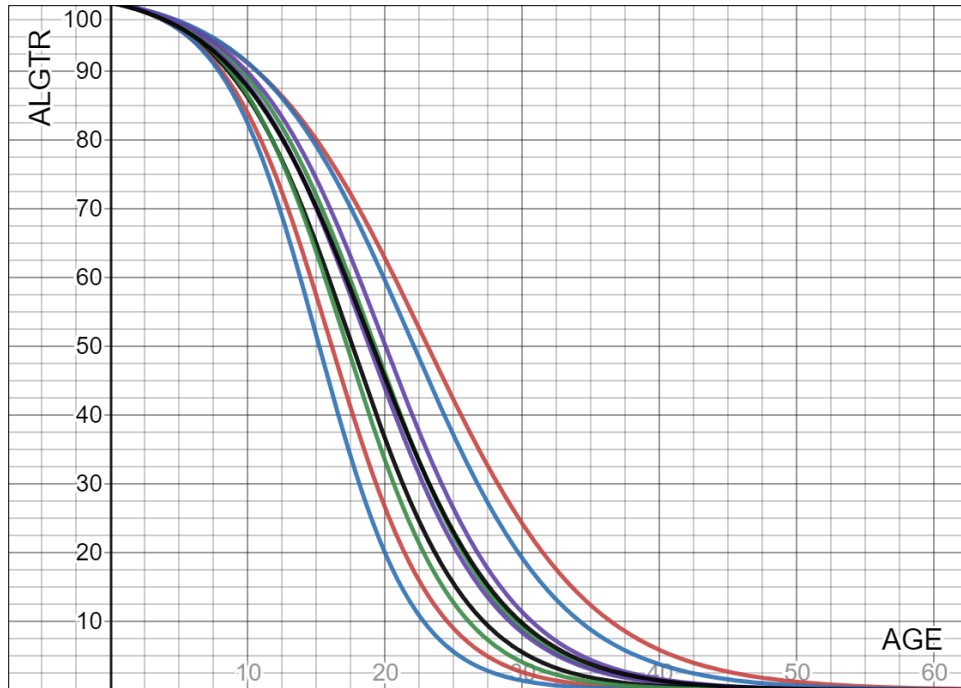


Figure 11. Initial US Alligator Cracking model curves

Visual inspection results are shown in Table 2. In this table, yellow, green, and blue color blocks in each column indicate that their corresponding initial family curves are close to each other and should be grouped together, and grey color blocks indicate that all initial family curves are close to each other, and it was challenging to distinguish between each other. The final AADTT breakpoints were determined by grouping as many blocks as possible with the same color across all the columns in the table. These breakpoints are included in the last column of the table. They are:

- Interstate: **3,000, 5,700**
- US: **280, 520, 880, 1,670**
- NC: **250, 420, 850**

Therefore, the final pavement families are:

- Interstate0_3000, Interstate3000_5700, Interstate5700plus
- US0_280, US280_520, US520_880, US880_1670, US1670plus
- NC0_250, NC250_420, NC420_580, NC580plus

3.4 Final Distress Models

Final distress models for Transverse Cracking, Alligator Cracking, Raveling, Longitudinal Cracking, Longitudinal Lane Joint Cracking, Wheel Path Patching, Non-Wheel Path Patching, and Rutting were developed using Equation (22). The same data cleaning process described in Section 3.3.2 was used and resulting model parameters a, b, and c are included in Table 3 below. It should be noted that the Longitudinal Lane Joint Cracking model for NC250_420 is not reasonable and thus is not included in the table. Transverse Cracking model curves of US roadways are included in Figure 12 as an example. All distress model curves are included in Appendix A.

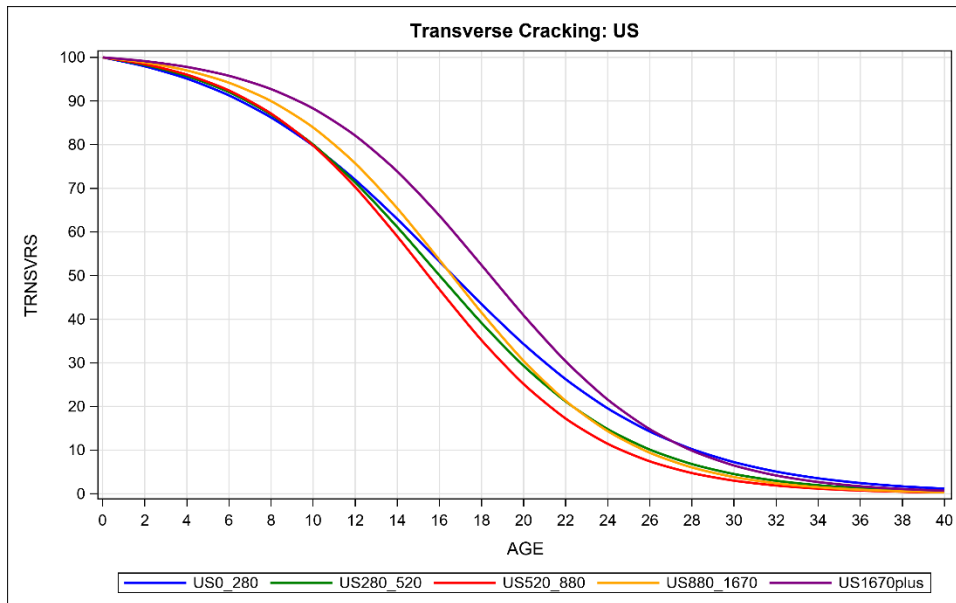


Figure 12. Transverse Cracking Model curves for US Roadways

Table 2. Final AADTT Breakpoints

| System | AADTT | TRNSVRS | ALGTR | LNGTDNL | LNGTDNL_LANE_JNT | RVL | WP_PTCH | NWP_PTCH | RUT | Break Points |
|------------|-----------|---------|-------|---------|------------------|-----|---------|----------|-----|--------------|
| Interstate | 0_2000 | | | | | | | | | 0_3000 |
| | 2000_3000 | | | | | | | | | |
| | 3000_4200 | | | | | | | | | |
| | 4200_5700 | | | | | | | | | |
| | 5700_6700 | | | | | | | | | 5700 plus |
| | 6700_8000 | | | | | | | | | |
| | 8000 plus | | | | | | | | | |
| US | 0_160 | | | | | | | | | 0_280 |
| | 160_280 | | | | | | | | | |
| | 280_400 | | | | | | | | | |
| | 400_520 | | | | | | | | | |
| | 520_660 | | | | | | | | | 520_880 |
| | 660_880 | | | | | | | | | |
| | 880_1200 | | | | | | | | | 880_1670 |
| | 1200_1670 | | | | | | | | | |
| | 1670_2460 | | | | | | | | | |
| | 2460 plus | | | | | | | | | |
| NC | 0_80 | | | | | | | | | 0_250 |
| | 80_140 | | | | | | | | | |
| | 140_190 | | | | | | | | | |
| | 190_250 | | | | | | | | | |
| | 250_320 | | | | | | | | | 250_420 |
| | 320_420 | | | | | | | | | |
| | 420_570 | | | | | | | | | 420_850 |
| | 570_850 | | | | | | | | | |
| | 850 plus | | | | | | | | | 850 plus |

Table 3. Final Distress Models

| Distress | | Interstate0_3000 | Interstate3000_5700 | Interstate5700plus | US0_280 | US280_520 | US520_880 | US880_1670 | US1670plus | NC0_250 | NC250_420 | NC420_850 | NC850plus |
|------------------|---|------------------|---------------------|--------------------|---------|-----------|-----------|------------|------------|---------|-----------|-----------|-----------|
| TRNSVRS | a | 101.15 | 102.36 | 103.22 | 104.78 | 103.37 | 102.66 | 101.96 | 101.51 | 102.73 | 102.53 | 102.00 | 101.77 |
| | b | 34.49 | 19.25 | 36.36 | 16.17 | 15.71 | 15.26 | 16.43 | 18.29 | 14.58 | 14.65 | 14.65 | 16.93 |
| | c | -7.73 | -5.14 | -10.58 | -5.32 | -4.63 | -4.21 | -4.18 | -4.36 | -4.05 | -3.98 | -3.75 | -4.20 |
| ALGTR | a | 100.76 | 100.78 | 101.85 | 102.13 | 101.80 | 101.85 | 101.50 | 101.83 | 101.44 | 101.53 | 101.54 | 101.44 |
| | b | 32.84 | 24.23 | 32.36 | 22.48 | 19.11 | 17.39 | 16.44 | 19.47 | 19.93 | 20.07 | 19.16 | 18.55 |
| | c | -6.73 | -4.99 | -8.10 | -5.84 | -4.75 | -4.36 | -3.92 | -4.87 | -4.70 | -4.80 | -4.59 | -4.37 |
| LNGTDNL | a | 101.27 | 101.18 | 102.60 | 102.65 | 101.78 | 101.41 | 100.75 | 101.13 | 101.47 | 101.34 | 101.43 | 101.33 |
| | b | 18.53 | 14.02 | 16.43 | 19.74 | 17.21 | 15.95 | 13.33 | 13.55 | 20.52 | 18.48 | 17.72 | 16.43 |
| | c | -4.25 | -3.16 | -4.50 | -5.44 | -4.27 | -3.74 | -2.72 | -3.02 | -4.87 | -4.28 | -4.17 | -3.80 |
| LNGTDNL-LANE-JNT | a | 100.68 | 101.75 | 100.66 | 100.03 | 101.27 | 100.04 | 100.05 | 100.16 | 100.36 | | 100.01 | 100.07 |
| | b | 39.88 | 36.65 | 80.14 | 708.48 | 18.53 | 697.63 | 251.84 | 96.83 | 46.02 | | 801.11 | 205.77 |
| | c | -7.99 | -9.05 | -15.94 | -87.75 | -4.25 | -88.07 | -33.17 | -14.98 | -8.17 | | -88.10 | -28.29 |
| RVL | a | 100.99 | 102.23 | 103.65 | 101.62 | 101.36 | 101.64 | 101.54 | 101.57 | 102.25 | 101.88 | 102.05 | 102.00 |
| | b | 16.24 | 30.63 | 41.45 | 24.51 | 24.75 | 24.86 | 28.81 | 27.84 | 21.27 | 22.95 | 22.61 | 24.26 |
| | c | -3.52 | -8.06 | -12.52 | -5.94 | -5.76 | -6.05 | -6.90 | -6.70 | -5.60 | -5.78 | -5.82 | -6.20 |
| WP-PTCH | a | 100.03 | 100.28 | 100.14 | 100.18 | 100.16 | 100.21 | 100.22 | 100.14 | 100.11 | 100.17 | 100.23 | 100.26 |
| | b | 234.45 | 45.66 | 76.32 | 151.75 | 112.54 | 241.49 | 185.65 | 99.63 | 87.76 | 86.64 | 210.29 | 77.21 |
| | c | -29.26 | -7.75 | -11.65 | -24.04 | -17.49 | -39.05 | -30.37 | -15.12 | -12.95 | -13.56 | -34.70 | -13.01 |
| NWP-PTCH | a | 100.04 | 100.30 | 100.11 | 100.17 | 100.13 | 100.15 | 100.19 | 100.10 | 100.11 | 100.14 | 100.20 | 100.25 |
| | b | 228.48 | 46.68 | 73.32 | 189.40 | 128.03 | 150.29 | 292.45 | 104.36 | 93.19 | 101.69 | 150.01 | 83.30 |
| | c | -28.89 | -8.04 | -10.72 | -29.83 | -19.22 | -23.18 | -46.76 | -15.15 | -13.72 | -15.56 | -24.05 | -13.86 |
| RUT | a | 102.08 | 101.11 | 101.34 | 101.25 | 101.43 | 101.87 | 101.76 | 102.31 | 100.81 | 101.07 | 101.43 | 101.69 |
| | b | 86.68 | 117.99 | 74.23 | 207.56 | 84.48 | 103.24 | 70.03 | 90.82 | 83.29 | 61.88 | 69.37 | 75.66 |
| | c | -22.37 | -26.20 | -17.21 | -47.35 | -19.89 | -25.95 | -17.34 | -24.10 | -17.29 | -13.64 | -16.34 | -18.54 |

3.4 Final Performance Models

Since pavement's pre-treatment condition can greatly impact the performance of pavement after it is treated, it was decided to include this information when developing pavement performance models. As concluded by a previous study [4], the average PCR values before Interstate, US, and NC roadways were treated, i.e., Pre_PCR values, are summarized in Table 4 below.

Table 4. Pre_PCR Values

| Pavement Classification | Pre_PCR |
|-------------------------|---------|
| Interstate | 69 |
| US | 61 |
| NC | 58 |

Using these Pre_PCR values, each of the roadway family can be further divided into two sub-families. For example, Interstate0_3000 is divided into Interstate0_3000_Poor (when roadways' Pre_PCR values are less than 69) and Interstate0_3000_Good (when roadways' Pre_PCR values are greater than 69). Therefore, the new pavement families are listed below and performance models were developed for all these families:

- Interstate0_3000_Poor, Interstate0_3000_Good, Interstate3000_5700_Poor, Interstate3000_5700_Good, Interstate5700plus_Poor, Interstate5700plus_Good
- US0_280_Poor, US0_280_Good, US280_520_Poor, US280_520_Good, US520_880_Poor, US520_880_Good, US880_1670_Poor, US880_1670_Good, US1670plus_Poor, US1670plus_Good
- NC0_250_Poor, NC0_250_Good, NC250_420_Poor, NC250_420_Good, NC420_580_Poor, NC420_580_Good, NC580plus_Poor, NC580plus_Good

These performance models were developed using the following model equation:

$$PCR = a / (1 + e^{(-Pavement_Age + b)/c}) \quad (23)$$

where a, b, c are model parameters.

Based on findings from a previous study [3], PCR values of asphalt pavements can be calculated as shown in equations below:

$$\text{NDR} = 0.5152640 \times \text{TRA} + 0.2729290 \times \text{LNG} + 0.2118080 \times \text{LNG_JNT} \quad (24)$$

$$\text{LDR} = 0.5316370 \times \text{ALGTR} + 0.1520450 \times \text{WP} + 0.0887566 \times \text{NWP} + 0.2275610 \times \text{RUT} \quad (25)$$

$$\text{PCR} = \min(\text{LDR}, \text{NDR}) \quad (26)$$

where:

- **NDR:** Non-Load Related Distress Rating
- **LDR:** Load Related Distress Rating
- **PCR:** Pavement Condition Rating
- **TRA:** Transverse Cracking index value
- **LNG:** Longitudinal Cracking index value
- **ALGTR:** Alligator Cracking index value
- **WP:** Wheel Path Patching index value
- **NWP:** Non Wheel Path Patching index value
- **RUT:** Rutting index value

The same data cleaning process described in Section 3.3.2 was used and resulting model parameters a, b, and c are included in Table 5 below.

Table 5. Final Performance Models

| Family | a | b | c |
|--------------------------|----------|----------|----------|
| Interstate0_3000_good | 101.2 | 23.25 | -5.35 |
| Interstate0_3000_poor | 104.5 | 14.70 | -4.79 |
| Interstate3000_5700_good | 102.0 | 21.05 | -5.45 |
| Interstate3000_5700_poor | 102.0 | 12.59 | -3.32 |
| Interstate5700plus_good | 104.5 | 48.81 | -15.94 |
| Interstate5700plus_poor | 117.0 | 12.46 | -7.09 |
| US0_280_good | 103.2 | 22.73 | -6.73 |
| US0_280_poor | 103.2 | 11.50 | -3.41 |
| US280_520_good | 103.0 | 21.97 | -6.23 |
| US280_520_poor | 105.0 | 13.02 | -4.42 |
| US520_880_good | 102.5 | 22.23 | -6.17 |
| US520_880_poor | 109.0 | 12.99 | -5.47 |
| US880_1670_good | 101.6 | 19.96 | -5.08 |
| US880_1670_poor | 105.0 | 12.96 | -4.44 |
| US1670plus_good | 102.0 | 21.01 | -5.37 |
| US1670plus_poor | 104.5 | 12.98 | -4.21 |
| NC0_250_good | 102.5 | 23.76 | -6.61 |
| NC0_250_poor | 102.5 | 12.84 | -3.65 |
| NC250_420_good | 102.0 | 21.43 | -5.61 |
| NC250_420_poor | 102.0 | 12.52 | -3.36 |
| NC420_850_good | 102.0 | 22.40 | -5.99 |
| NC420_850_poor | 103.0 | 12.72 | -3.76 |
| NC850plus_good | 101.7 | 23.11 | -5.94 |
| NC850plus_poor | 103.0 | 12.72 | -3.62 |

Performance model curves of Interstate0_3000 and US520_850 roadways are included in Figure 13 and Figure 14 below as examples. In these figures, the blue solid line represents the model curve that was developed using roadway sections that have greater Pre_PCR values than the corresponding Pre_PCR threshold, i.e., the *Roadway_Good* curve, the green solid line represents the *Roadway_Poor* curve, and the red dash line represent the overall model curve, *Roadway_Combined* curve, that was developed using the combined *Roadway_Good* and *Roadway_Poor* data. All performance model curves are included in Appendix B.

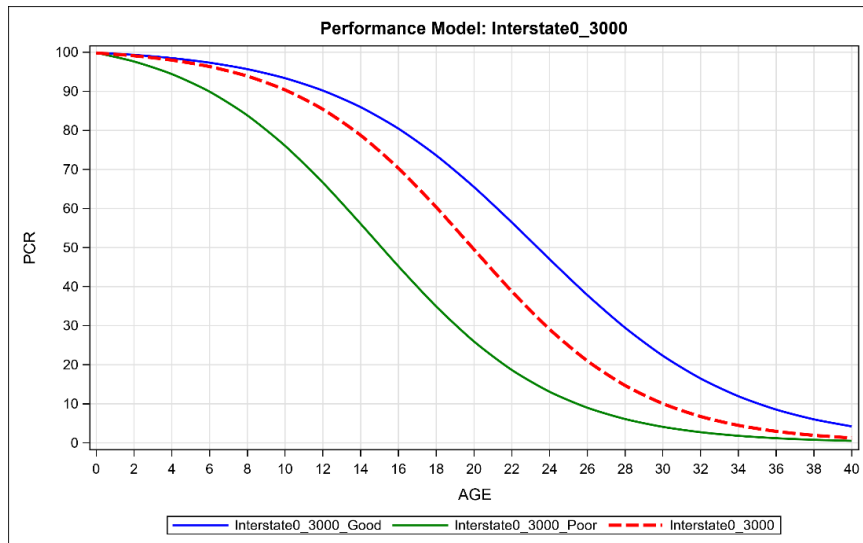


Figure 13. Performance Model Curves for Interstate0-3000

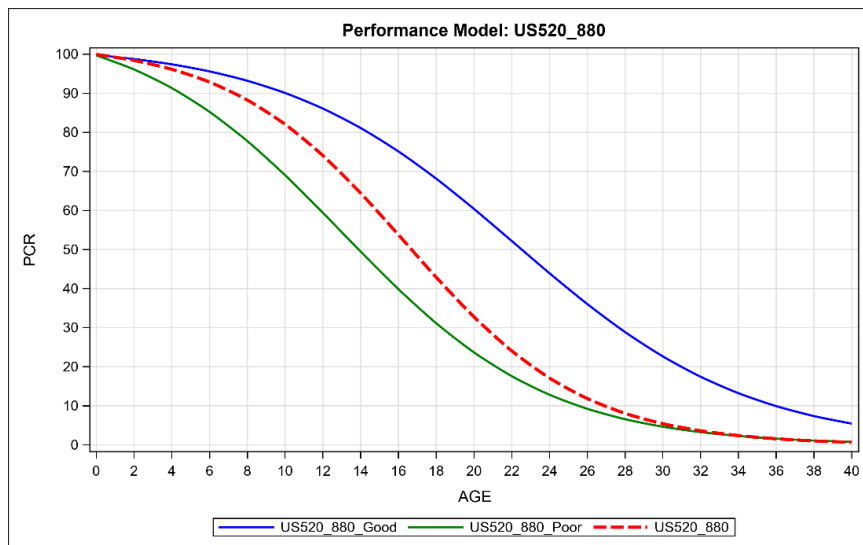


Figure 14. Performance Model Curves for US520-850

CHAPTER 4 A Pilot Study on ESAL

This chapter describes the procedures used to develop pavement distress and performance models for Interstate routes using an alternative traffic loading parameter, ESAL, and its breakpoints as well as pre-treatment pavement conditions. The flow chart is the same as the procedure used for AADTT except for AADTT being replaced with ESAL (the red box in Figure 15 below).

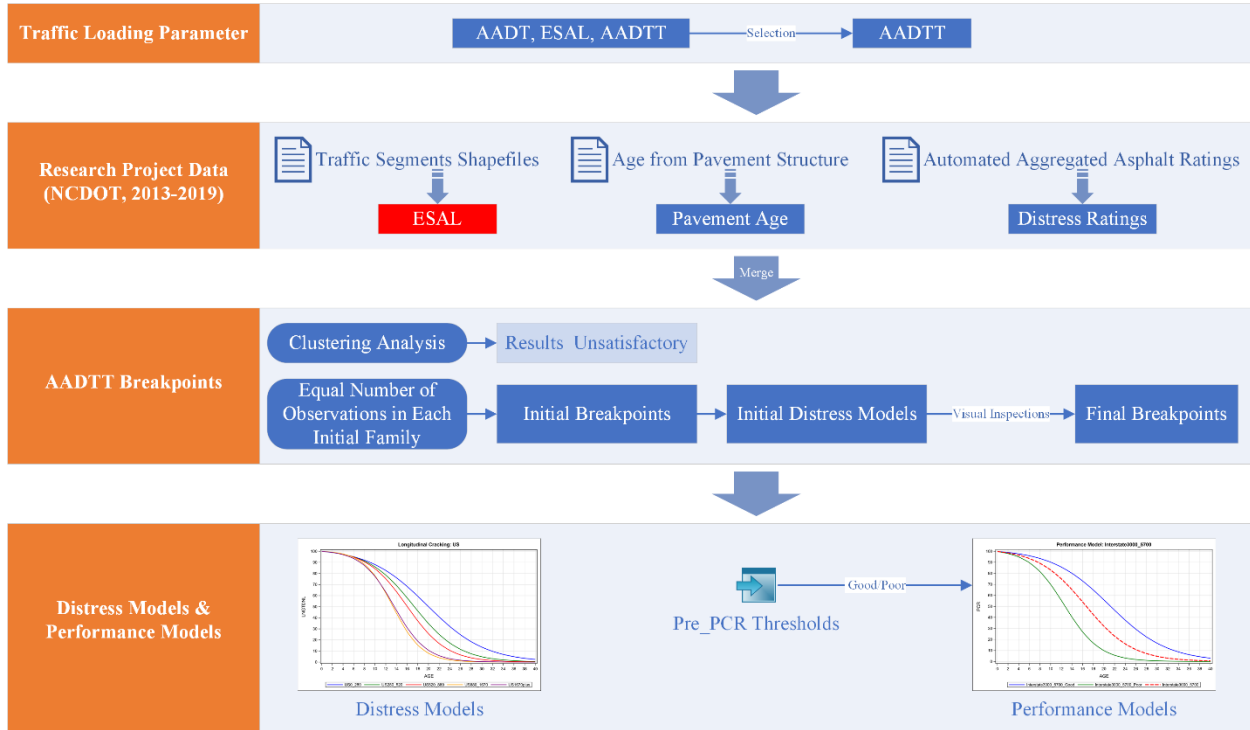


Figure 15. Flow Chart for ESAL

As described in Chapter 3, ESAL was not initially selected as the new traffic loading parameter because quite some additional information is required for each roadway section to calculate ESAL values (equations below), whereas AADTT values are included in the segment shapefiles for this research project to use directly.

According to the NCDOT Pavement Design Procedure [25], ESAL can be calculated using the following equations:

$$ESALS_{Total} = \frac{\left(\left(1 + \frac{\%Growth}{100 + 365.25} \right)^{(365.25 \times N_D)} - 1 \right) \times \left(ADT_c \times \frac{\%TTST}{100} \times TTST_F \times \frac{\%Duals}{100} \times Duals_F \right) \times \frac{\%Direction}{100} \times L_D}{\ln \left(1 + \frac{\%Growth}{100 + 365.25} \right)} \quad (27)$$

where,

$$\% \mathbf{Growth} = \left(10^{\left(\frac{\log_{10} \frac{ADT_{Future}}{ADT_{Initial}}}{(Year_{Future} - Year_{Initial}) \times 365.25} \right)} \times 365.25 - 365.25 \right) \times 100 \quad (28)$$

$$\mathbf{ADT}_C = ADT_{Initial} \times \left(1 + \frac{\% \mathbf{Growth}}{100 \times 365.25} \right)^{((Year_{Construction} - Year_{Initial}) \times 365.25)} \quad (29)$$

N_D = Design Number of Years

ADT_C = Average Annual Daily Traffic in the year of construction

TTST_F = Tractor Trailer Semi Truck (TTST) Loading Factor

Dual_F = Duals Factor

L_D = Lane Distribution Factors (a lane distribution factor of 0.50 will be used for the design of inside (median) lane widening of existing facilities with 2 or more lanes per direction):

| No. of Lanes <u>In One Direction</u> | Lane Distribution <u>Factor</u> |
|---|------------------------------------|
| 1 | 1.0 |
| 2 | 0.9 |
| 3 or more | 0.8 |

Truck Loading Factors (Flexible Pavement, 18-kip ESALs):

| | DUALS | TTST |
|-----------------------------|-------|------|
| Rural Freeway & Interstates | 0.30 | 1.15 |
| Rural Other | 0.30 | 0.95 |
| Urban Freeway & Interstates | 0.30 | 0.85 |
| Urban Other | 0.25 | 0.80 |

% Direction: a direction split of 50% is typically used in all designs.

For this pilot study, a simplified equation was suggested by NCDOT to calculate ESAL:

$$ESAL = 0.3 \times SU_AADT + 1.05 \times MU_AADT \quad (30)$$

where,

SU_AADT = Annual average daily traffic of single unit single axle trucks, “Duals”

MU_AADT = Annual average daily traffic of various combinations of multiple unit and multiple axle trucks, “TTST”

Calculated ESAL values were then used as the new alternative traffic loading parameter to develop distress and performance models for Interstate routes only.

4.1 Initial ESAL Breakpoints

Using the equal number of observations in each initial family method, it was decided to develop 7 initial Interstate families of 500 roadway sections, 10 initial US families of 2,000 sections, and 10 initial NC families of 3,000 sections. Corresponding initial ESAL breakpoints are:

- Interstate: **1,500, 2,300, 3,700, 5,200, 6,400, 7,700**
- US: **50, 110, 180, 250, 340, 450, 600, 820, 1,200**
- NC: **30, 60, 100, 130, 170, 220, 300, 410, 660**

4.2 Initial Distress Models

After outliers were removed using the same process described in Chapter 3, initial distress models were developed, and model curves were visually inspected to group similar curves. One example, Interstate Transverse Cracking model curves, are shown below (Figure 16).

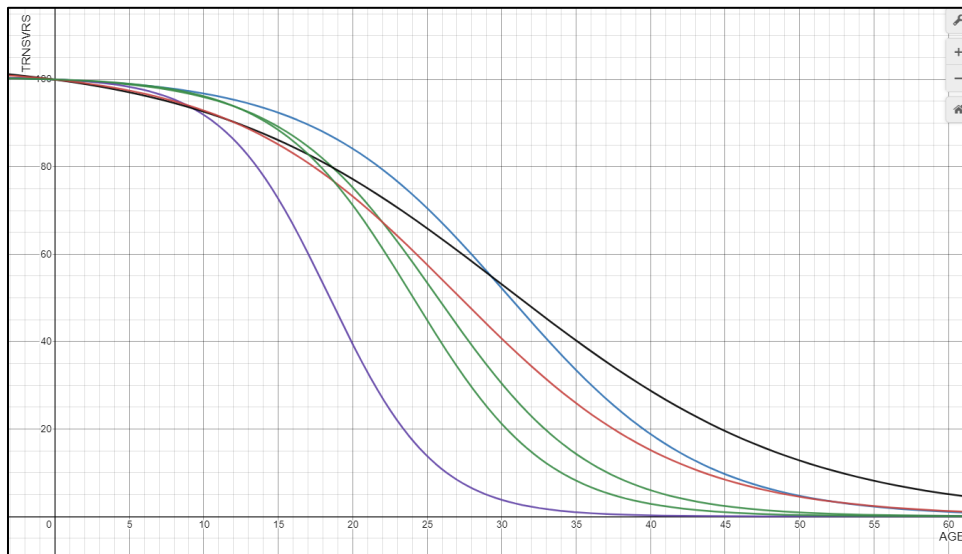


Figure 16. Initial Interstate Transverse Cracking model curves

Visual inspection results are shown in Table 6. In this table, differing color blocks in each column indicate that their corresponding initial family curves are close to each other and should be grouped together.

Table 6. Final ESAL Breakpoint (Interstate Routes)

| System | ESAL | TRNSVRS | ALGTR | LNGTDNL | LNGTDNL_LANE_JNT | RVL | WP_PTCH | NWP_PTCH | RUT | Break Points |
|------------|-----------|---------|--------|---------|------------------|--------|---------|----------|--------|--------------|
| Interstate | 0-1500 | Yellow | Yellow | Yellow | Yellow | Yellow | Yellow | Yellow | Yellow | 0-1500 |
| | 1500-2300 | Green | Green | Yellow | Green | Green | Yellow | Yellow | Green | 1500-2300 |
| | 2300-3700 | Orange | Yellow | Yellow | Green | Orange | Green | Green | Orange | 2300-5200 |
| | 3700-5200 | Yellow | Yellow | Yellow | Orange | Blue | Orange | Orange | Blue | |
| | 5200-6400 | Green | Orange | Green | Blue | Green | Blue | Green | Orange | 5200-7700 |
| | 6400-7700 | Grey | Orange | Green | Blue | Grey | Blue | Green | Green | |
| | 7700 plus | Green | Green | Yellow | Orange | Orange | Blue | Green | Green | 7700 plus |

The final ESAL breakpoints were determined by grouping as many blocks as possible with the same color across all the columns in the table. These breakpoints are included in the last column of the table. They are:

- Interstate: **1,500, 2,300, 5,200, 7,700**

Therefore, the final Interstate pavement families are:

- Interstate0_1500, Interstate1500_2300, Interstate2300_5200, Interstate5200_7700, Interstate7700plus

4.3 Final Distress Models

Final distress models for Transverse Cracking, Alligator Cracking, Raveling, Longitudinal Cracking, Longitudinal Lane Joint Cracking, Wheel Path Patching, Non-Wheel Path Patching, and Rutting were developed using Equation (22). The same data cleaning process described in Section 3.3.2 was used and resulting model parameters a, b, and c are included in Table 7 below. Transverse Cracking model curves of Interstate roadways are included in Figure 17 as an example. All distress model curves are included in Appendix F.

Table 7. Final Distress Models for Interstate Routes (ESAL)

| Distress | | Interstate_E_0_1500 | Interstate_E_1500_2300 | Interstate_E_2300_5200 | Interstate_E_5200_7700 | Interstate_E_7700plus |
|------------------|---|---------------------|------------------------|------------------------|------------------------|-----------------------|
| TRNSVRS | a | 100.9 | 100.7 | 101.7 | 104 | 100.5 |
| | b | 30.46200818 | 25.64414652 | 21.101897 | 370.985241 | 24.02716255 |
| | c | -6.48155643 | -5.203086327 | -5.134310916 | -115.5202975 | -4.530896571 |
| ALGTR | a | 100.5 | 100.3 | 100.5 | 101.5 | 100.4 |
| | b | 29.79158571 | 23.96676485 | 41.00879646 | 118.541268 | 23.26348119 |
| | c | -5.567784068 | -4.022073291 | -7.760868368 | -28.49631158 | -4.124833706 |
| LNGTDNL | a | 100.4 | 100.2 | 100.5 | 104.3 | 100.8 |
| | b | 18.00055101 | 15.81804042 | 17.01757405 | 52.05476974 | 17.88383666 |
| | c | -3.301935126 | -2.572078442 | -3.20114607 | -16.46921987 | -3.743364604 |
| LNGTDNL-LANE-JNT | a | 101.9 | 100.1 | 100.6 | 100.8 | 100.5 |
| | b | 24.74019771 | 12.50137132 | 15.19824058 | 15.01003277 | 16.62965384 |
| | c | -6.185674379 | -1.808939741 | -3.014184853 | -3.148038624 | -3.095278283 |
| RVL | a | 101.1 | 100.8 | 102.6 | 107.5 | 101.3 |
| | b | 19.20674883 | 16.72243498 | 27.99596232 | 33.95666223 | 21.49364764 |
| | c | -4.276868206 | -3.482180236 | -7.701692953 | -13.08393945 | -4.922031145 |
| WP-PTCH | a | 100.5 | 100.3 | 101.1 | 101 | 100.95 |
| | b | 167.271779 | 83.96452929 | 29.84304886 | 38.60612198 | 35.1711101 |
| | c | -32.04710207 | -14.16865825 | -6.620403566 | -8.33878383 | -7.558877921 |
| NWP-PTCH | a | 100.5 | 100.3 | 101.05 | 101.05 | 101.05 |
| | b | 323.615484 | 81.07287713 | 28.38759874 | 39.43206828 | 36.50056583 |
| | c | -61.77984868 | -13.90167611 | -6.240470472 | -8.587812704 | -7.992856132 |
| RUT | a | 101.4 | 102.05 | 101.65 | 101.6 | 101.12 |
| | b | 39.47051099 | 66.85133209 | 191.7035046 | 87.53173572 | 66.34072338 |
| | c | -9.26547041 | -17.19207189 | -46.83488666 | -21.22425491 | -14.81575485 |

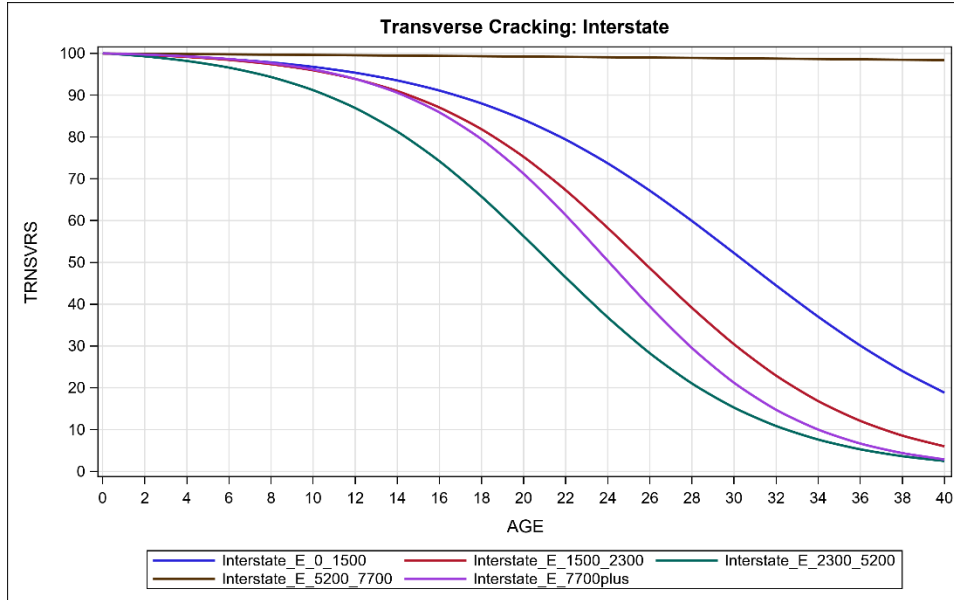


Figure 17. Transverse Cracking Model Curves for Interstate Routes (ESAL)

4.4 Final Performance Models

Using the same Pre_PCR values listed in Table 4, final performance models were developed for the following Interstate families:

- Interstate0_1500_Poor, Interstate0_1500_Good, Interstate1500_2300_Poor, Interstate1500_2300_Good, Interstate2300_5200_Poor, Interstate2300_5200_Good, Interstate5200_7700_Poor, Interstate5200_7700_Good, Interstate7700plus_Poor, Interstate7700plus_Good

Resulting model parameters, a, b, and c are included in Table 8 below.

Table 8. Final Performance Models for Interstate Routes (ESAL)

| Family | a | b | c |
|-----------------------------|--------|--------------|--------------|
| Interstate_E_0_1500_good | 101.63 | 25.146009659 | -6.155948602 |
| Interstate_E_0_1500_poor | 100.00 | -23.15220801 | 31.278934863 |
| Interstate_E_1500_2300_good | 100.90 | 19.333423522 | -4.087873165 |
| Interstate_E_1500_2300_poor | 104.20 | 14.845647092 | -4.694104871 |
| Interstate_E_2300_5200_good | 102.60 | 23.375366909 | -6.418199513 |
| Interstate_E_2300_5200_poor | 113.40 | 15.838415118 | -7.890229436 |
| Interstate_E_5200_7700_good | 105.70 | 58.249022104 | -20.40296632 |
| Interstate_E_5200_7700_poor | 114.70 | 11.059762499 | -5.773810448 |
| Interstate_E_7700plus_good | 102.20 | 26.578801103 | -6.962505814 |
| Interstate_E_7700plus_poor | 100.00 | 5.4214545976 | 8.8478152996 |

Performance model curves of the Interstate1500_2300 family are included in Figure 18 below as an example. In this figure, the blue solid line represents the model curve that was developed using roadway sections that have greater Pre_PCR values than the corresponding Pre_PCR threshold, i.e., the *Roadway_Good* curve, the green solid line represents the *Roadway_Poor* curve. It should be noted that the Interstate0_1500_Poor model and the Interstate7700plus_Good models are not reasonable mainly because of the small sample size of these two families and thus are not included in the final plots. All performance model curves are included in Appendix G.

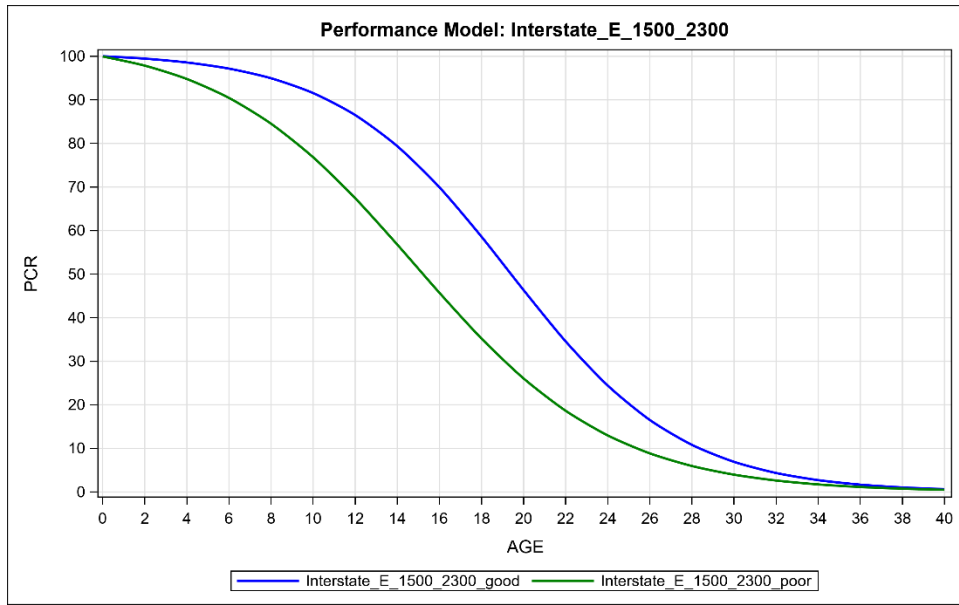


Figure 18. Performance Model Curves for Interstate1500-2300 (ESAL)

CHAPTER 5 FINDINGS AND CONCLUSIONS

This research project was conducted to develop pavement distress and performance models using a new traffic loading indicator, a new set of breakpoints for dividing roadway families, and pavement pre-treatment conditions. Several steps were involved in this study: (1) traffic segment shapefiles, pavement age files, and automated asphalt pavement rating files were obtained from NCDOT and merged to create a master data file; (2) distress ratings were normalized and distress index values were calculated, outliers were removed, and two different methods, clustering analysis and equal number of observations in each initial roadway family, were used to determine the initial breakpoints; (3) initial distress models were developed and visual inspections were conducted to group the model curves that are close to each other, then the final breakpoints were determined; (4) final distress models were developed, and final performance models were developed using Pre_PCR conditions. Findings and conclusions of this research project are provided below:

- Data availability. Research data needed for this research project, e.g., AADTT, Pavement Age, Pavement Distress Ratings, etc., have been frequently updated and made available to the research team by NCDOT engineers. These raw data are either published on a website that can be accessed publicly or provided to researchers upon request on a timely basis.
- Development of pavement families. Clustering analysis and the equal number of observations method were used to determine the AADTT breakpoints, which were then used to group new pavement families. It was observed that clustering analysis used in this project did not provide sufficient accuracy, as shown in Figure 19, Figure 20, and Figure 21. In these histograms, counts of AADTT are shown at the top of each bin, (a) includes color blocks that have boundaries ending at the AADTT values resulting from clustering analysis, (b) includes color blocks that have boundaries ending at pre-selected number of roadway sections in each initial pavement family, i.e., 500 for Interstate, 2,000 for US, and 3,000 for NC, and (c) includes color blocks that have boundaries ending at final AADTT breakpoints determined by visual inspections. It can be observed that the resolution of (a) is not sufficient to capture intermediate AADTT values as final breakpoints. It can be concluded that for a similar research project, it is recommended to use the equal number of observations method to determine breakpoints.

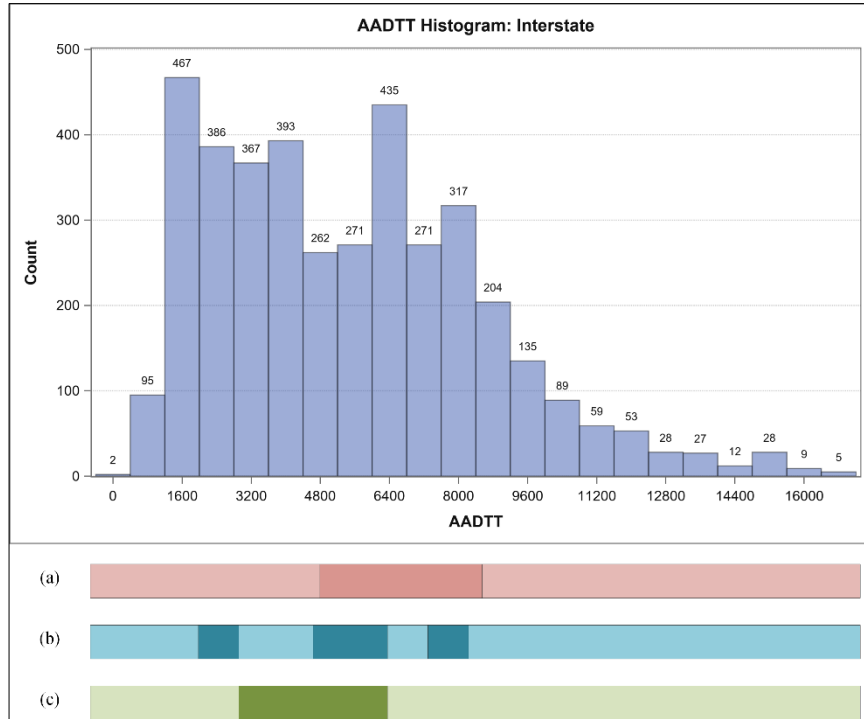


Figure 19. AADTT Breakpoints for Interstate

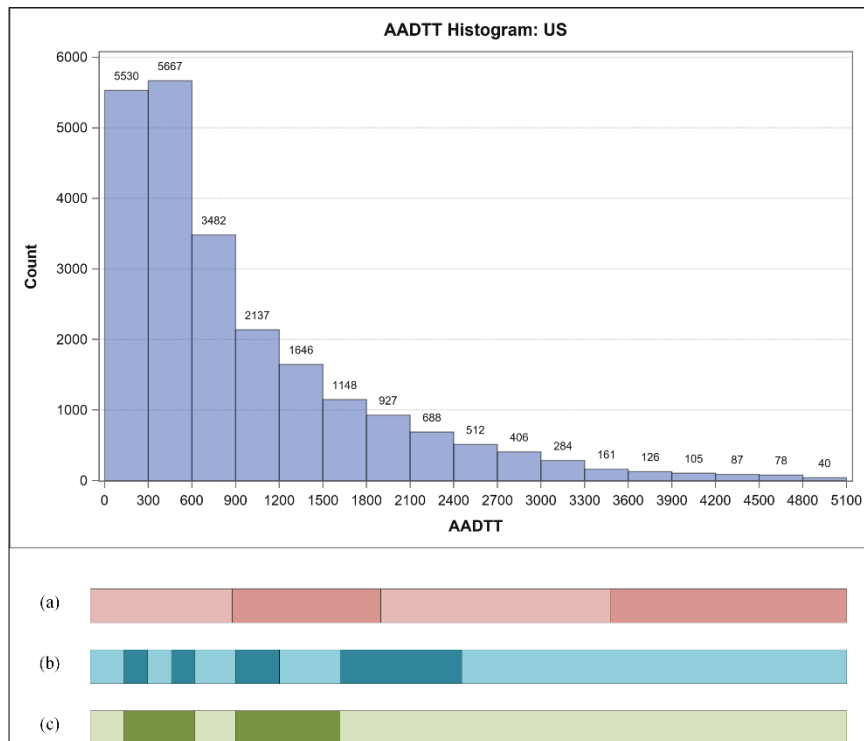


Figure 20. AADTT Breakpoints for US

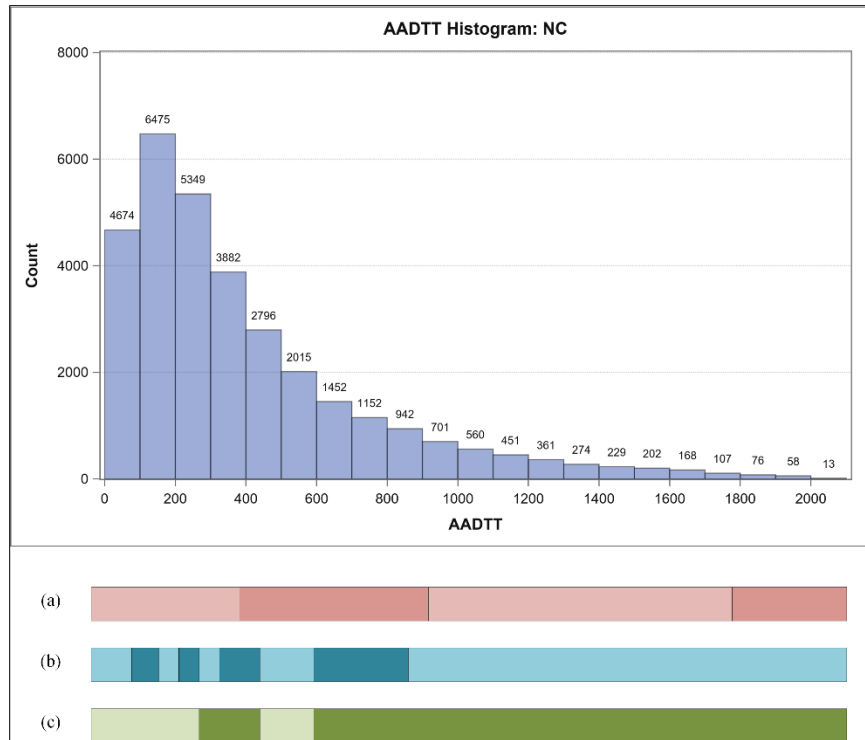


Figure 21. AADTT Breakpoints for NC

- Distress models. A comparison of distress model curves (Figure 22) developed using AADT [3] (referring to as AADT distress curves) with the model curves developed in this project using AADTT (referring to as AADTT distress curves) indicates the following:
 - The Wheel Path Patching, Non Wheel Path Patching, and Rutting AADTT distress curves are flat. One possible reason is that these three types of load related distresses (LDRs) are not severe in asphalt pavements in North Carolina. Another possible reason is that the data collection vendor has recently changed, and it is reasonable to assume that algorithms used to process raw images are different, which can lead to distress ratings that are different than the ones provided by the previous vendor. If the latter is true, it is necessary to conduct a detailed comparison between AADT distress curves and AADTT distress curves, and then update the NCDOT PMS Decision Trees accordingly.
 - Alligator Cracking AADTT distress curves are flatter than corresponding AADT distress curves. Alligator Cracking is another type of load related distress. This indicates that very likely the vendor's processing algorithms for LDRs are quite different, and special attention should be given to LDRs if the NCDOT PMS

- Performance models. For performance models developed using AADTT breakpoints (referring to as the AADTT performance models), their curvature is as expected (Figure 23). The *Roadway_Good* curves (blue solid lines) are flatter than the *Roadway_Combined* curves, and the *Roadway_Poor* curves are steeper than the *Roadway_Combined* curves (green solid lines). A comparison of AADT and AADTT performance curves indicates that in general AADTT curves are flatter (Figure 24) (all curves are included in Appendix D). A further comparison of AADT performance curves (dash lines) and AADTT *Roadway_Poor* performance curves (solid lines), however, indicates that they share the same deterioration trends (Figure 25) (all curves are included in Appendix E).

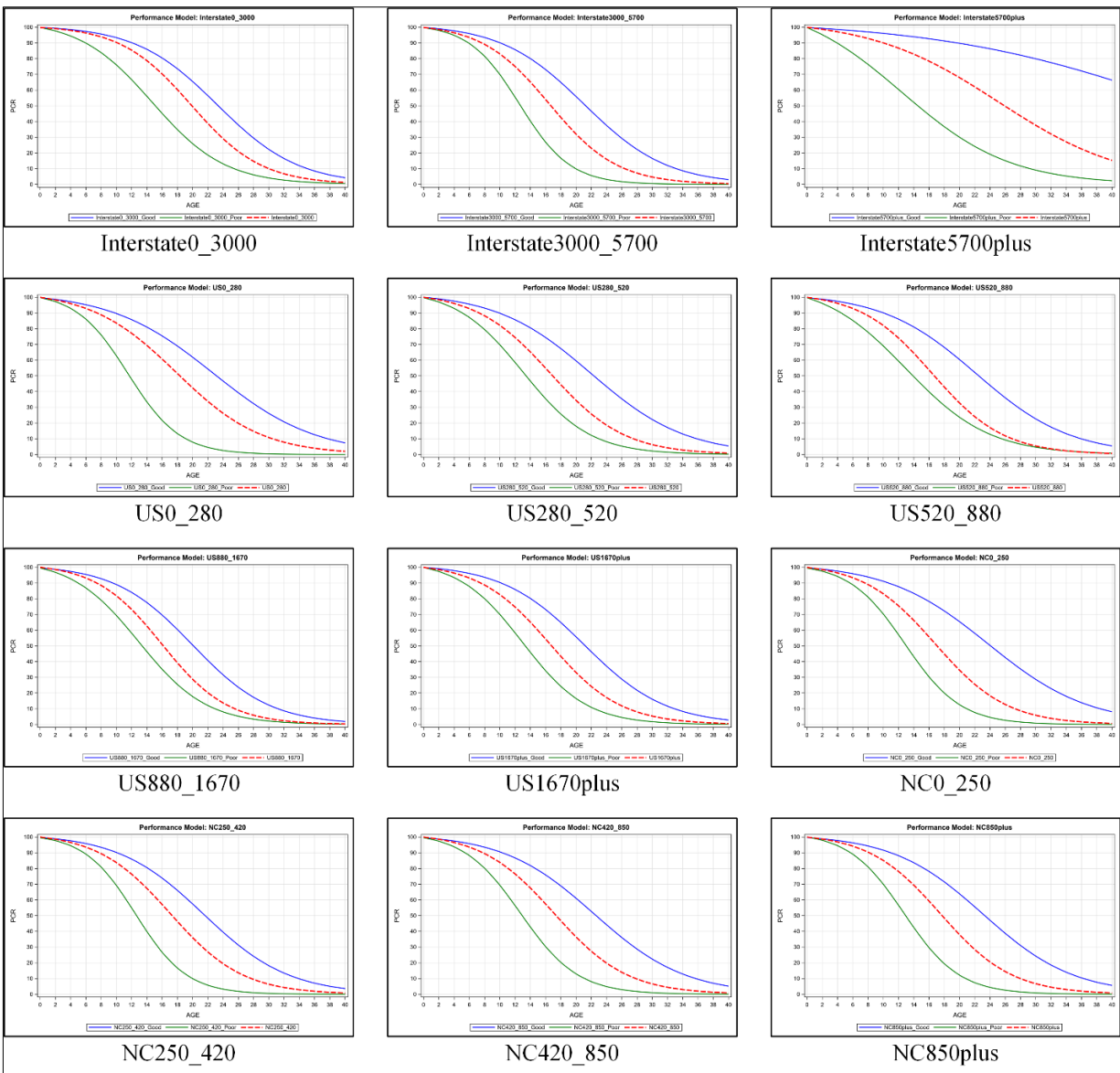


Figure 23. Performance Models: Combined, Good, and Poor

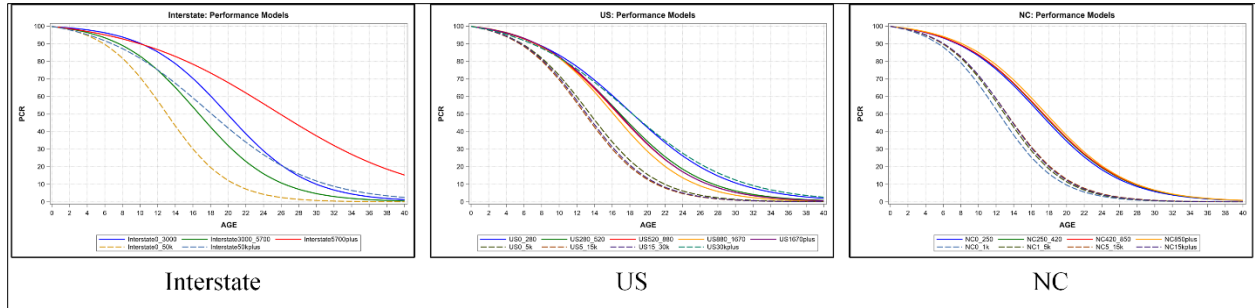


Figure 24. AADT Performance Models and AADTT Performance Models

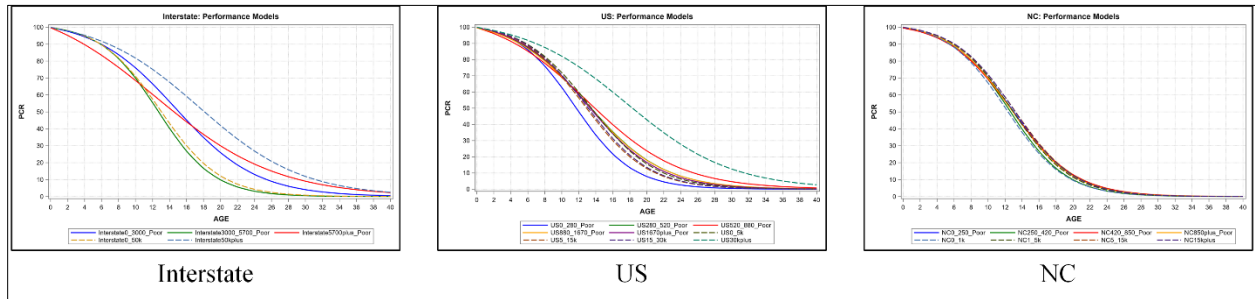


Figure 25. AADT Performance Models and AADTT Roadway_Poor Performance Models

- A pilot study was conducted to use Equivalent Single Axle Load (ESAL) as an alternative new traffic loading parameter. Due to the time constraint, only Interstate routes were analyzed, and corresponding distress and performance models were developed. In this pilot study, ESAL values were calculated using a simplified equation. The resulting distress model curves lay between the AADT curves and AADTT curves, indicating that ESAL distress curves reflect NCDOT preventive maintenance practices closer than AADTT curves.

CHAPTER 6 RECOMMENDATIONS

Based on findings and conclusions obtained from this research project, the following recommendations are provided for future research endeavors:

- Comparing to clustering analysis, the same number of observations per family method is more appropriate to be used to create pavement families, mainly because pavement distress data is variable in nature. The latter method is sufficiently accurate to capture reasonable intermediate AADTT values as family breakpoints.
- A subsequent research project is recommended to quantify the differences between AADT and AADTT distress and performance curves. Current Decision Trees in the NCDOT PMS are using the critical thresholds derived from obsolete AADT models. With the use of a new data collection vendor and the newly developed AADTT models, current Decision Trees should be updated to achieve PMS' maximum level of performance.
- Two sub-distress models, *Roadway_Good* and *Roadway_Poor*, should be developed for each distress type. Sub-performance models were developed in this research project. The model curves provide the ranges of PCR values at a given age. The similar procedure should be implemented to distress models to provide the ranges of distress index values, which can be used to fine tune the NCDOT PMS' Decision Trees.
- ESAL should be further studied as the alternative traffic loading parameter to develop distress and performance models for US and NC routes, and a comparison of ESAL and AADTT model curves should be conducted to study the differences between these two traffic loading parameters, and the results can assist NCDOT with an enhanced ability to update the decision trees, and thus make informative pavement management decisions.

CITED REFERENCES

1. Chen, D., Cavalline, T. L., and Ogunro, V. O. (2014). "Development and validation of pavement deterioration models and analysis weight factors for the NCDOT pavement management system (phase I: windshield survey data)." Rep. No. FHWA/NC/2011-01, Federal Highway Administration (FHWA), Washington, DC.
2. Chen, D., Hildreth, J., Nicholas, T., and Dye, M. (2014). "Development and validation of pavement deterioration models and analysis weight factors for the NCDOT pavement management system (phase II: automated data)." Rep. No. FHWA/NC/2011-01, Federal Highway Administration (FHWA), Washington, DC.
3. Chen, D., Hildreth, J., Nicholas, T., and James, S. (2015). " Evaluation of Benefit Weight Factors and Decision Trees for Automated Distress Data Models." Rep. No. FHWA/NC/2015-01, Federal Highway Administration (FHWA), Washington, DC.
4. Chen, D., Hildreth, J. and Finger, R. (2020). "Determination of Performance Jumps for Treatments of Asphalt Pavements in North Carolina's Pavement Management System." *Journal of Transportation Engineering: Part B: Pavements*, ASCE, Vol. 146(3): 04020046.
5. Madanat, S. M., Nakat, Z. E., and Sathaye, N. (2005). Development of Empirical-Mechanistic Pavement Performance Models using Data from the Washington State PMS Database. UC Davis: Institute of Transportation Studies (UCD).
6. Serigos, P.A., Smit, A, and Prozzi, J.A. (2017). Performance of Preventive Maintenance Treatments for Flexible Pavements in Texas. Technical Report 0-6878-2, TXDOT Project Number 0-6878.
7. Hong, F., Perrone, E., Mikhail, M., and Eltahan, A. (2017). Planning Pavement Maintenance and Rehabilitation Projects in the New Pavement Management System in Texas. proceedings of the 96th Transportation Research Board Annual Meeting, Washington D.C., Jan. 8-12, 2017.
8. A.T. Papagiannakis, M. Bracher, J. Li, and N. Jackson. (2006). Optimization of Traffic Data Collection for Specific Pavement Design Applications, FHWA-HRT-05-079.
9. Raheel, M., Khan, R., Khan, A., Khan, M. T., Ali, I., Alam, B., & Wali, B. (2018) Impact of axle overload, asphalt pavement thickness and subgrade modulus on load equivalency factor using modified ESALs equation, *Cogent Engineering*, Volume 5, 2018 - Issue 1.
10. Llopis-Castelló, D., García-Segura, T., Montalbán-Domingo, L., Sanz-Benlloch, A., & Pellicer, E. (2020). Influence of Pavement Structure, Traffic, and Weather on Urban Flexible Pavement Deterioration. *Sustainability* 2020, Vol. 12, Page 9717, 12(22), 9717.
11. Onayev, A., & Swei, O. (2021). IRI deterioration model for asphalt concrete pavements: capturing performance improvements over time. *Construction and Building Materials*, 271.

12. Yamany, M. & Abraham, D. (2020). Prediction of Pavement Performance using Non-homogeneous Markov Models: Incorporating the Impact of Preventive Maintenance.
13. Dong, Q., Huang, B., Richards, S.H., and Yan, X. (2013). Cost-Effectiveness Analyses of Maintenance Treatments for Low- and Moderate-Traffic Asphalt Pavements in Tennessee. *Journal of Transportation Engineering (ASCE)*, 2013, 139(8): 797-803.
14. Gong, H., Dong, Q., Huang, B., and Jia X. (2016). Effectiveness Analyses of Flexible Pavement Preventive Maintenance Treatments with LTPP SPS-3 Experiment Data. *Journal of Transportation Engineering (ASCE)*, 2016, 142(2): 04015045.
15. Vargas, A. (2018). PG Study – Performance of Southern Sections. Proceedings of the 2018 NCAT Pavement Test Track Conference, Auburn, AL, March 27-29, 2018.
16. Haider, S. W., and Dwaikat, M. B. (2011). Estimating optimum timing for preventive maintenance treatment to mitigate pavement roughness. *Transportation Research Record*, 2235(1), 43–53.
17. Labi, S., and Sinha, K. C. (2004). Effectiveness of highway pavement seal coating treatments. *Journal of Transportation Engineering* 10.1061/(ASCE)0733-947X (2004)130:1(14), 14–23.
18. Eltahan, A.A., Daleiden, J.F., and Simpson, A.L. (1999). Effectiveness of maintenance treatments of flexible pavements. *Transportation Research Record*, 1680(1), 18–25.
19. Shahin, M., Nunez, M., Broten, M., & Carpenter, S. (1987). New techniques for modeling pavement deterioration. *Transportation Research Record*. Issue Number: 1123.
20. Geoffrey, L., Labi, S., & Li, Z. (2008). Decision support for optimal scheduling of highway pavement preventive maintenance within resurfacing cycle. *Decision Support Systems*, 46(1), 376–387.
21. Faghri, A., & Hua, J. (1995). Roadway Seasonal Classification Using Neural Networks. *Journal of Computing in Civil Engineering*, 9(3), 209–215.
22. Rossi, R., Gastaldi, M., & Gecchele, G. (2014). Comparison of Clustering Methods for Road Group Identification in FHWA Traffic Monitoring Approach: Effects on AADT Estimates. *Journal of Transportation Engineering*, 140(7), 04014025.
23. “Traffic Survey GIS Data Products & Documents,” NCDOT, <https://connect.ncdot.gov/resources/State-Mapping/Pages/Traffic-Survey-GIS-Data.aspx>. Accessed 12/5/2021.
24. Chen, D. and Mastin, N. (2016). “Sigmoidal Models for Predicting Pavement Performance Conditions.” *Journal of Performance of Constructed Facilities*, ASCE, Vol. 30(4): 04015078.

25. NCDOT PAVEMENT DESIGN PROCEDURE AASHTO 1993 METHOD (2019), North Carolina Department of Transportation, Materials and Tests Unit – Pavement Section, January 4, 2019

Appendix A. Distress Model Curves

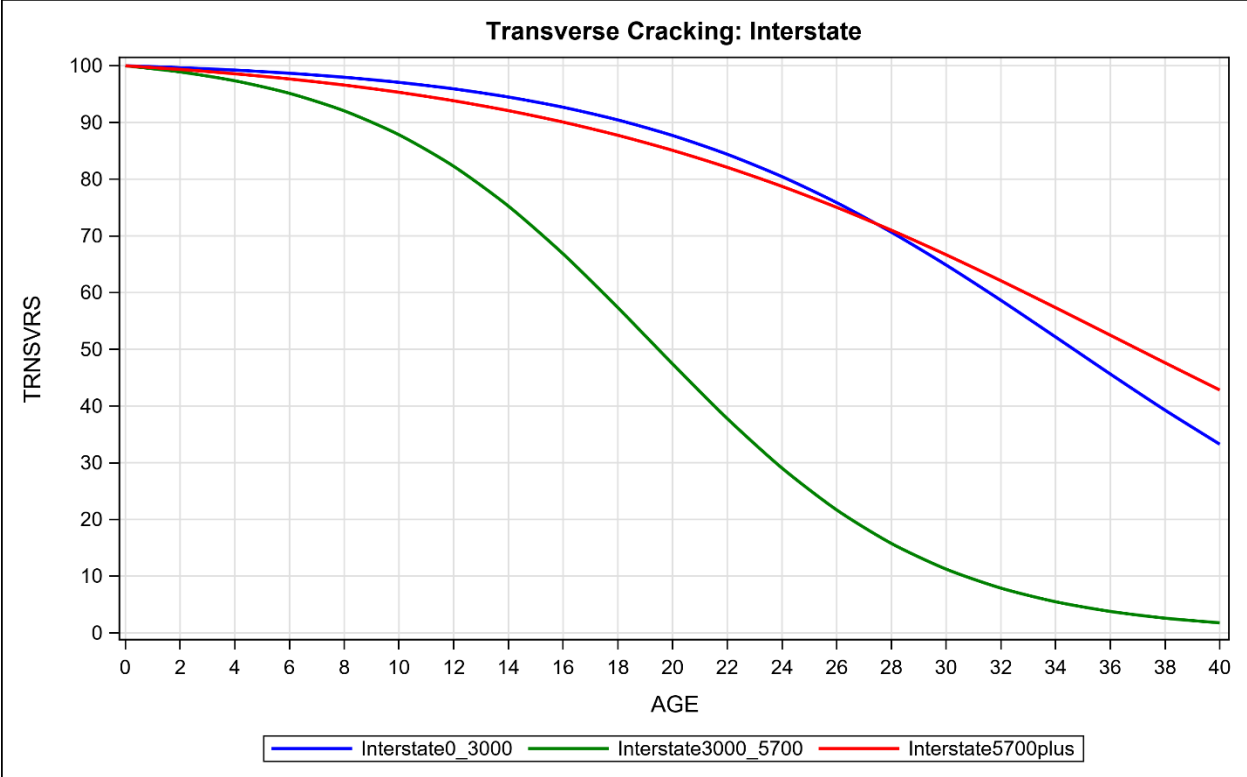


Figure A 1. Transverse Cracking: Interstate

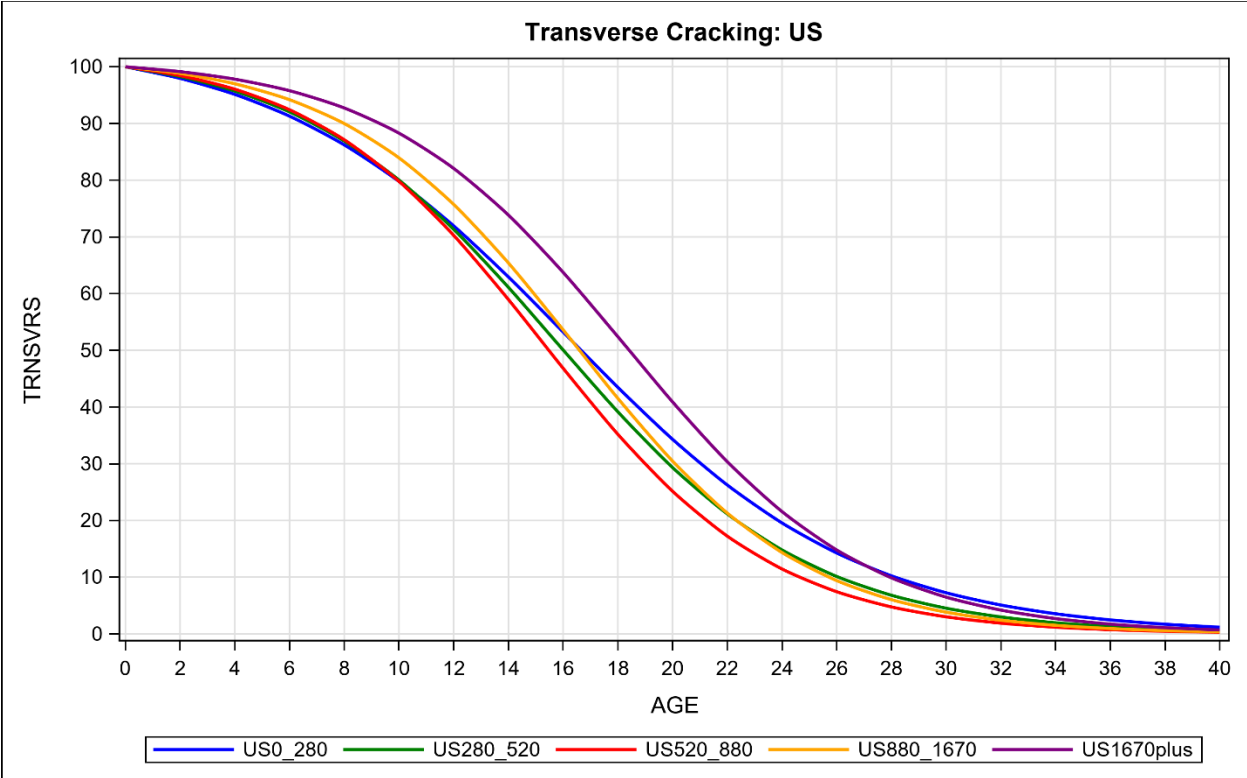


Figure A 2. Transverse Cracking: US

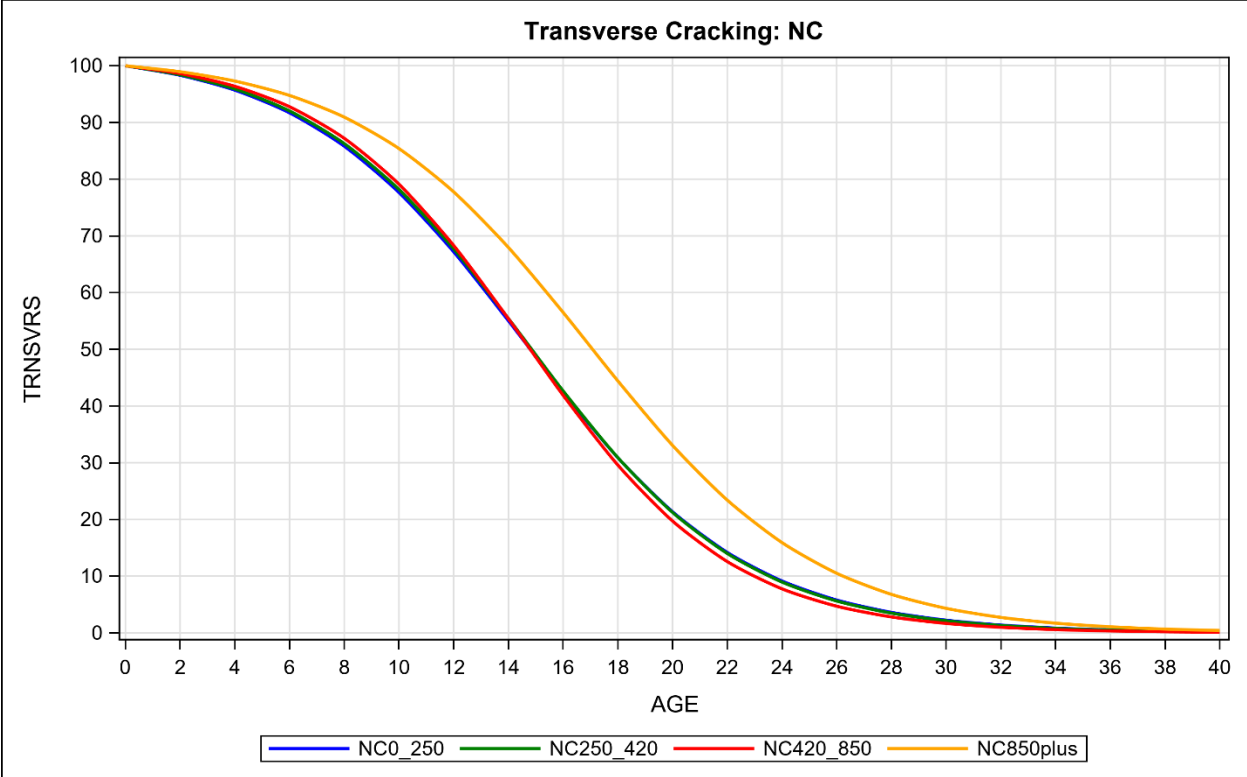


Figure A 3. Transverse Cracking: NC

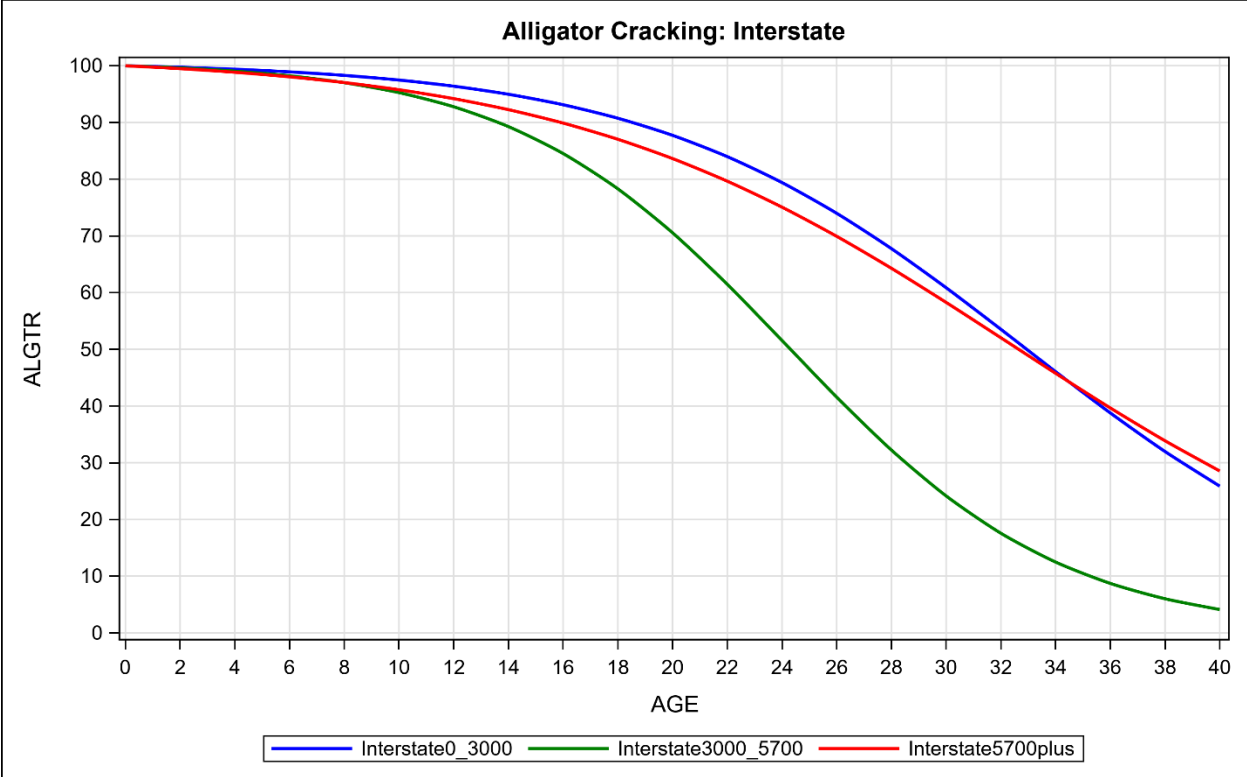


Figure A 4. Alligator Cracking: Interstate

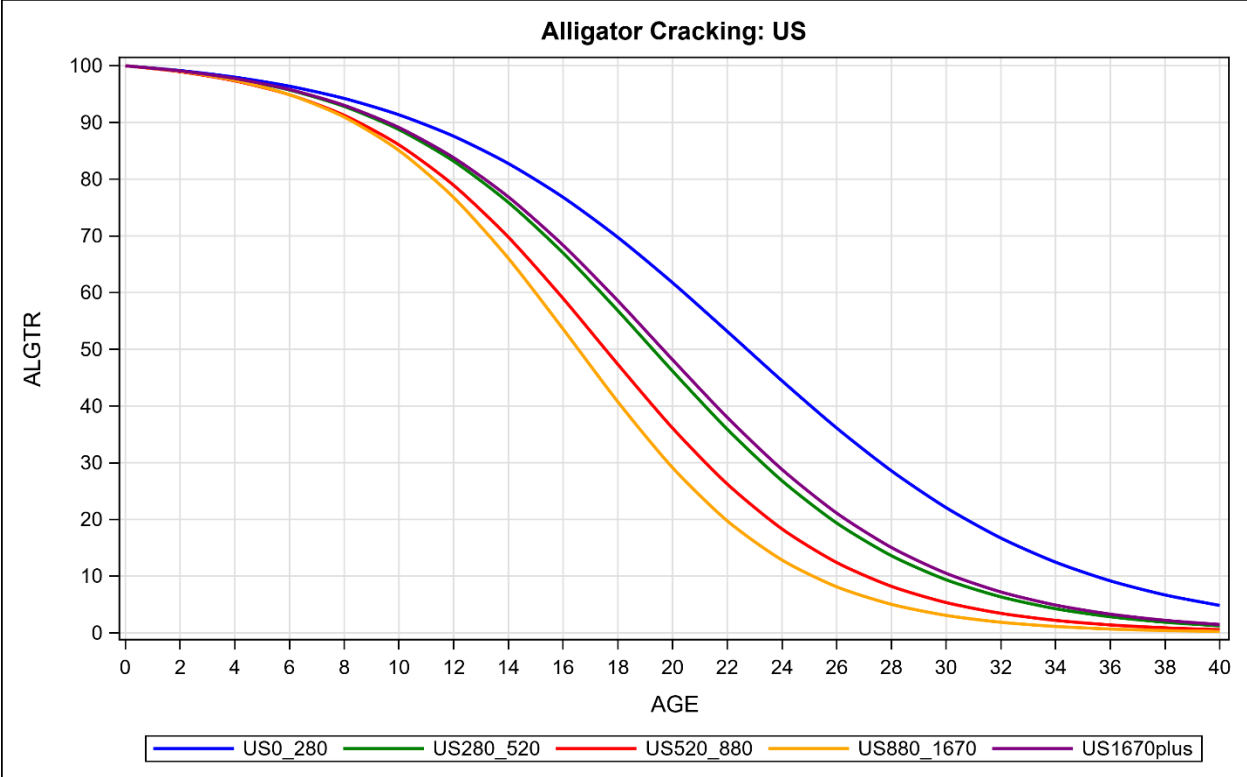


Figure A 5. Alligator Cracking: US

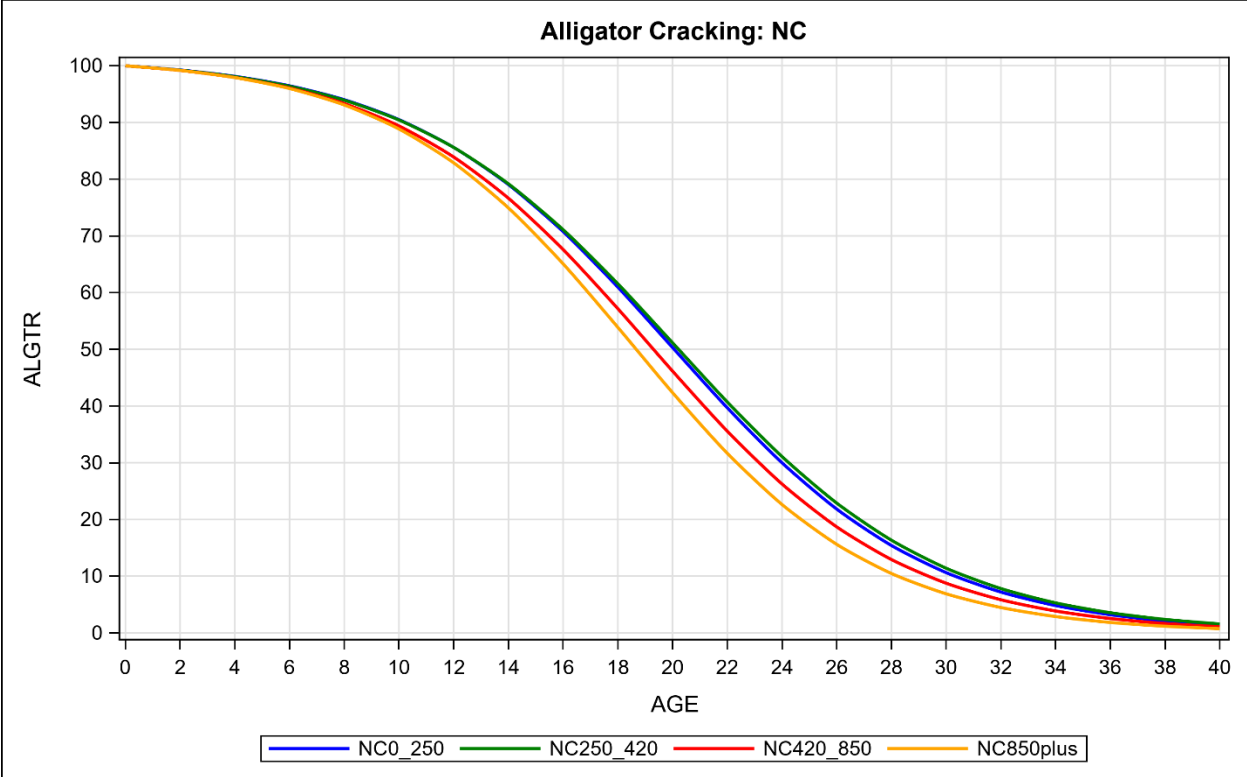


Figure A 6. Alligator Cracking: NC

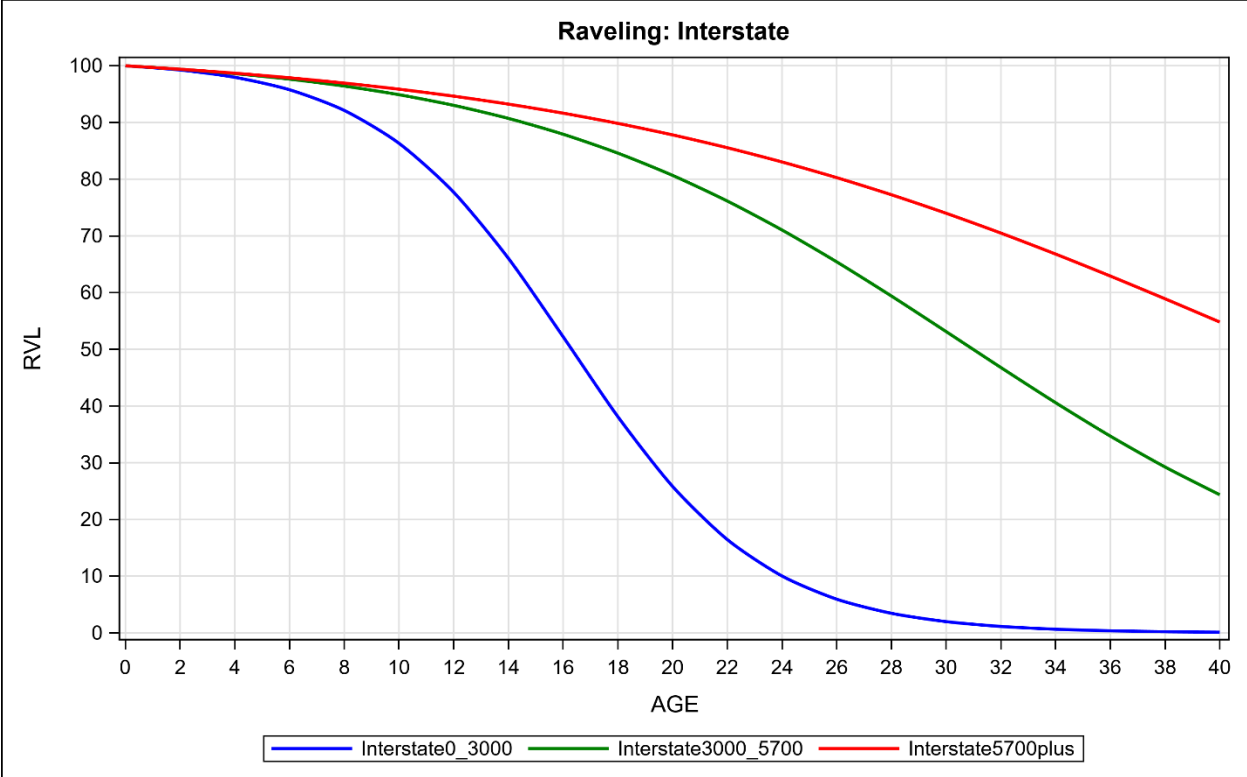


Figure A 7. Raveling: Interstate

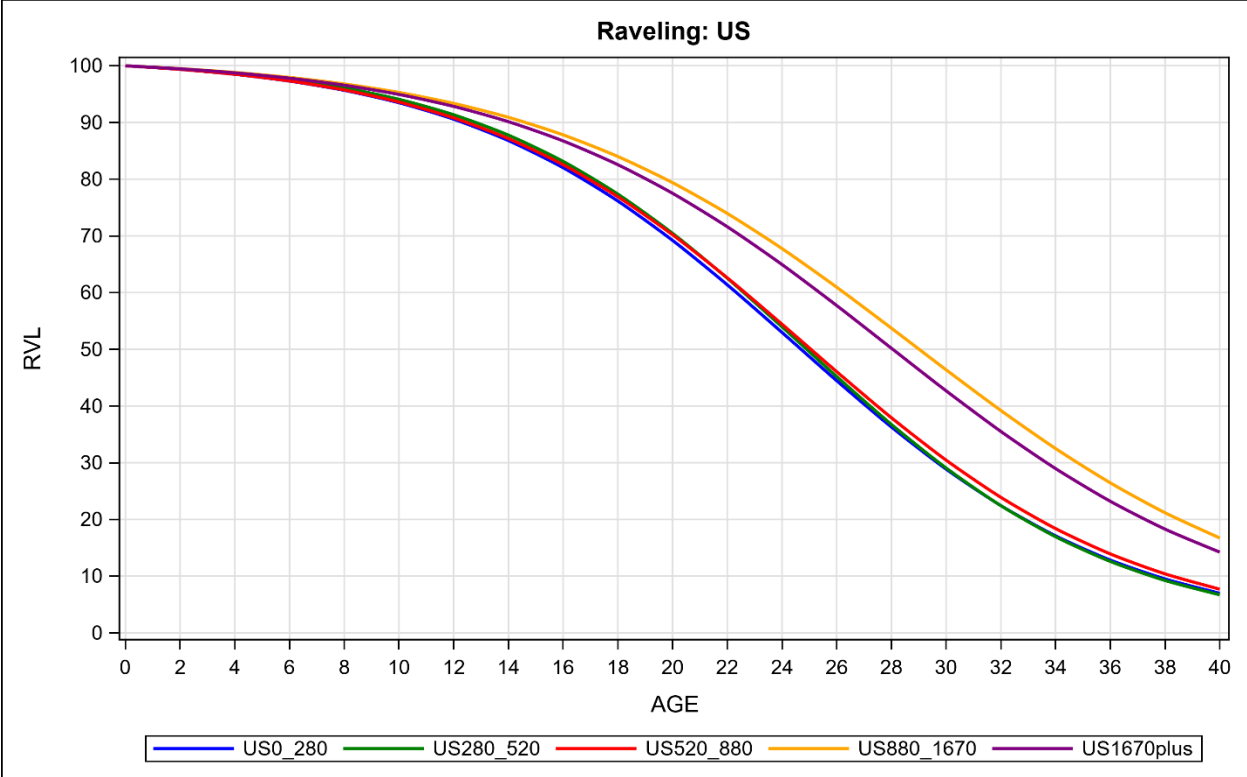


Figure A 8. Raveling: US

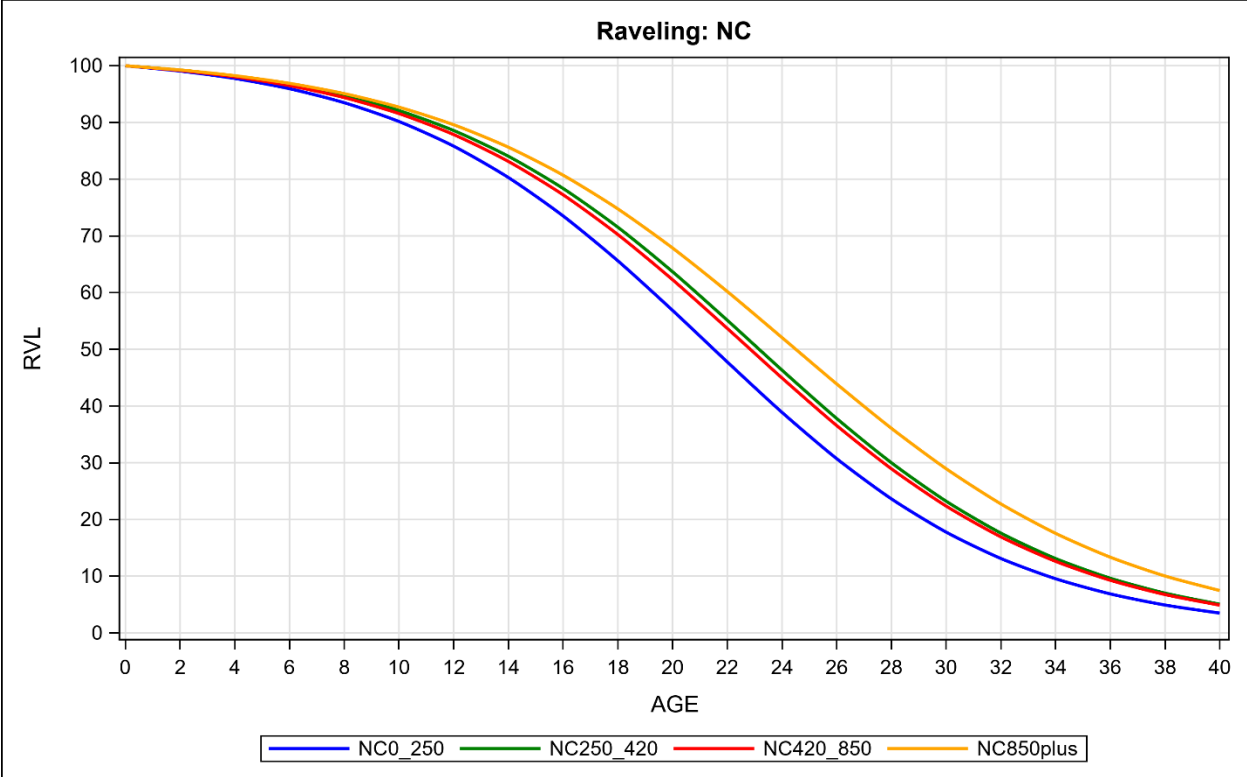


Figure A 9. Raveling: NC

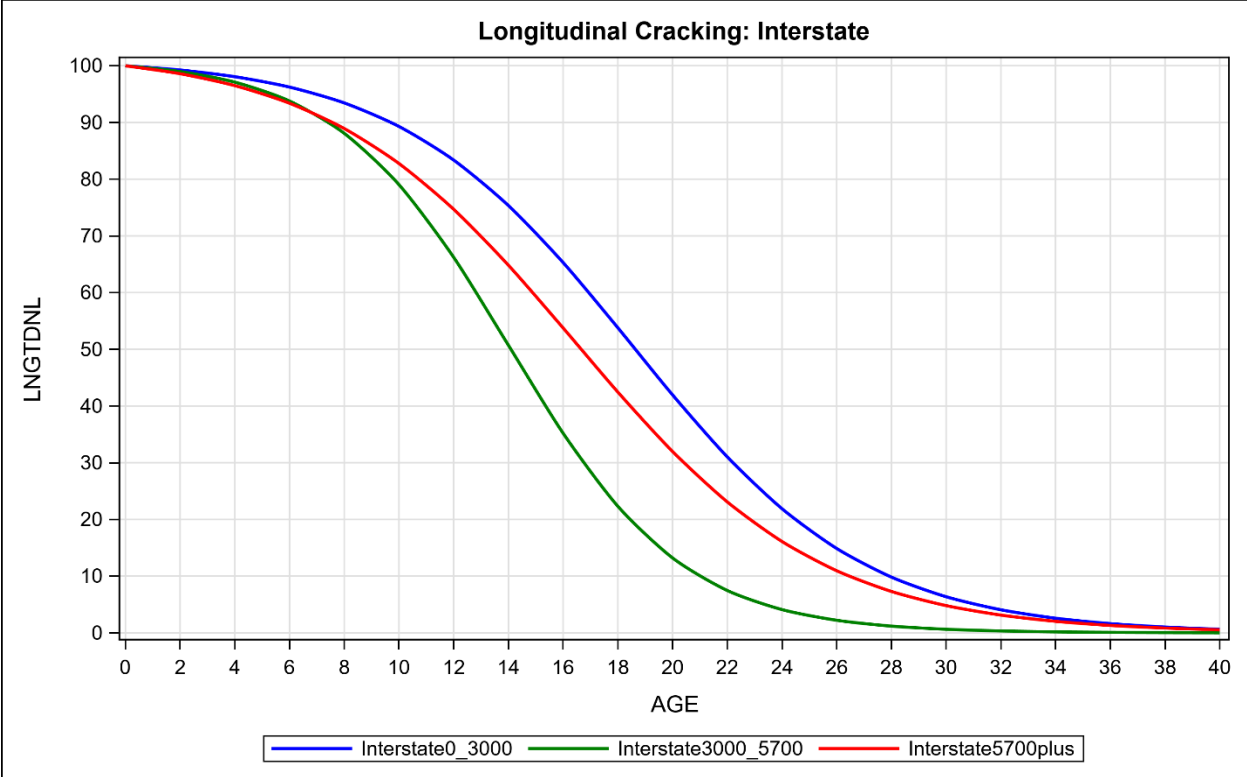


Figure A 10. Longitudinal Cracking: Interstate

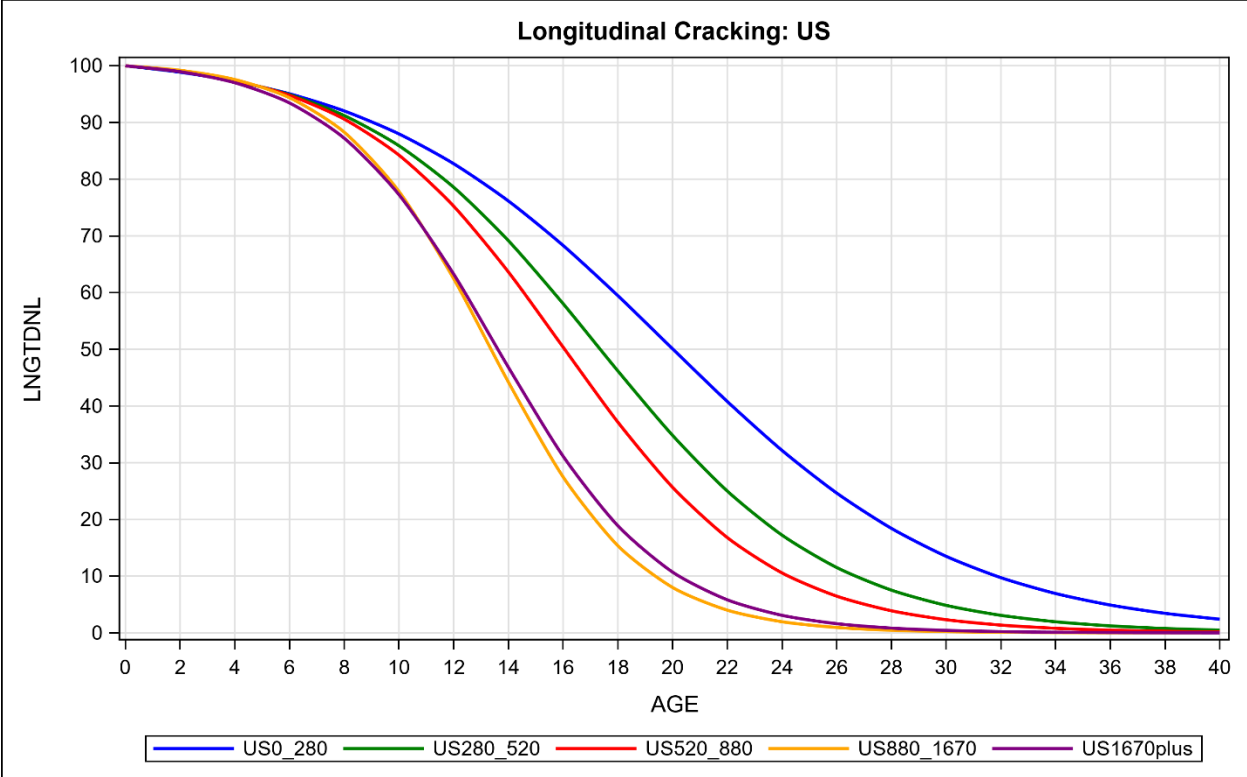


Figure A 11. Longitudinal Cracking: US

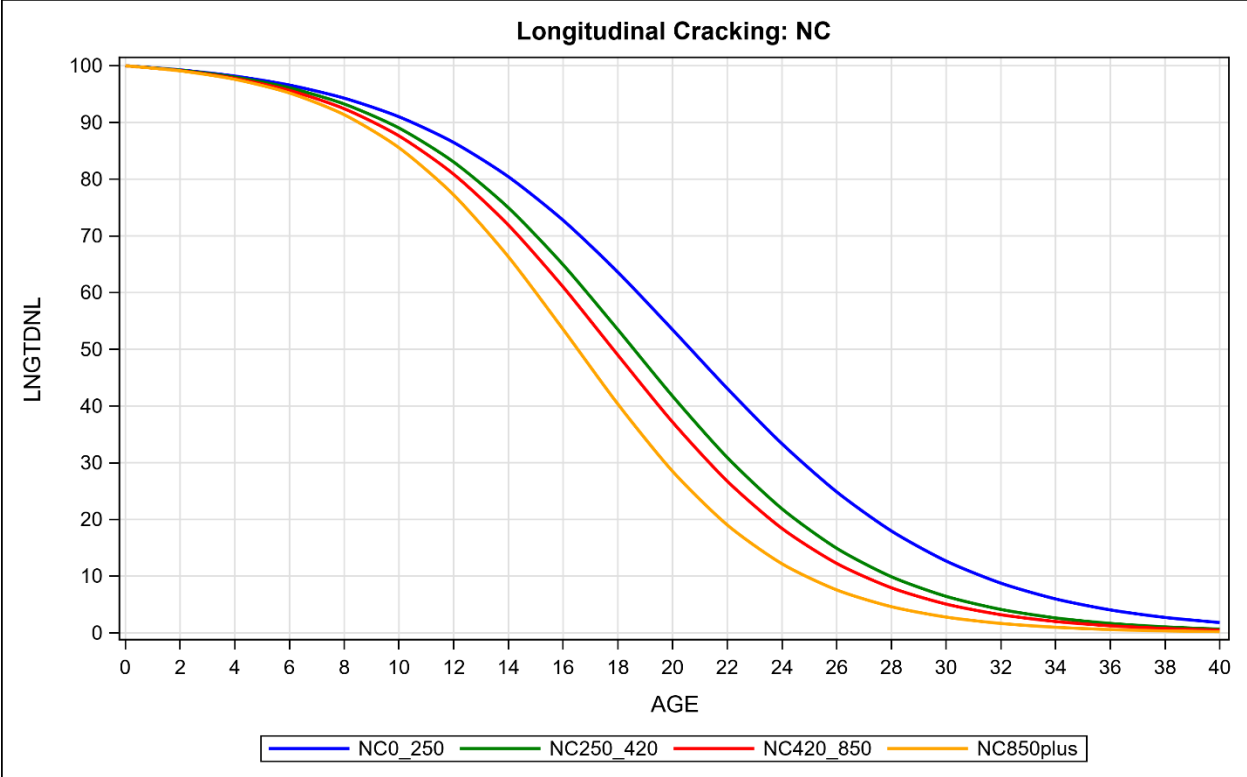


Figure A 12. Longitudinal Cracking: NC

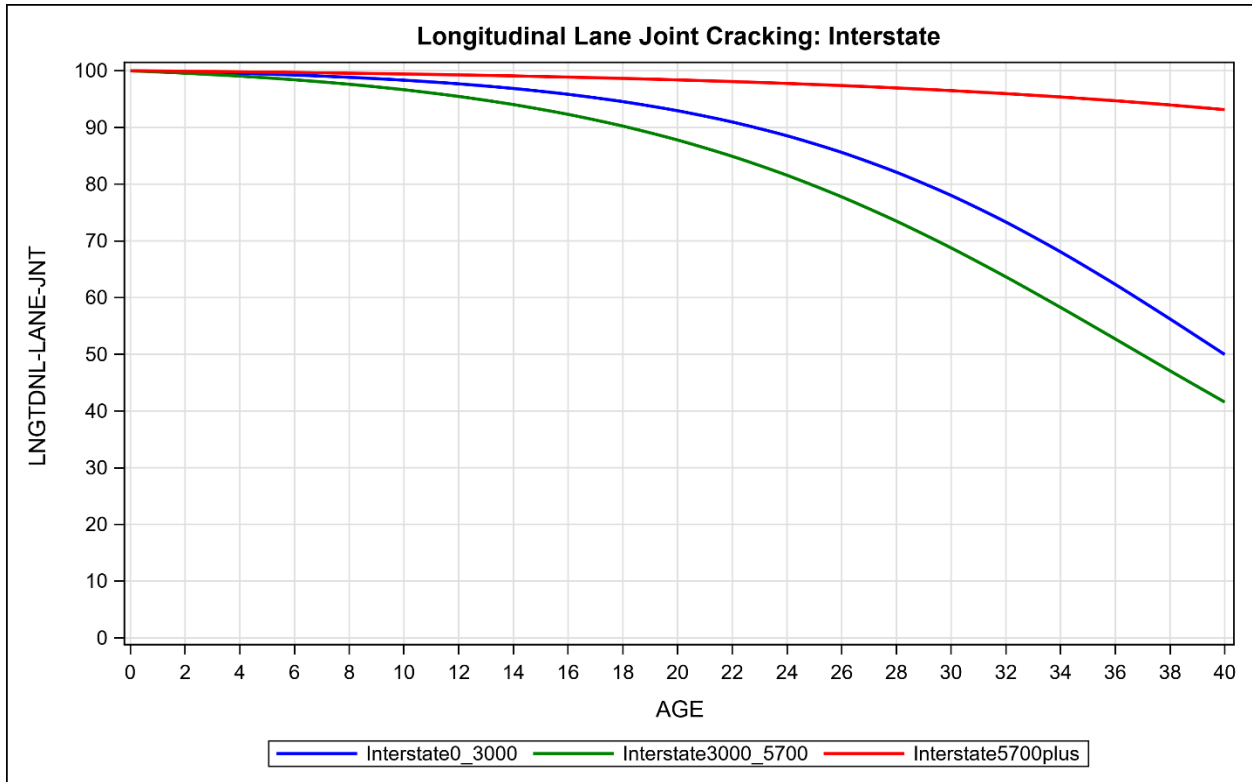


Figure A 13. Longitudinal Lane Joint Cracking: Interstate

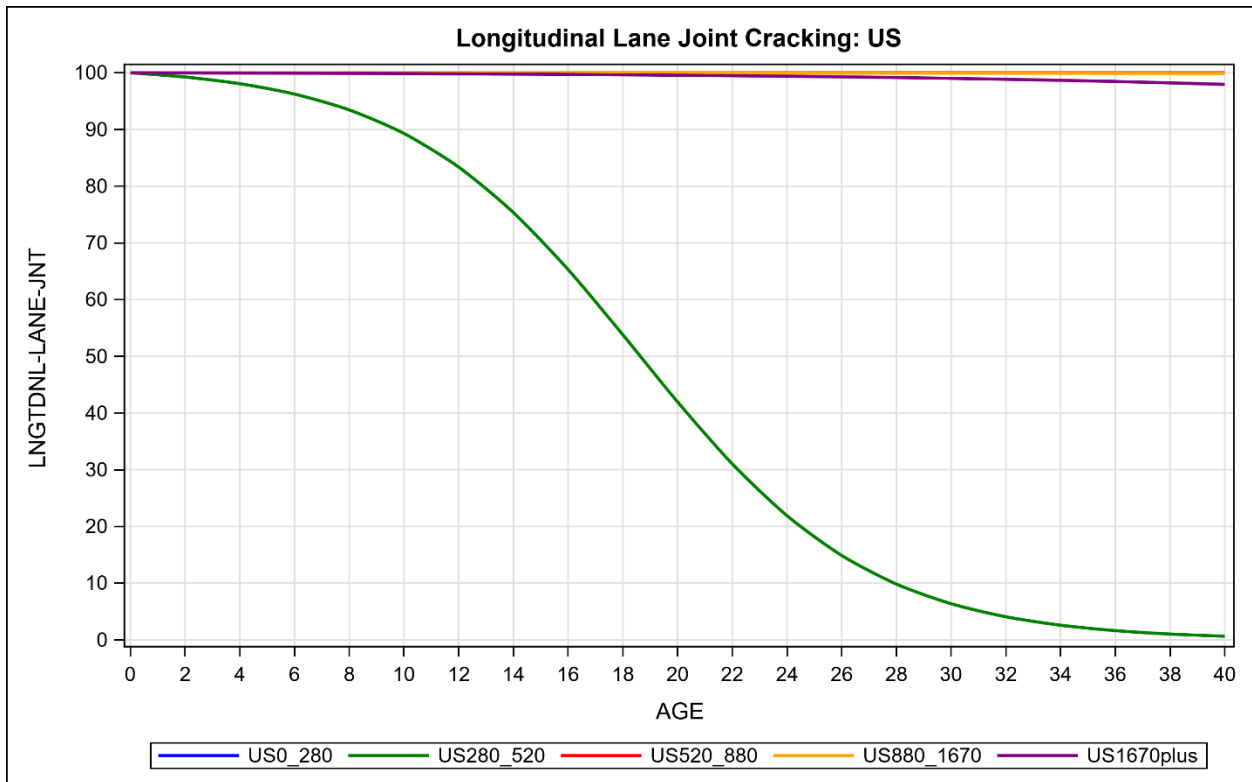


Figure A 14. Longitudinal Lane Joint Cracking: US

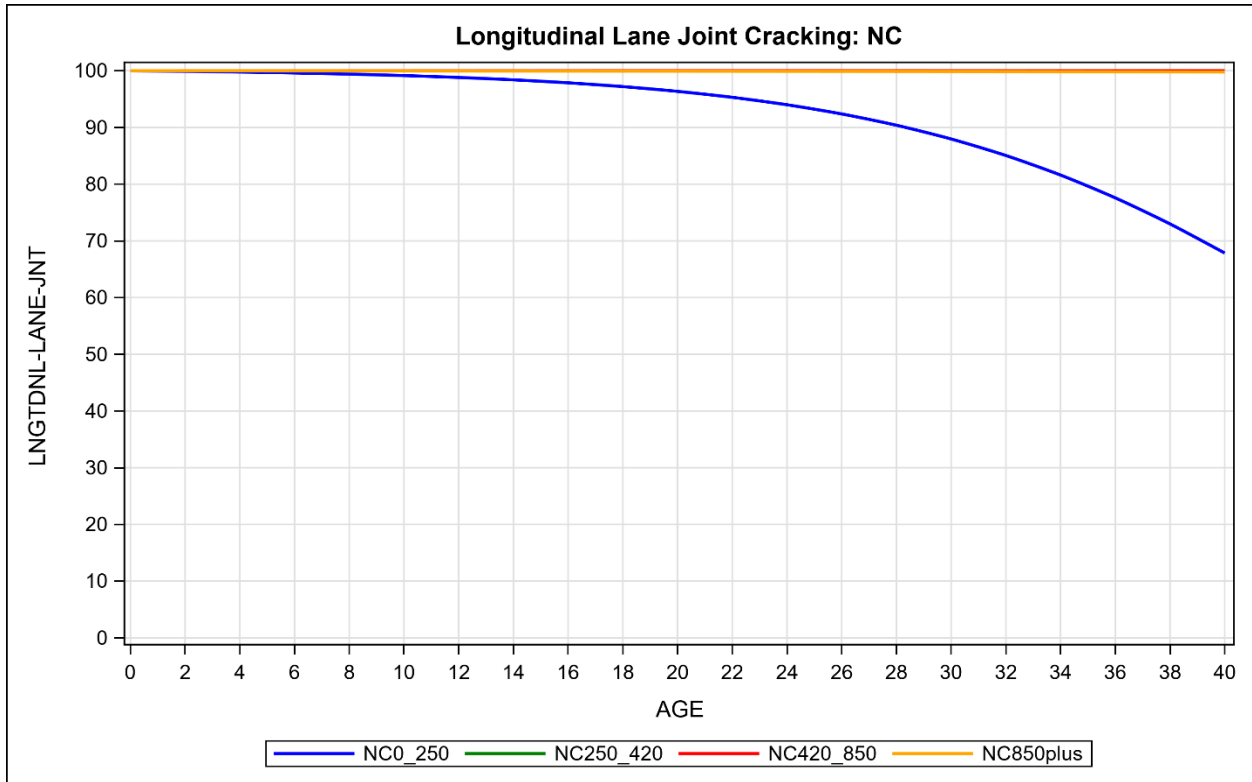


Figure A 15. Longitudinal Lane Joint Cracking: NC

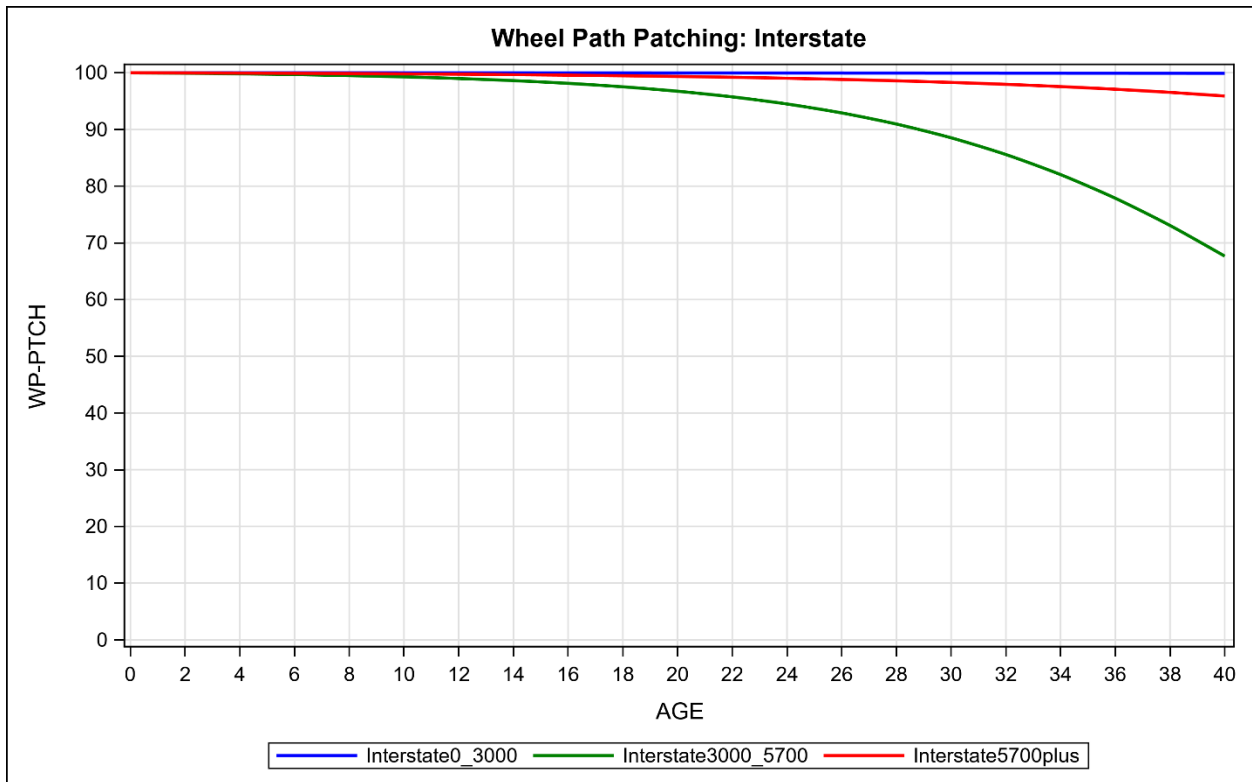


Figure A 16. Wheel Path Patching: Interstate

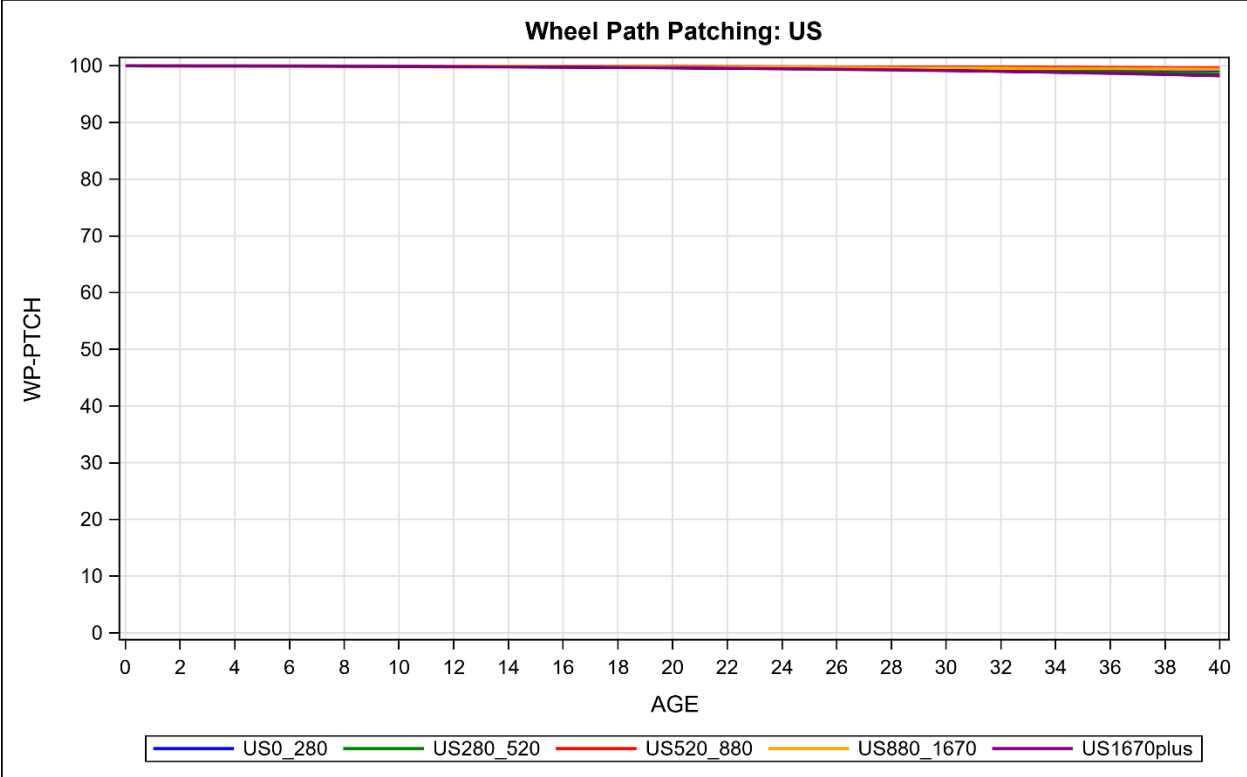


Figure A 17. Wheel Path Patching: US

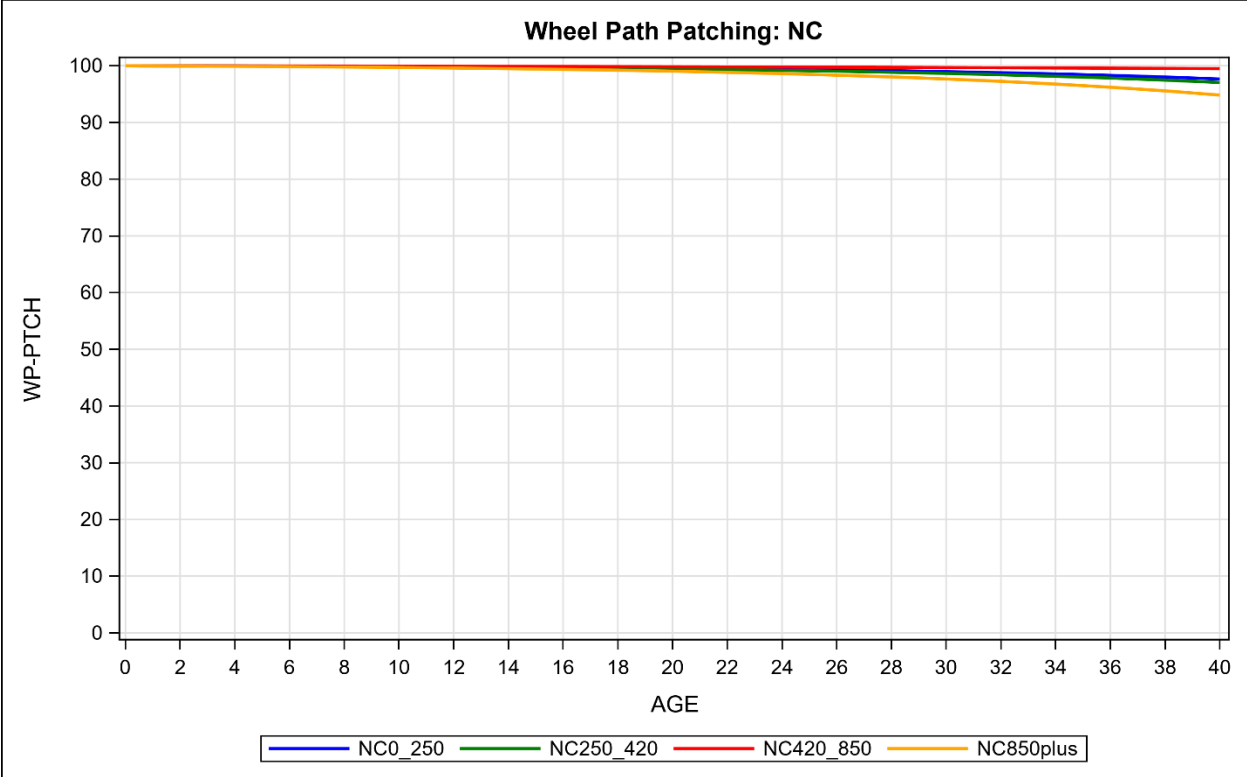


Figure A 18. Wheel Path Patching: NC

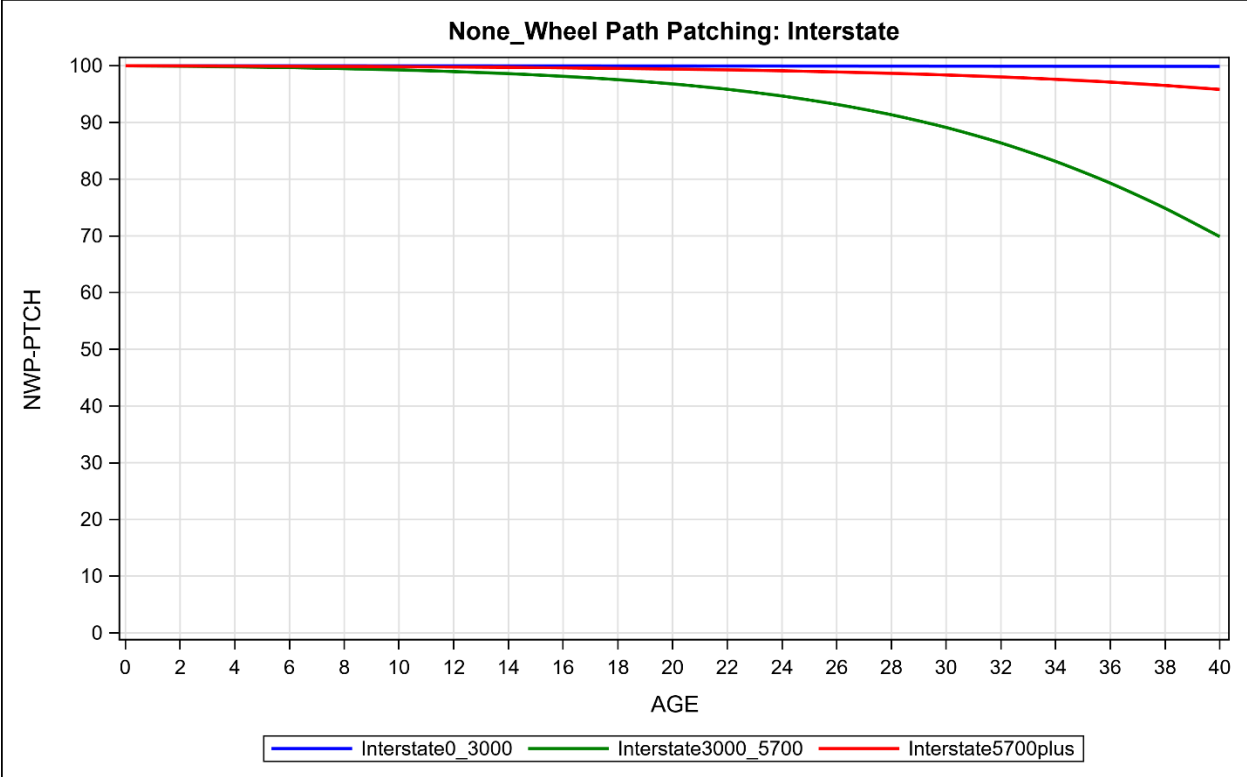


Figure A 19. Non-Wheel Path Patching: Interstate

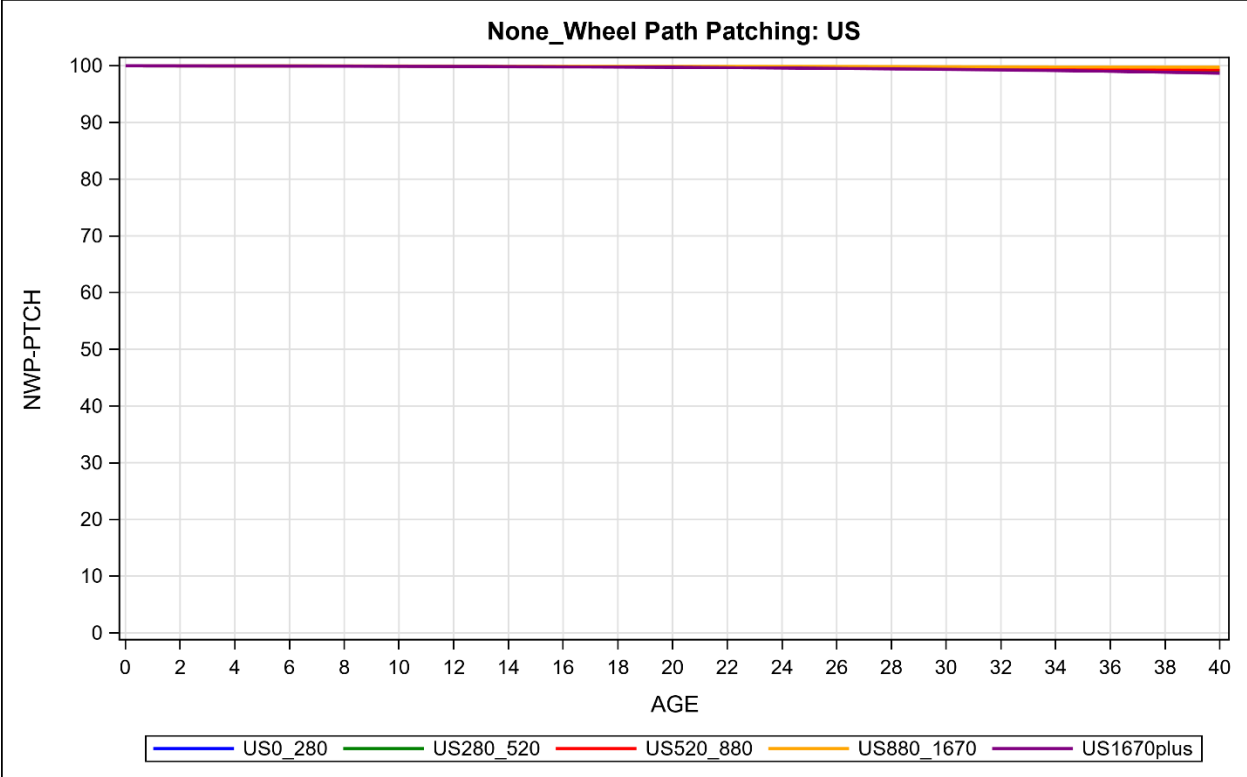


Figure A 20. Non-Wheel Path Patching: US

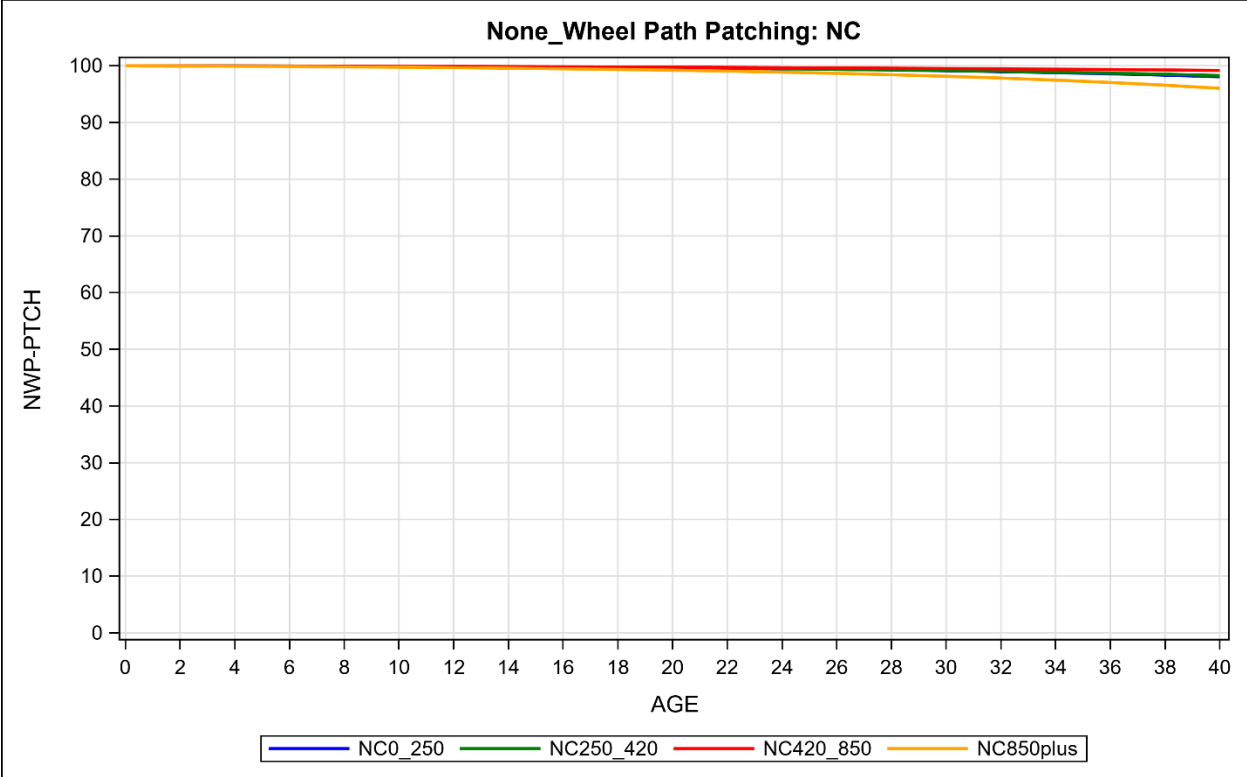


Figure A 21. Non-Wheel Path Patching: NC

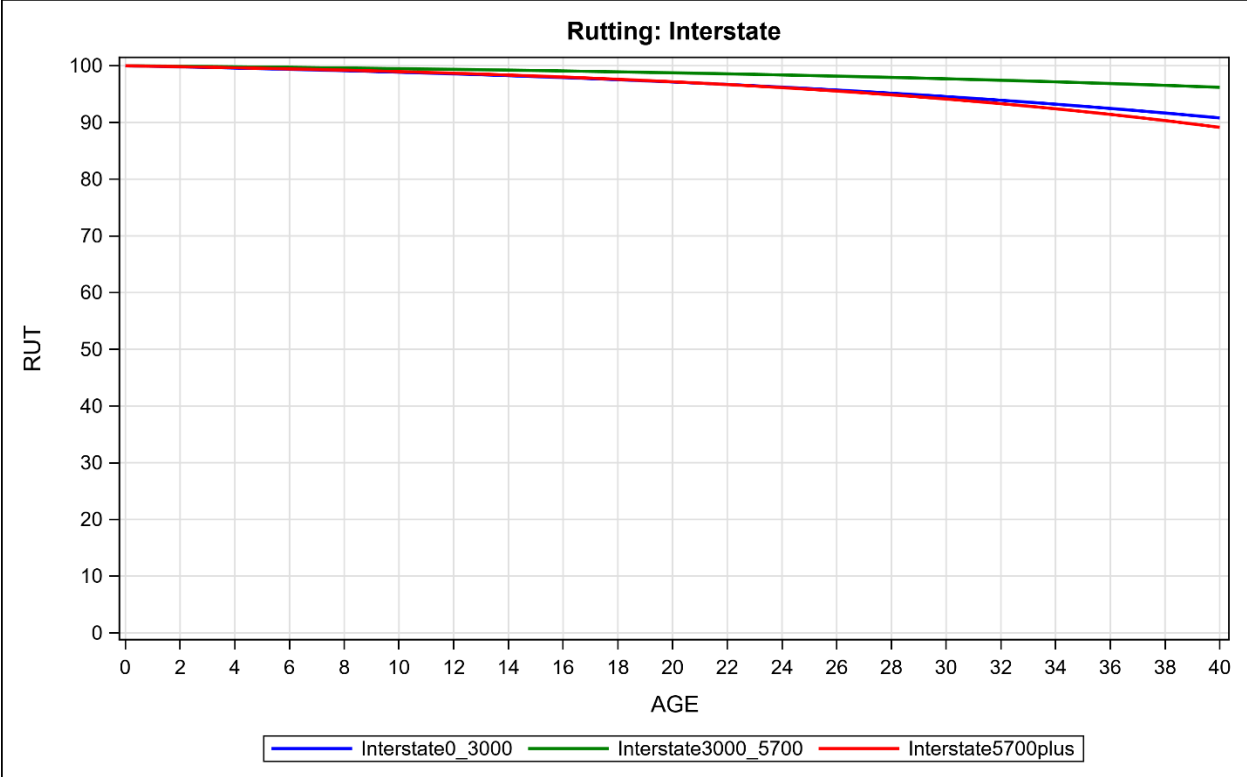


Figure A 22. Rutting: Interstate

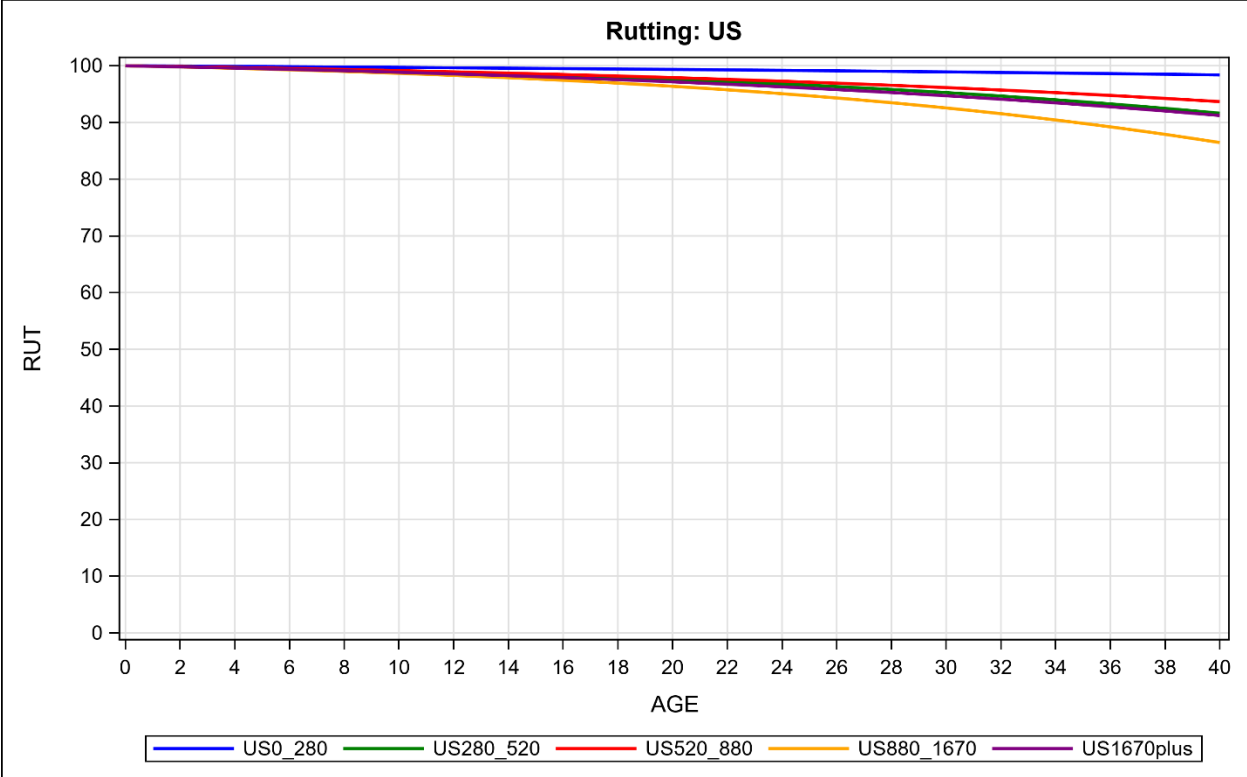


Figure A 23. Rutting: US

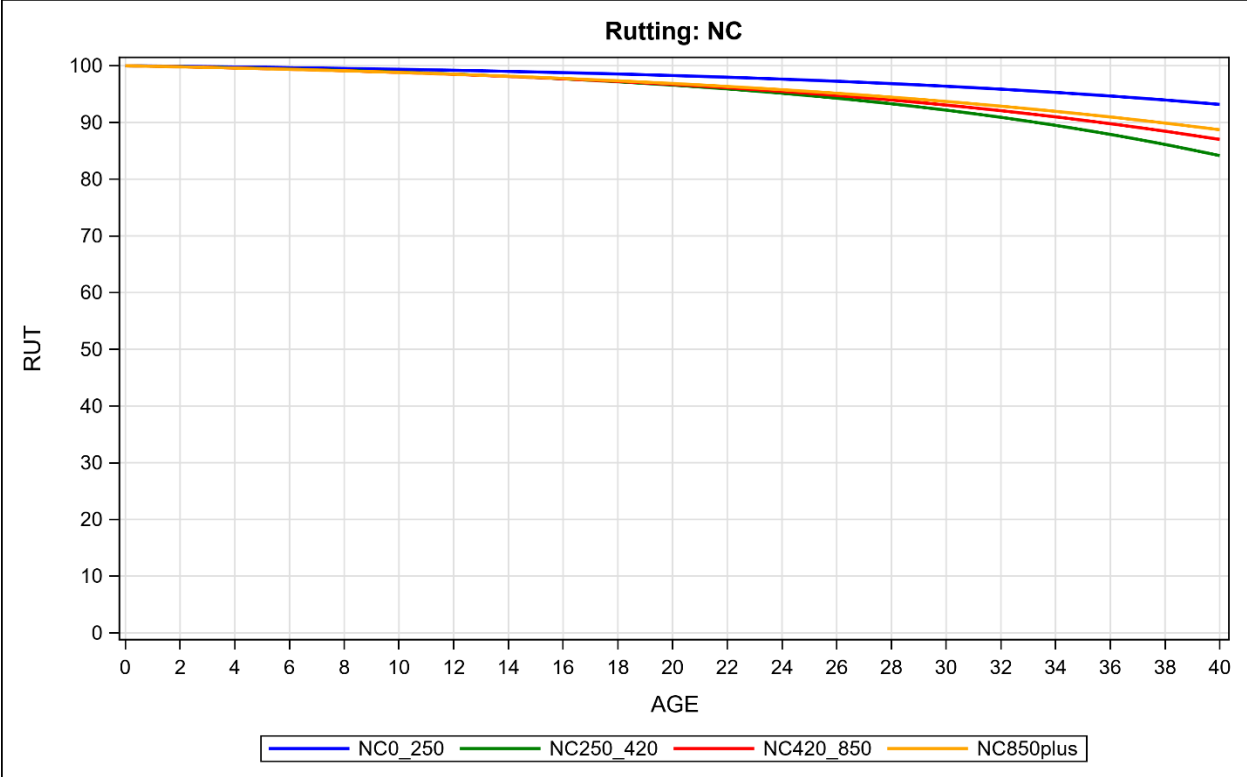


Figure A 24. Rutting: NC

Appendix B. Performance Model Curves

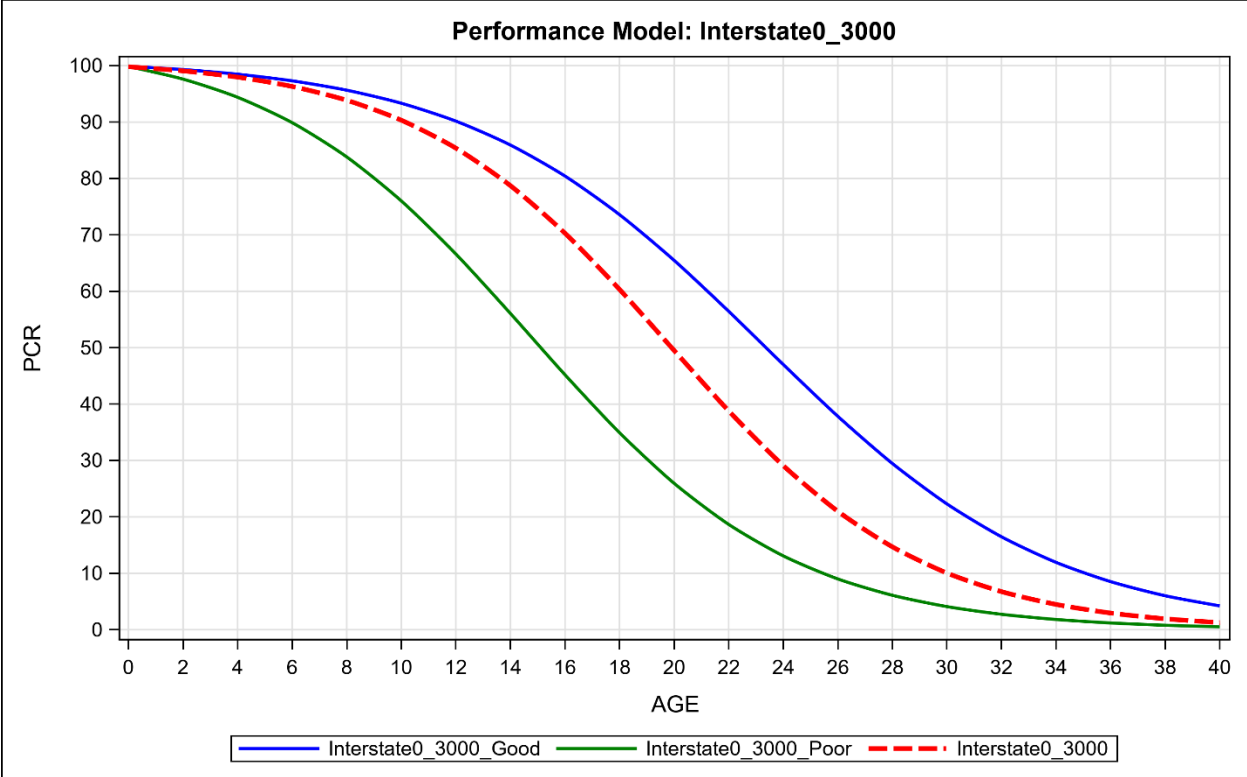


Figure B 1. Performance Model: Interstate0_3000

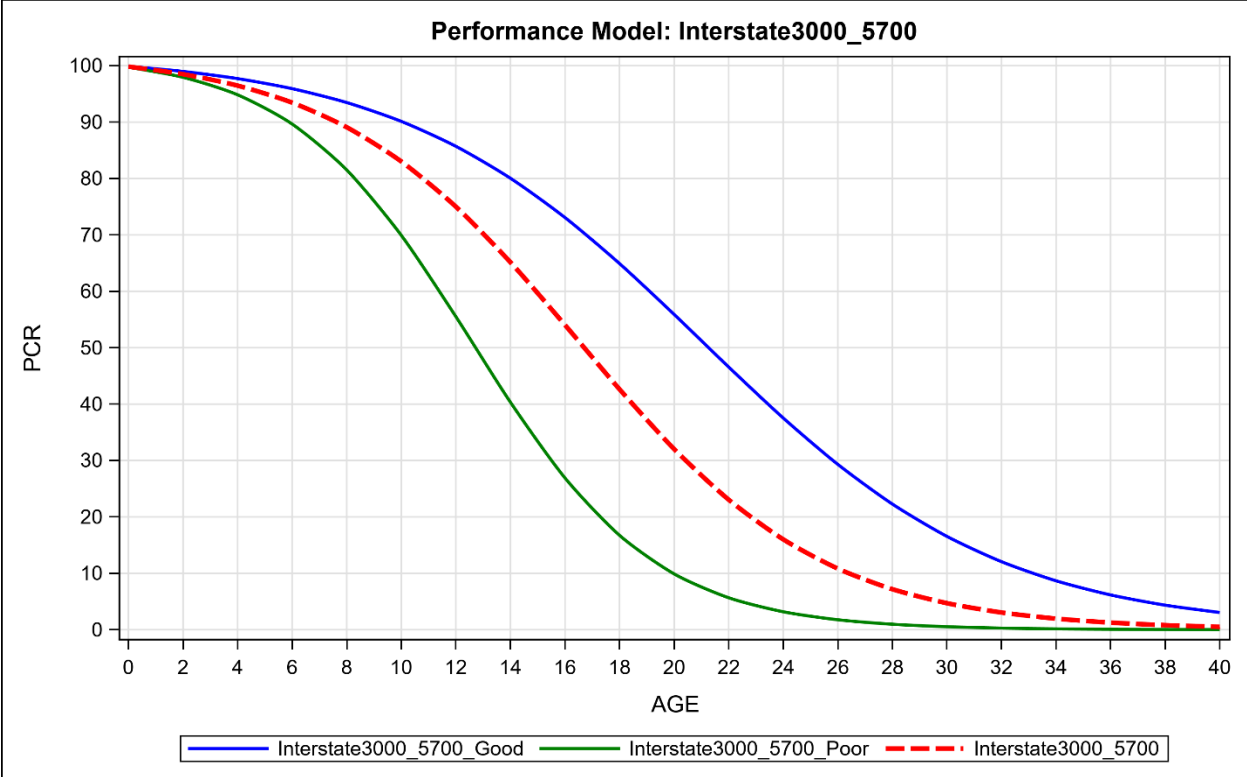


Figure B 2. Performance Model: Interstate3000_5700



Figure B 3. Performance Model: Interstate5700plus

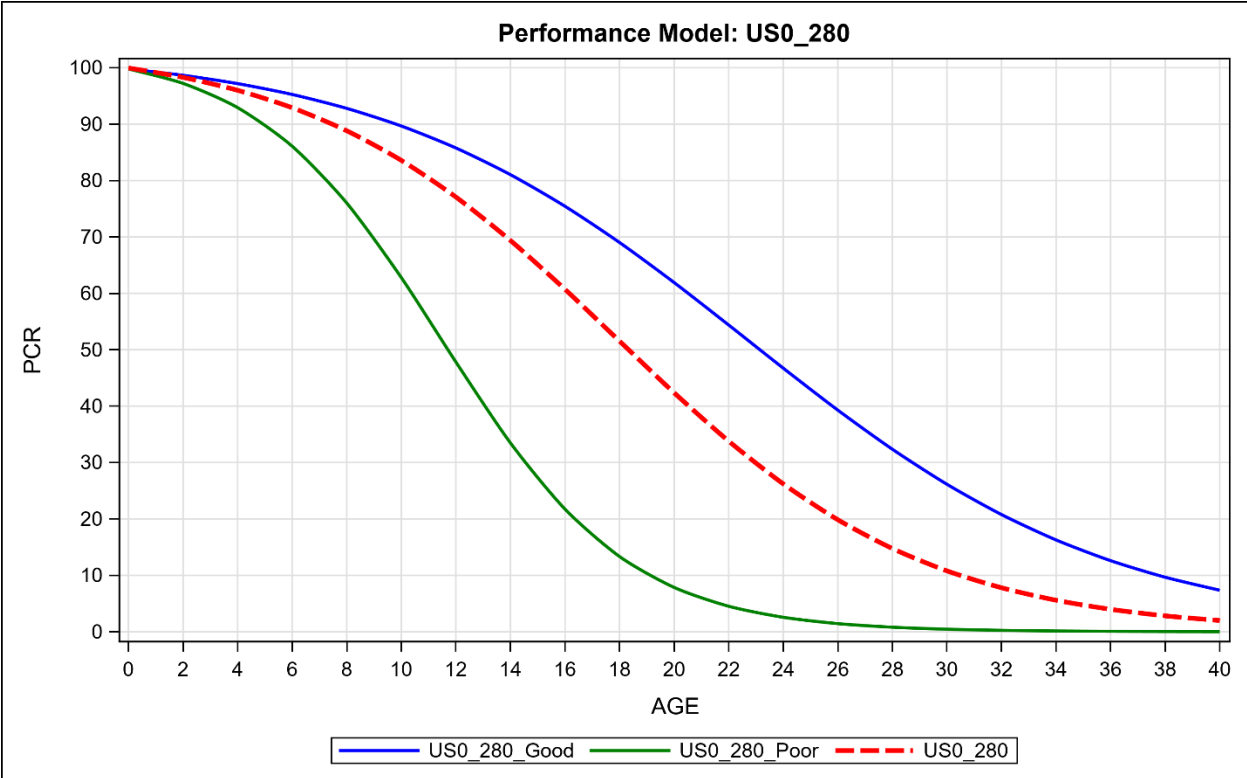


Figure B 4. Performance Model: US0_280

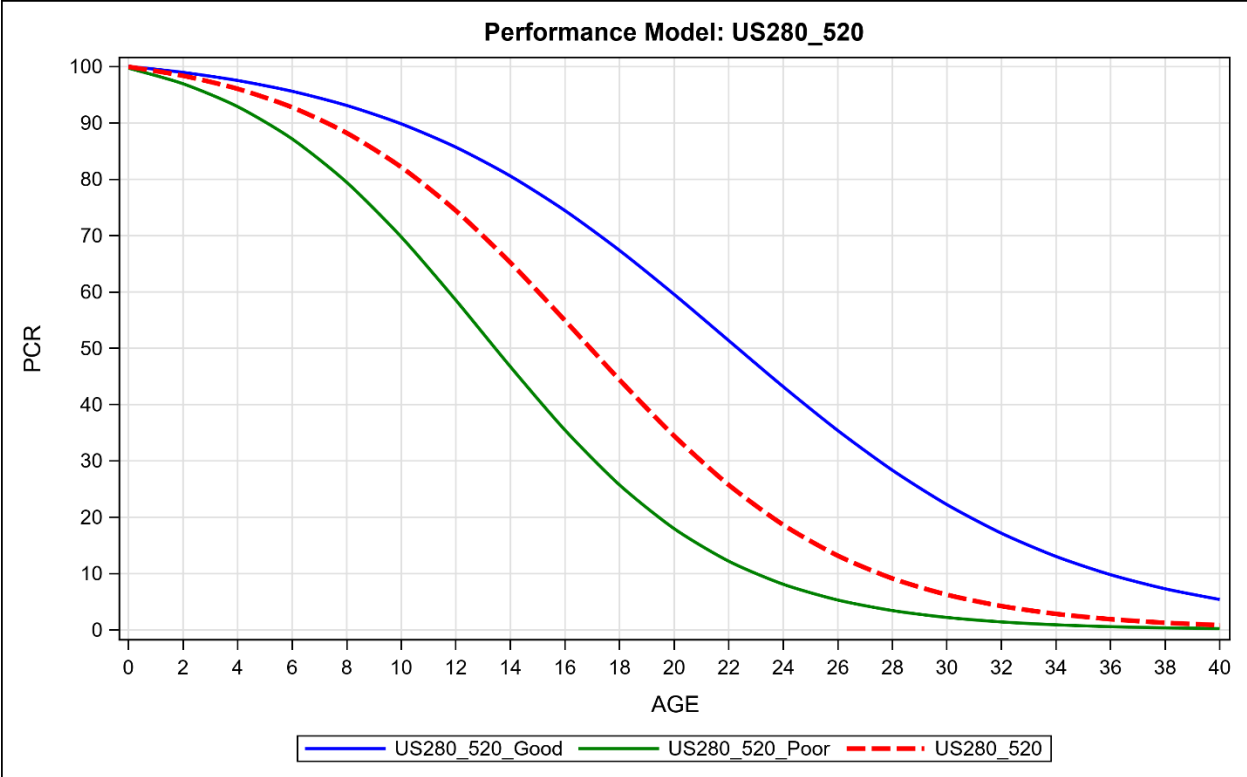


Figure B 5. Performance Model: US280_520

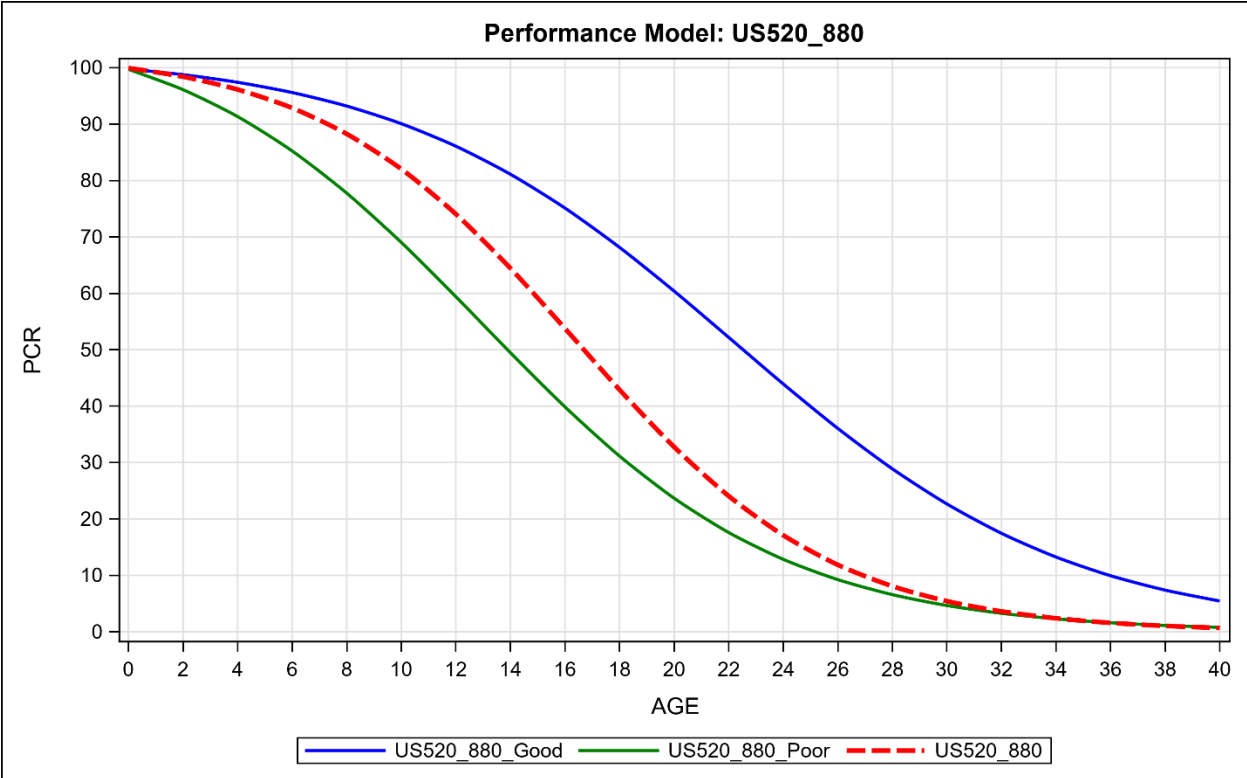


Figure B 6. Performance Model: US520_880

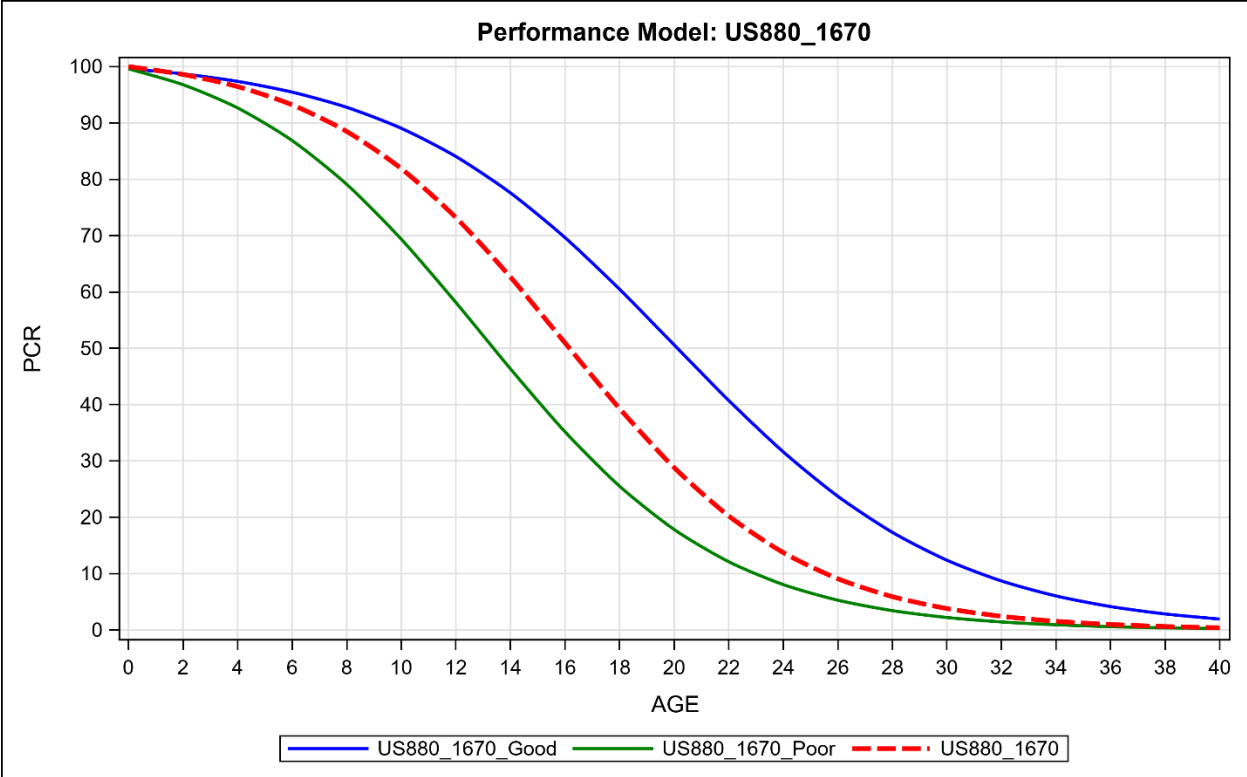


Figure B 7. Performance Model: US880_1670

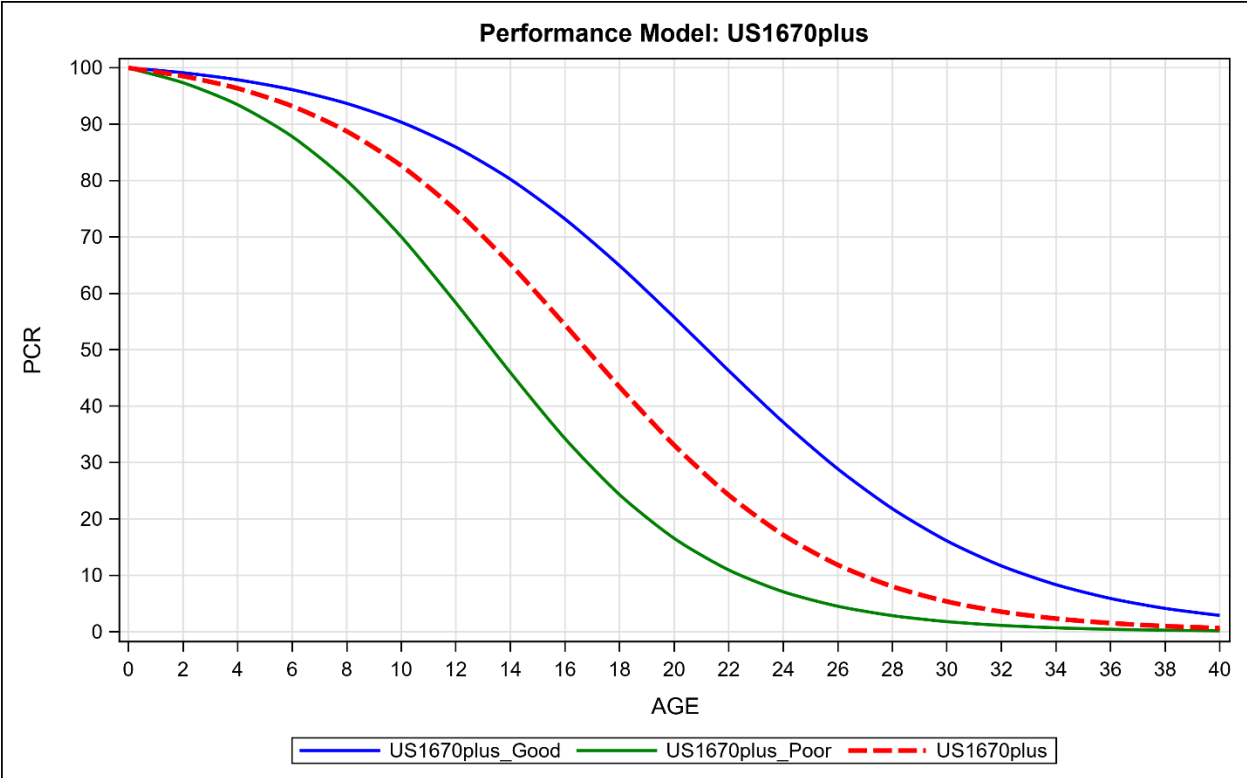


Figure B 8. Performance Model: US1670plus

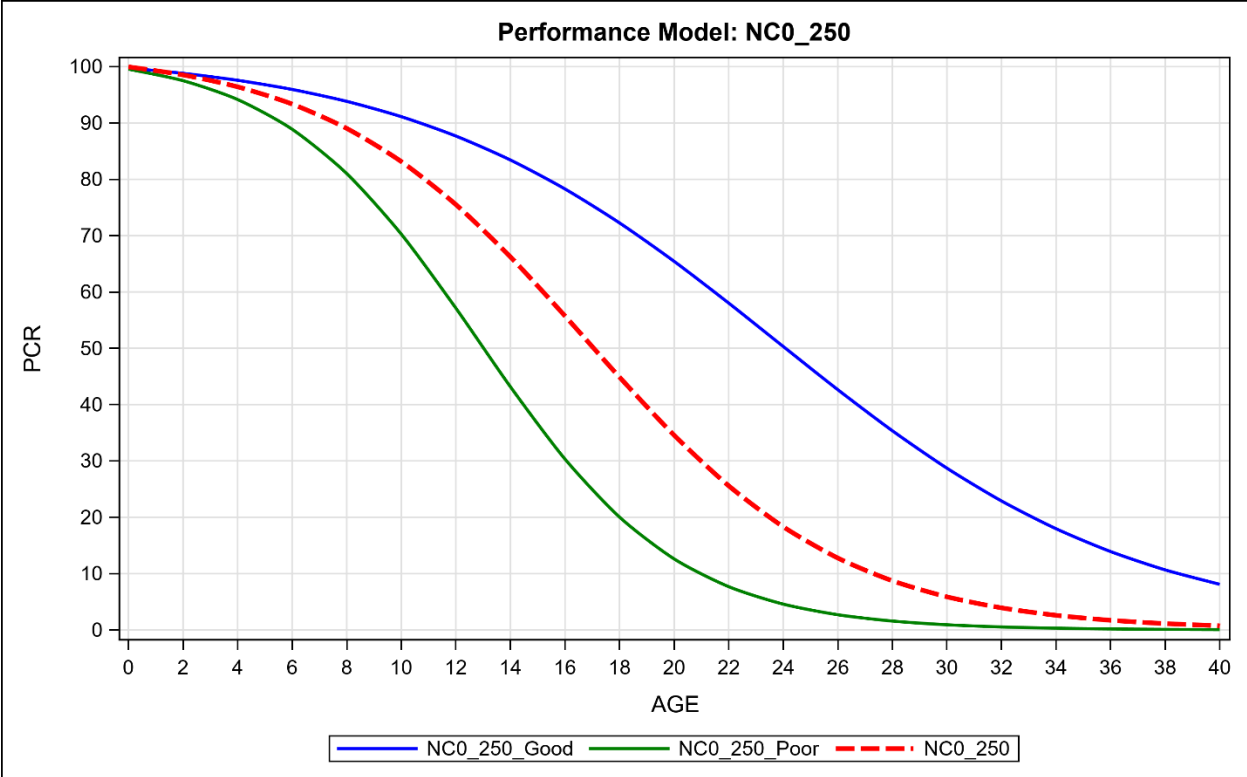


Figure B 9. Performance Model: NC0_250

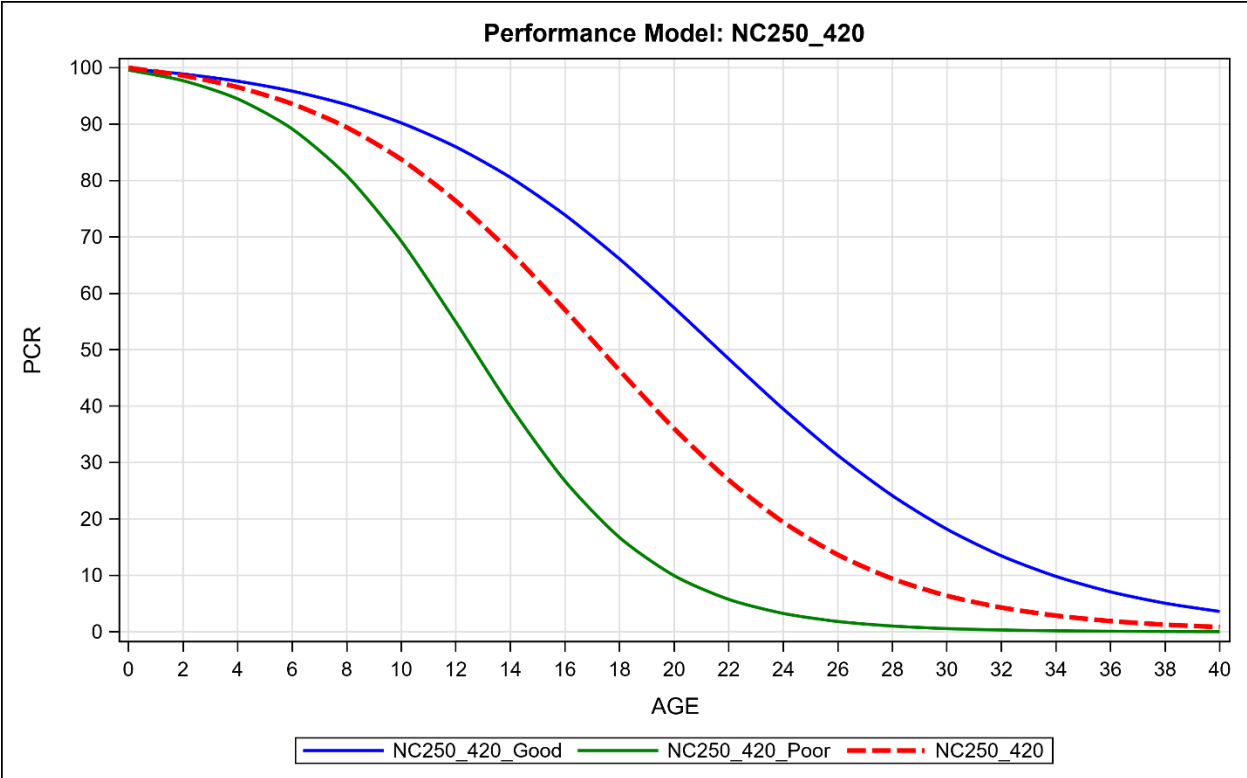


Figure B 10. Performance Model: NC250_420

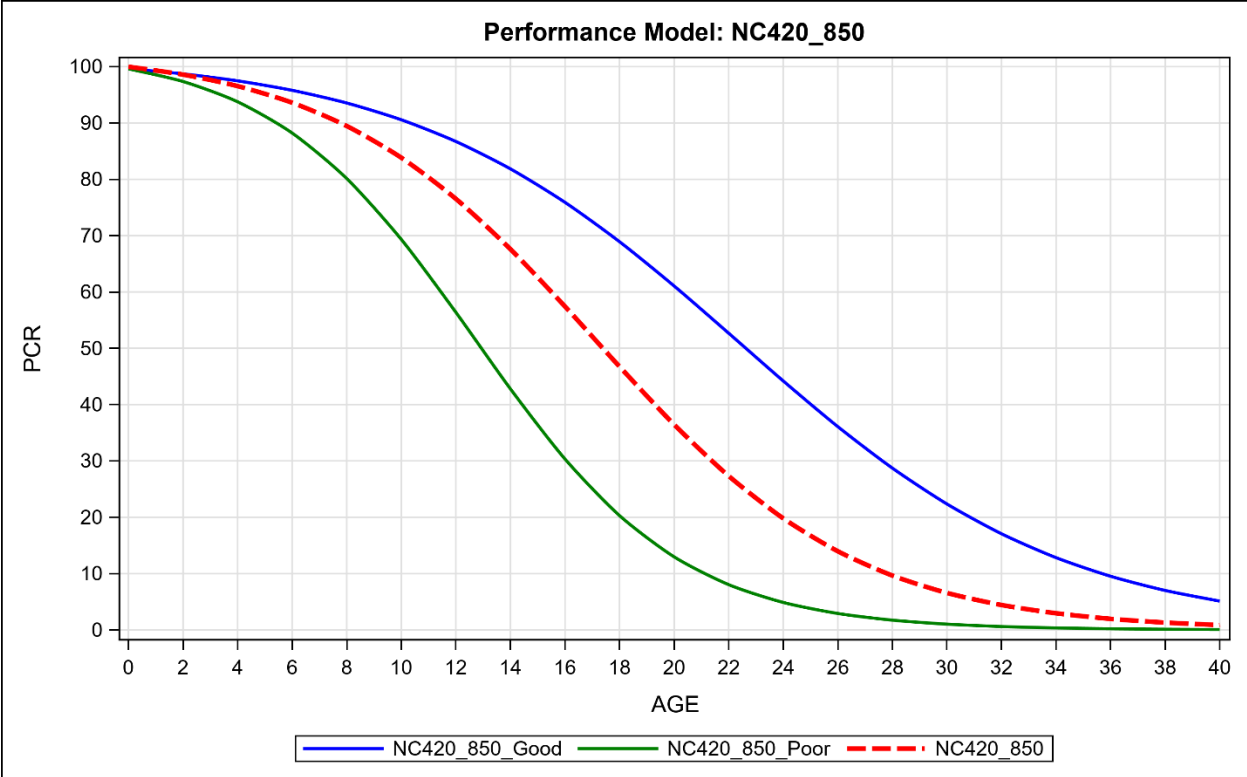


Figure B 11. Performance Model: NC420_850

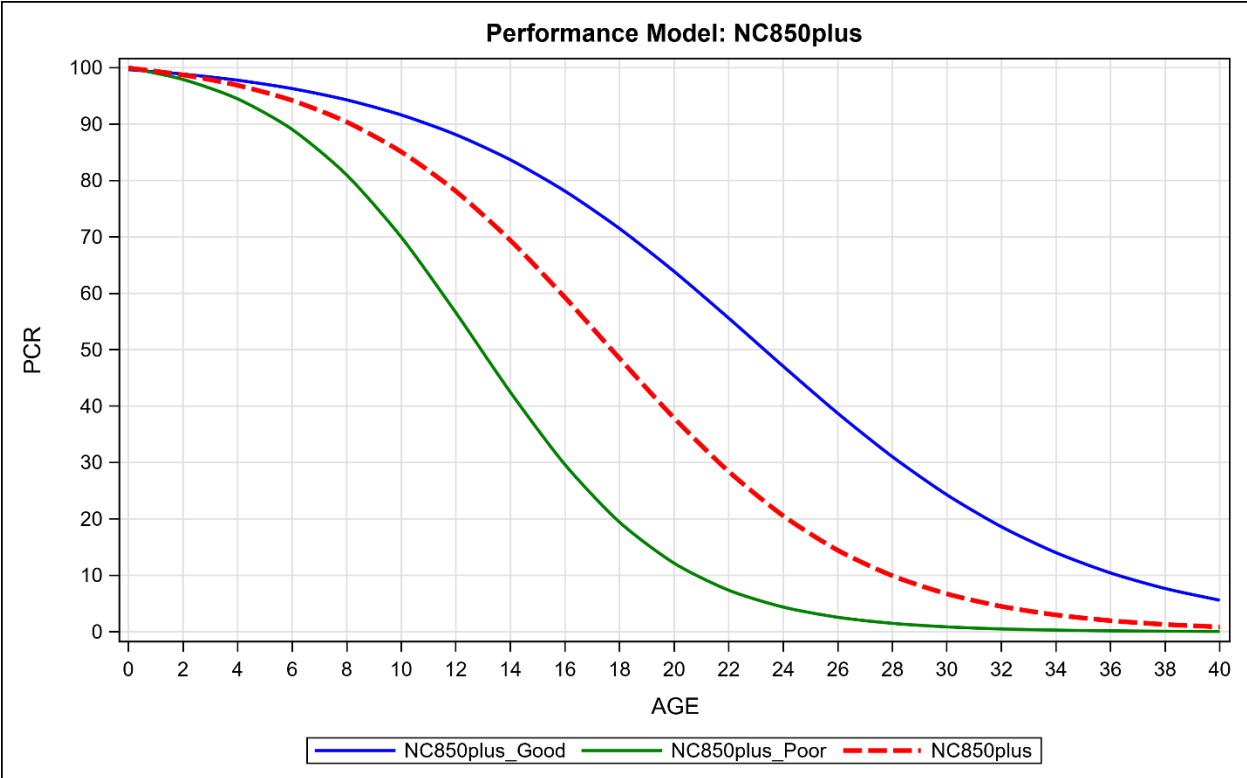


Figure B 12. Performance Model: NC850plus

Appendix C. AADT vs. AADTT Distress Model Curves

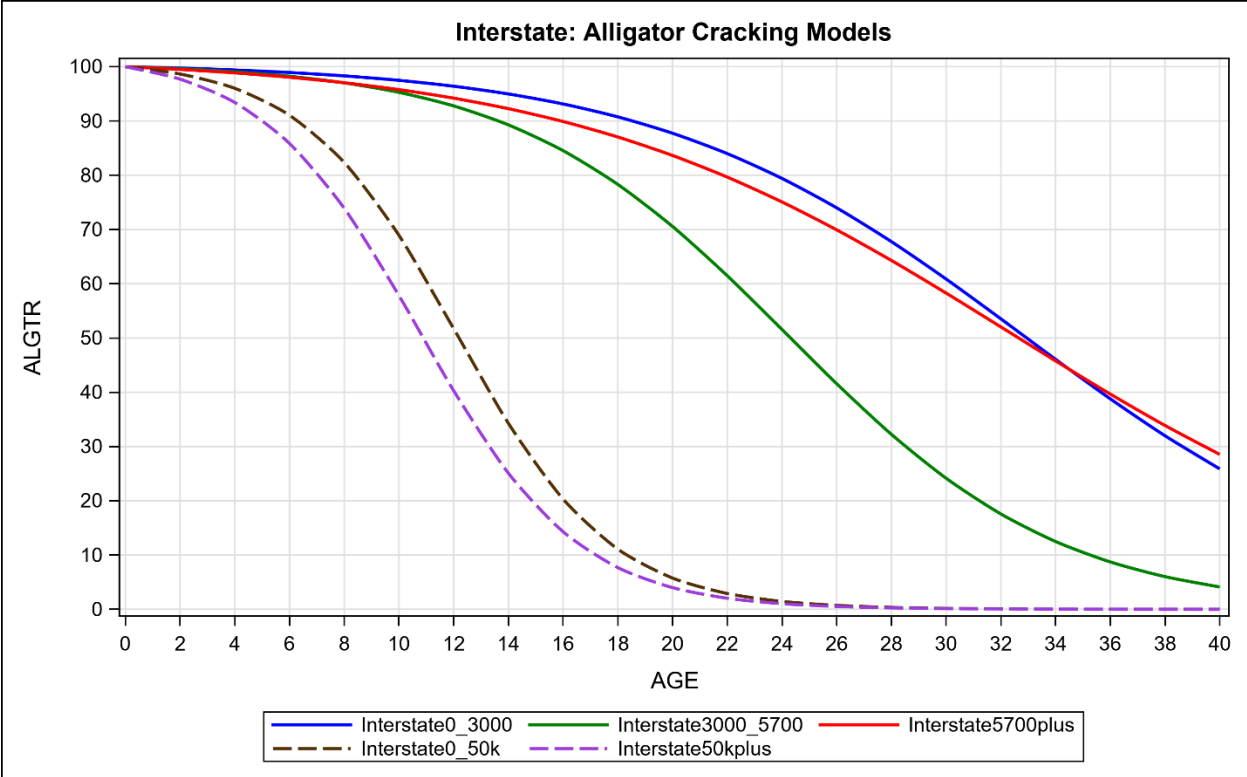


Figure C 1. Interstate: Alligator Cracking Models

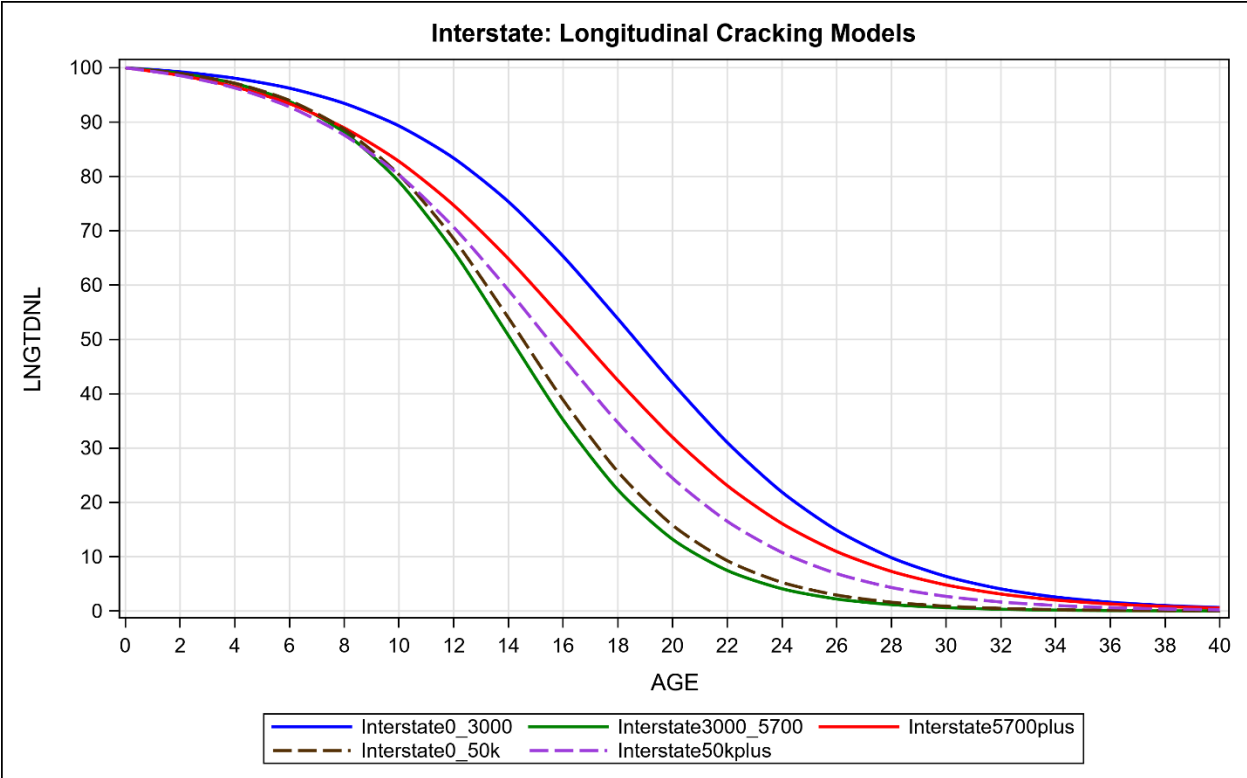


Figure C 2. Interstate: Longitudinal Cracking Models

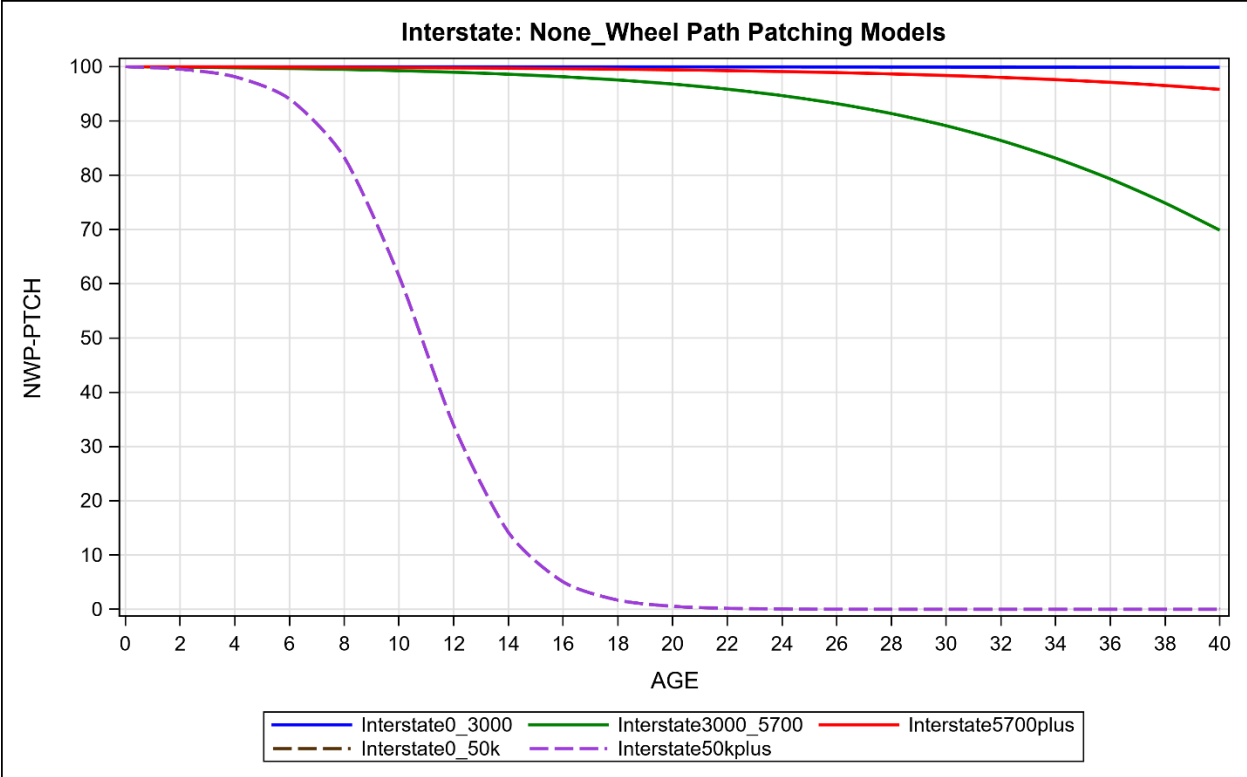


Figure C 3. Interstate: Non_Wheel Path Practicing Models

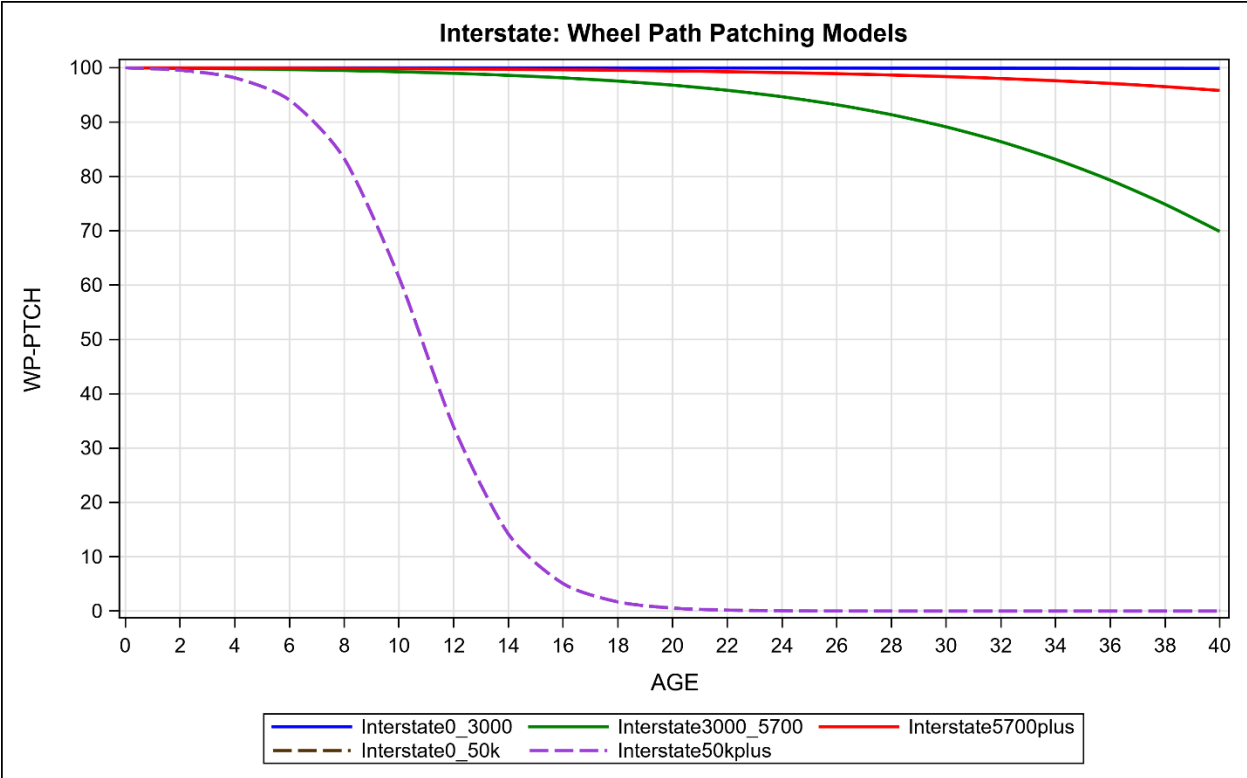


Figure C 4. Interstate: Wheel Path Practicing Models

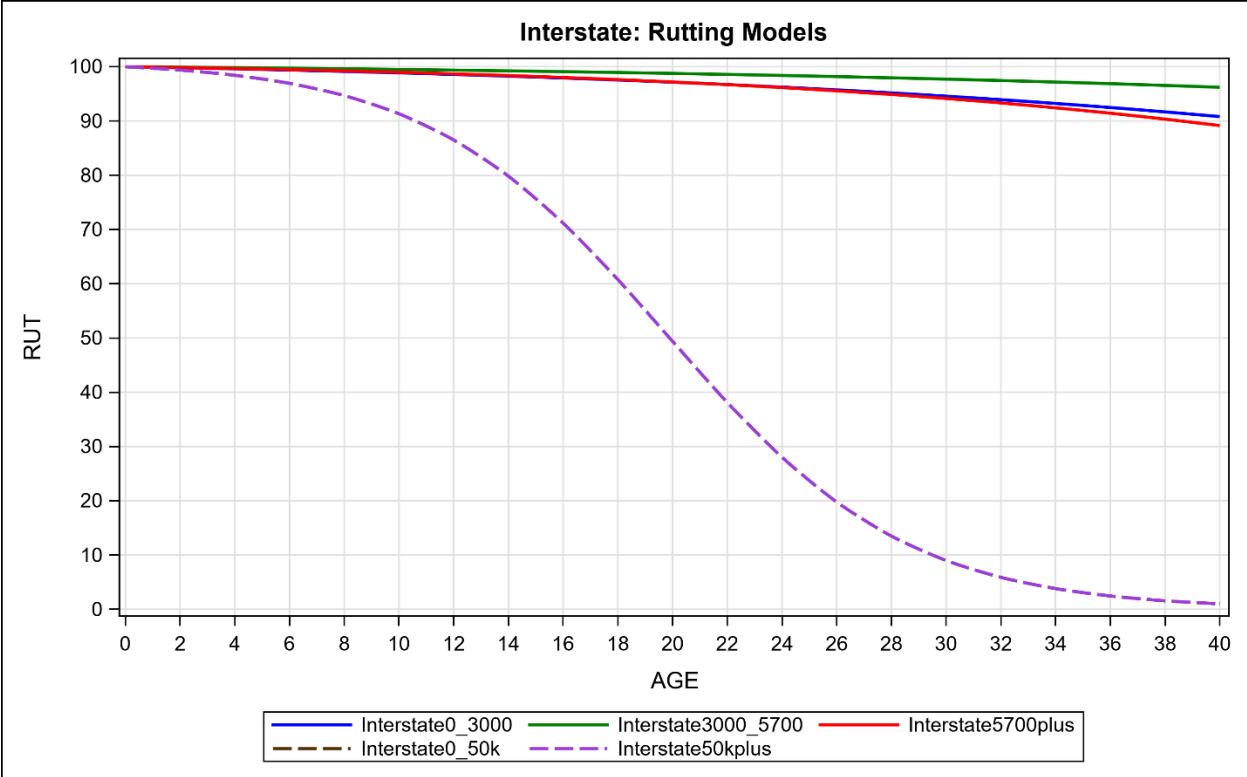


Figure C 5. Interstate: Rutting Models: Interstate: Rutting Models

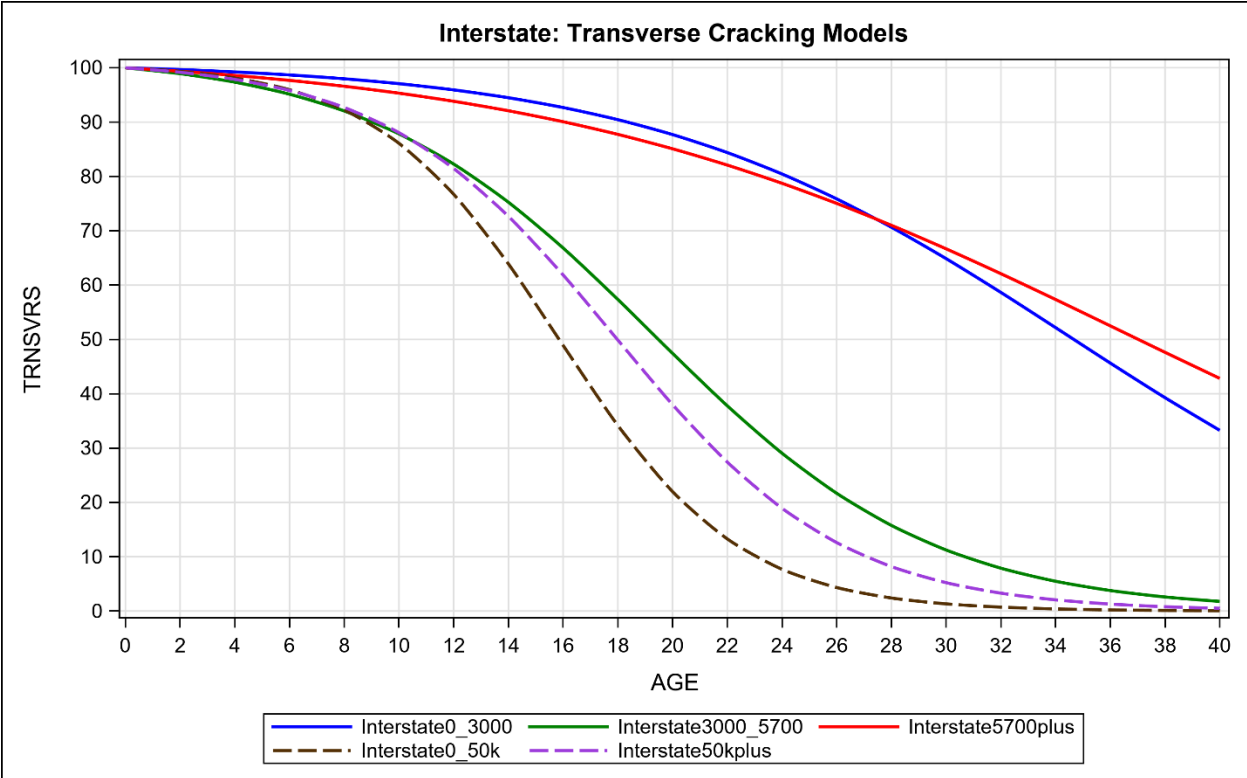


Figure C 6. Interstate: Transverse Cracking Models

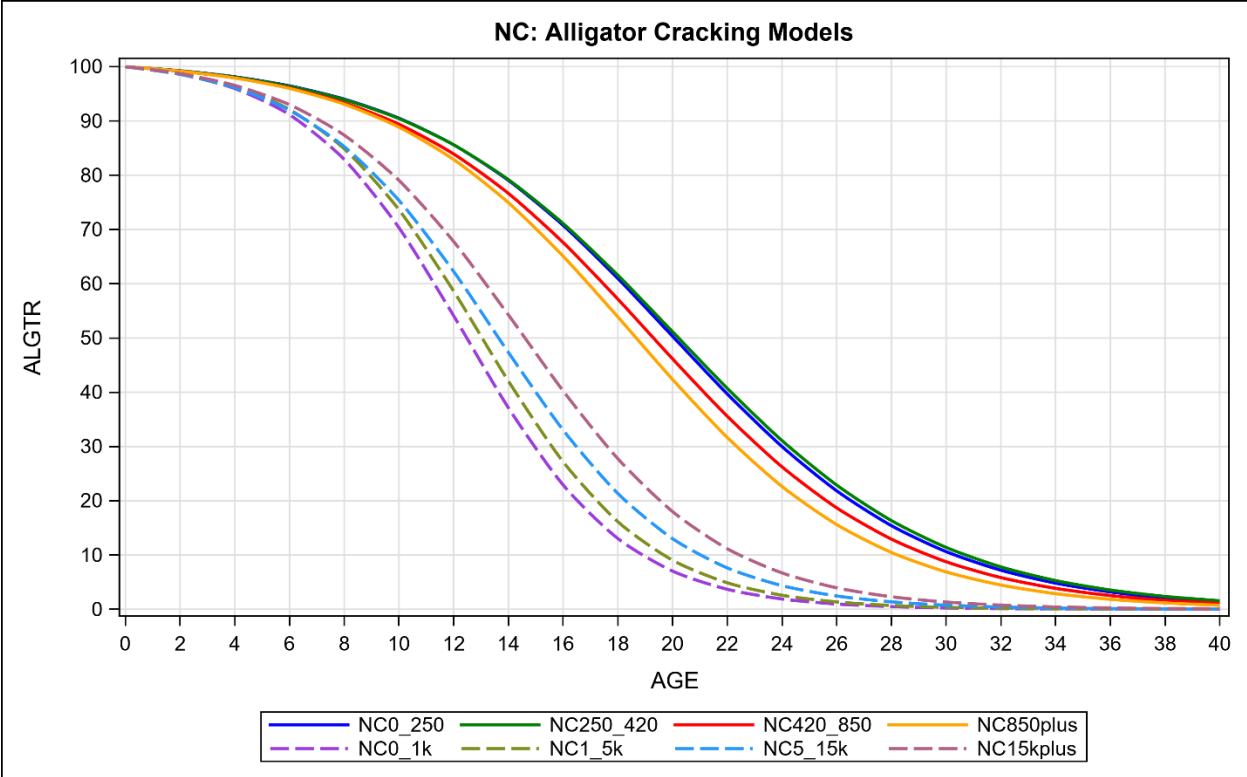


Figure C 7. NC: Alligator Cracking Models

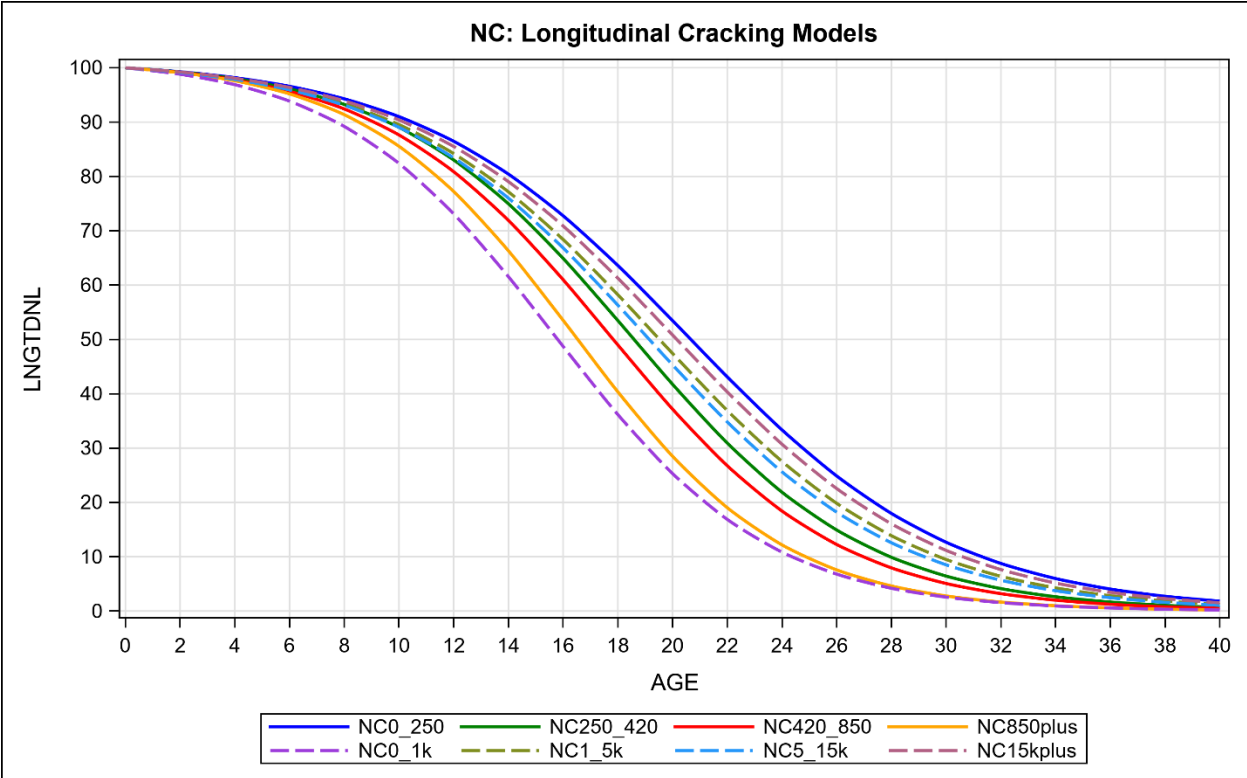


Figure C 8. NC: Longitudinal Cracking Models

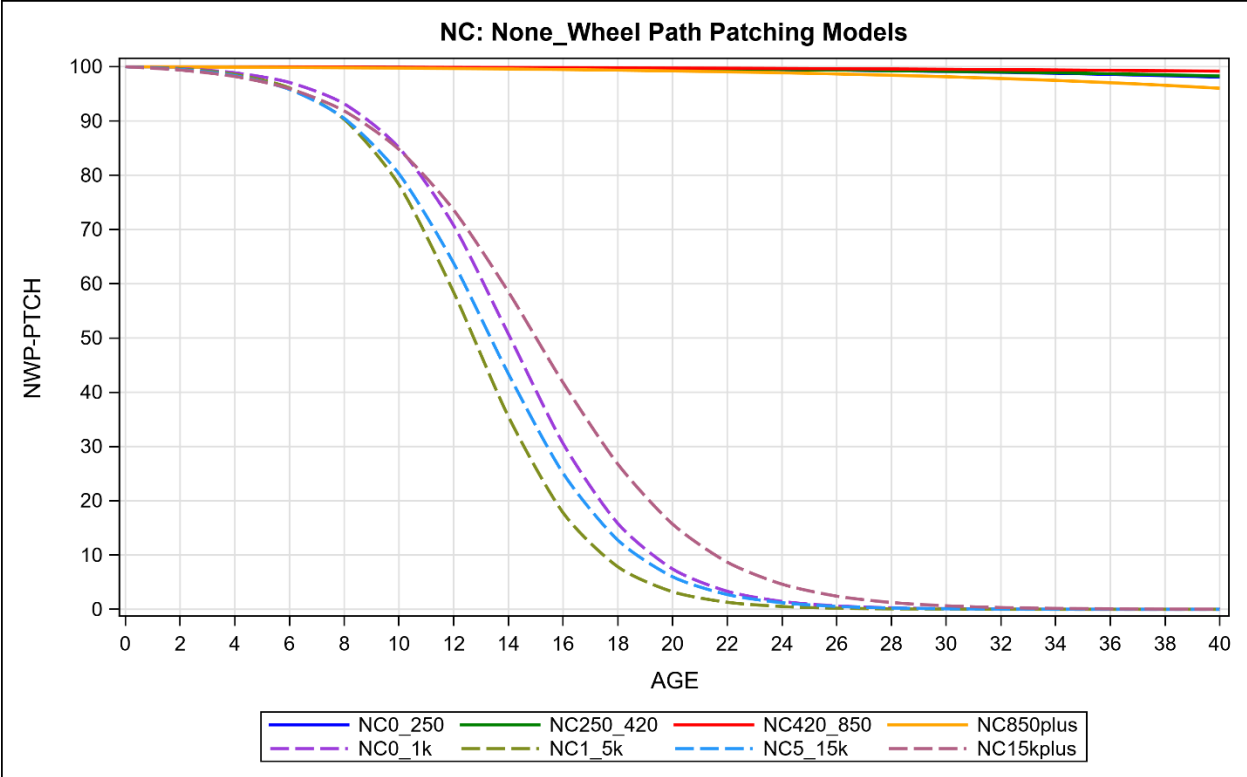


Figure C 9. NC: Non_Wheel Path Patching Models

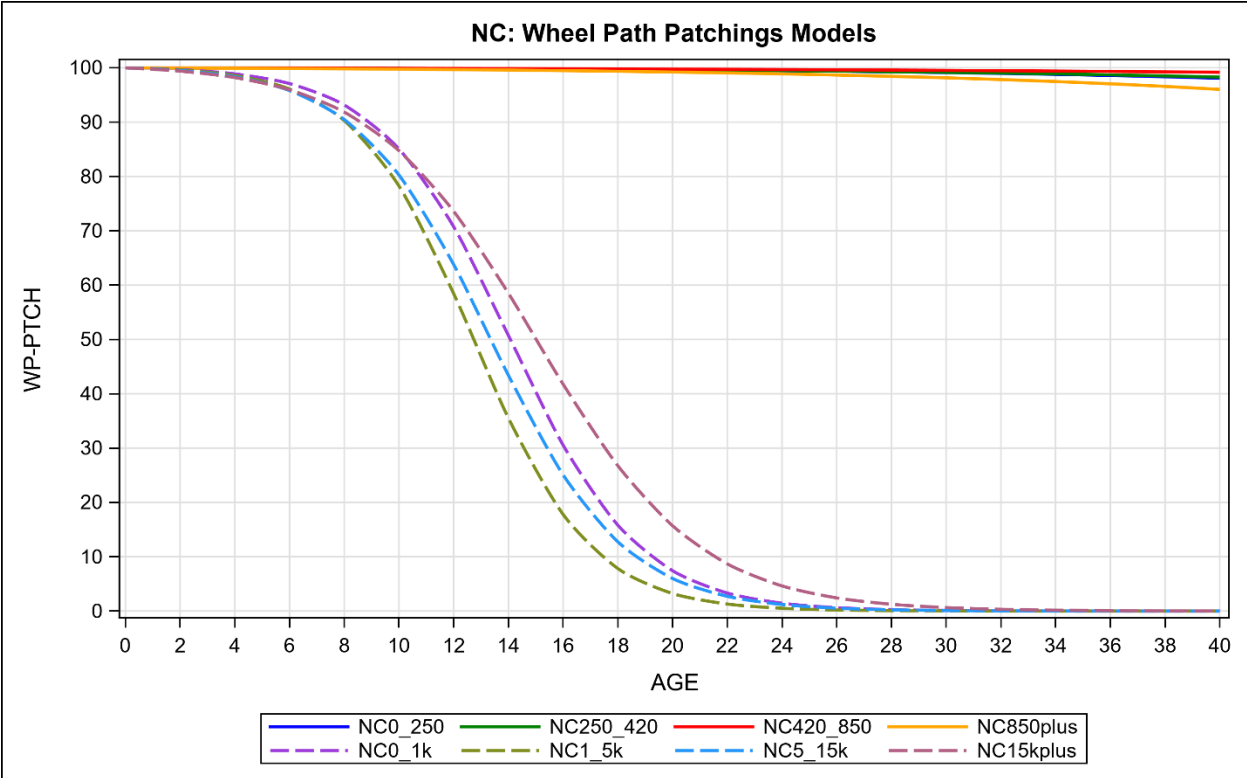


Figure C 10. NC: Wheel Path Patching Models

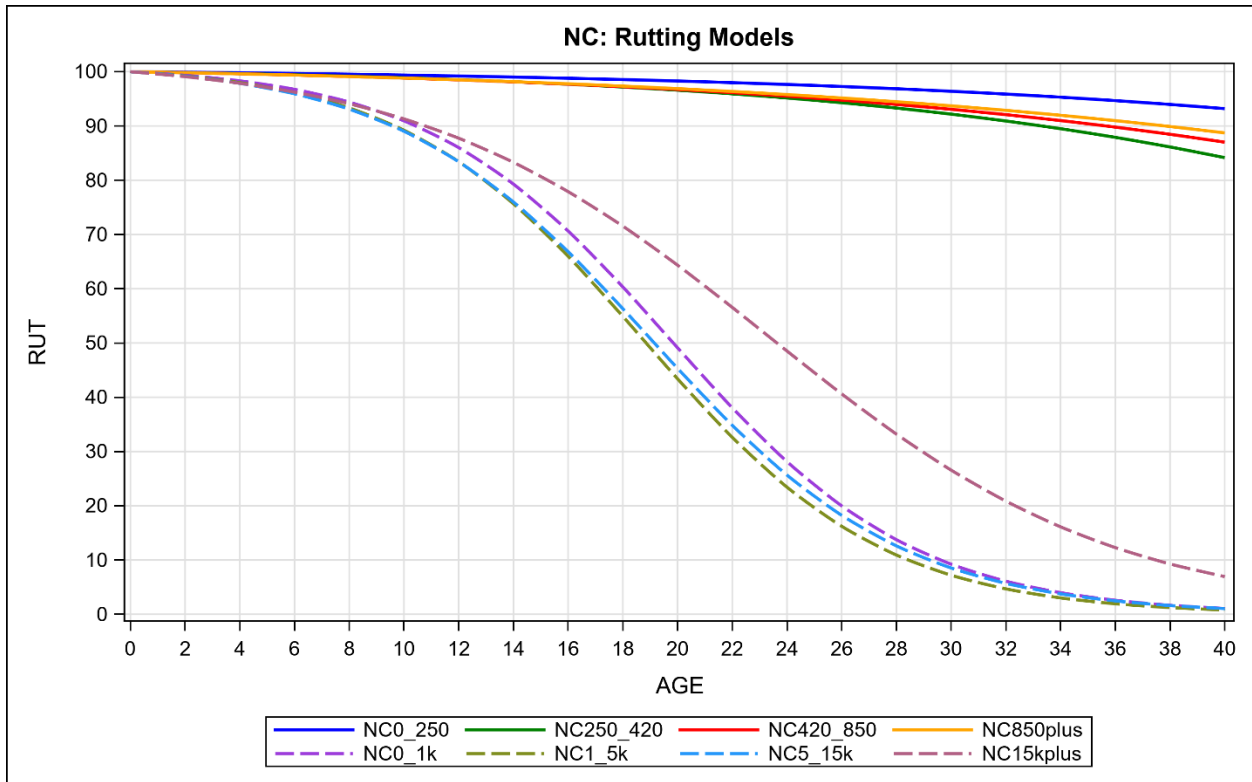


Figure C 11. NC: Rutting Models

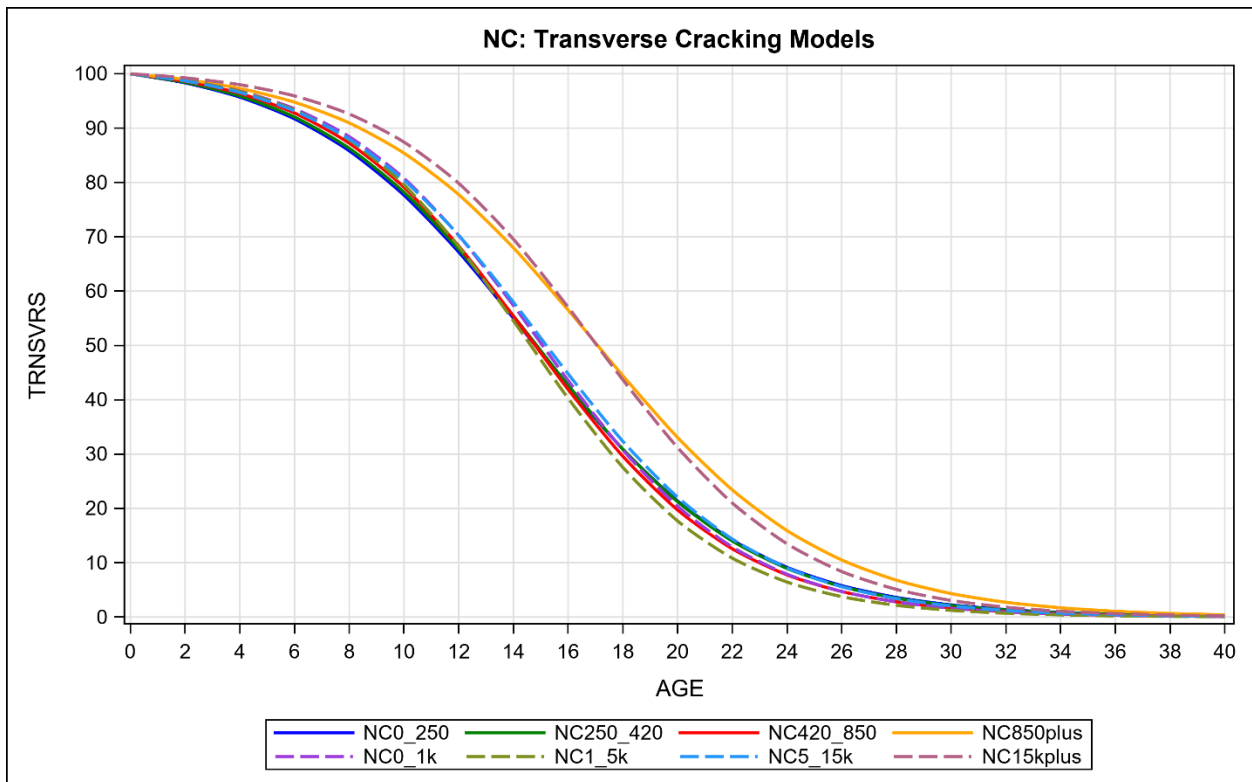


Figure C 12. NC: Transverse Cracking Models

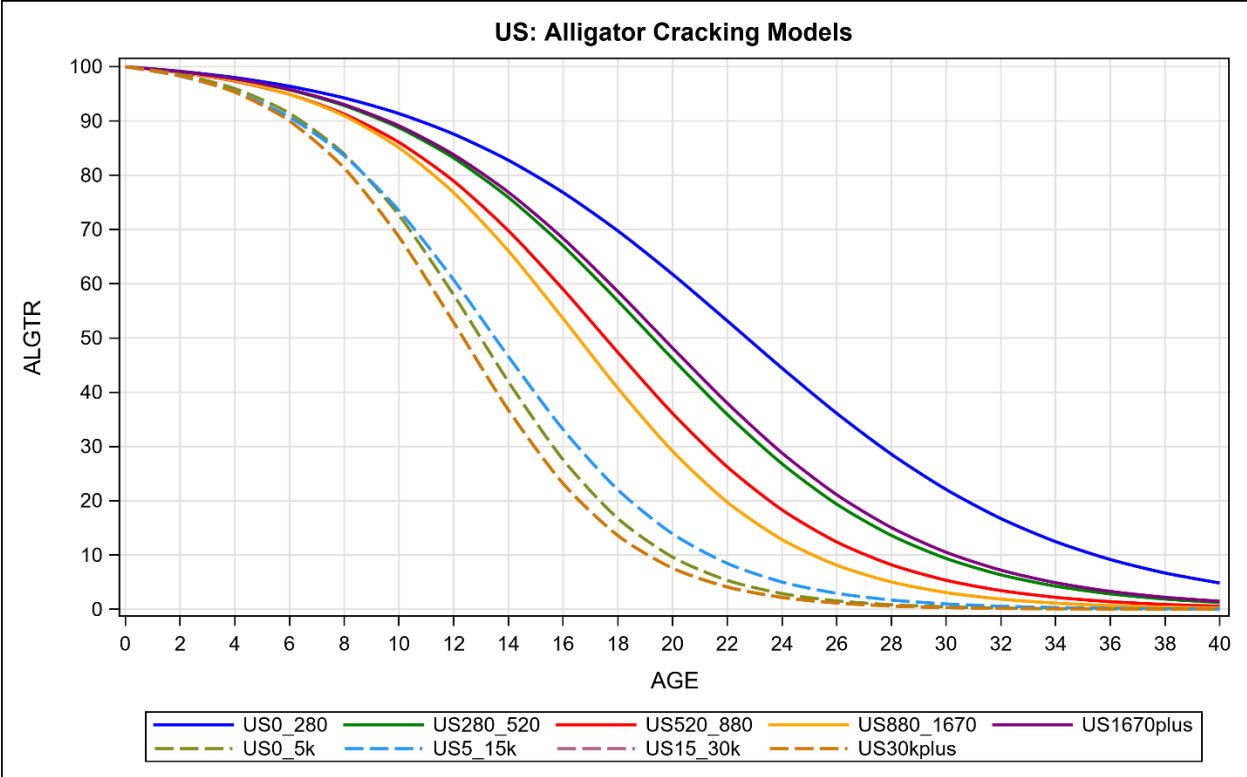


Figure C 13. US: Alligator Cracking Models

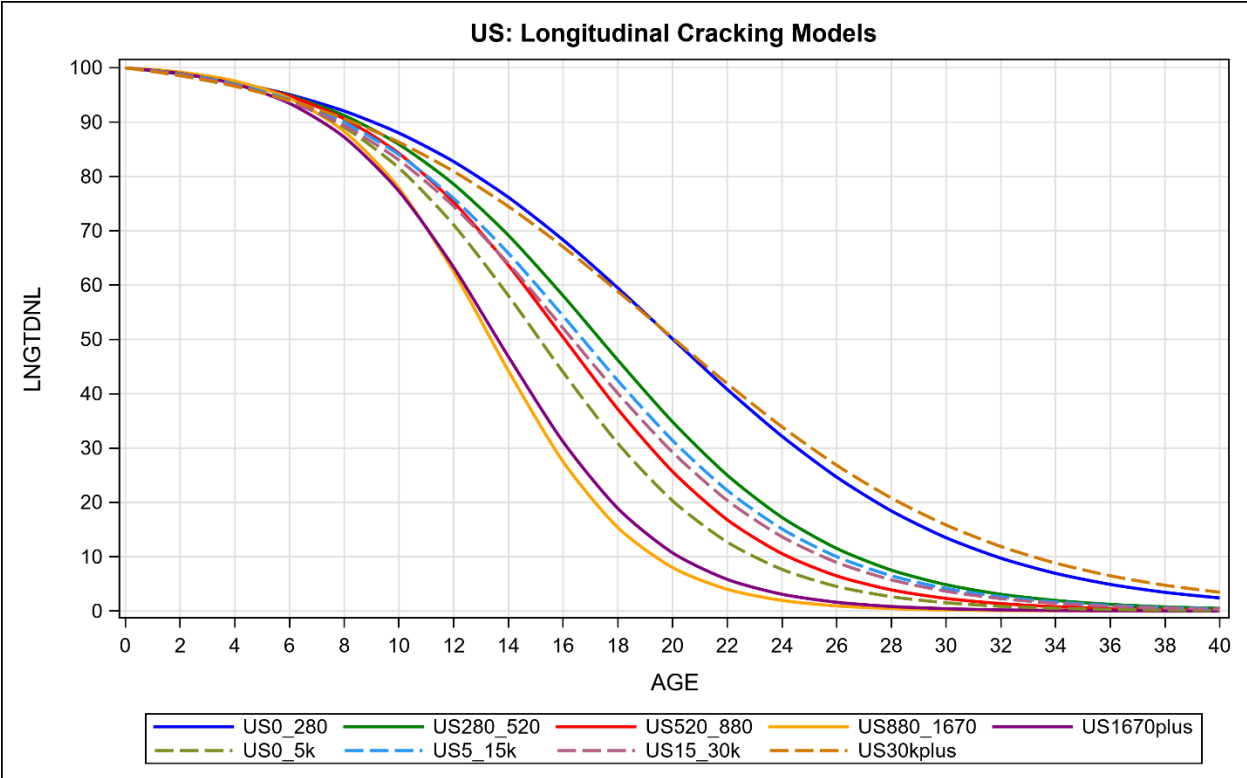


Figure C 14. US: Longitudinal Cracking Models

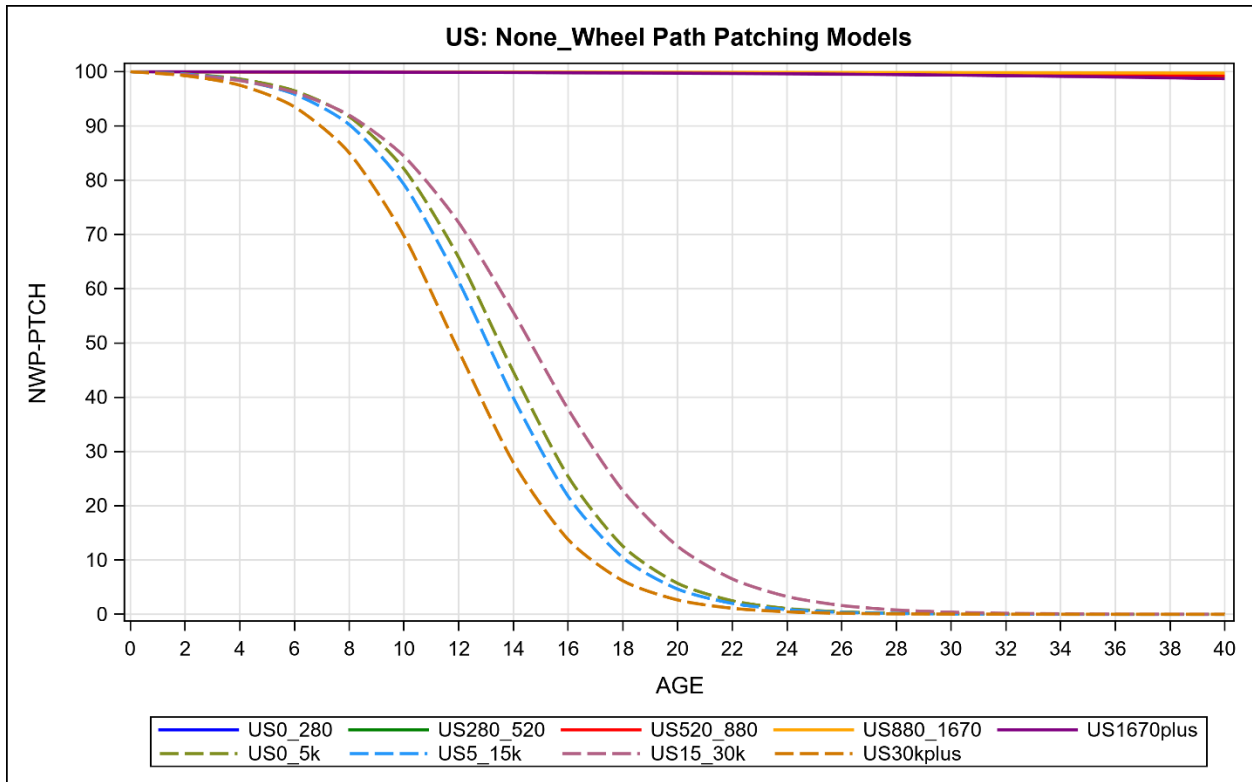


Figure C 15. US: Non_Wheel Path Patching Models

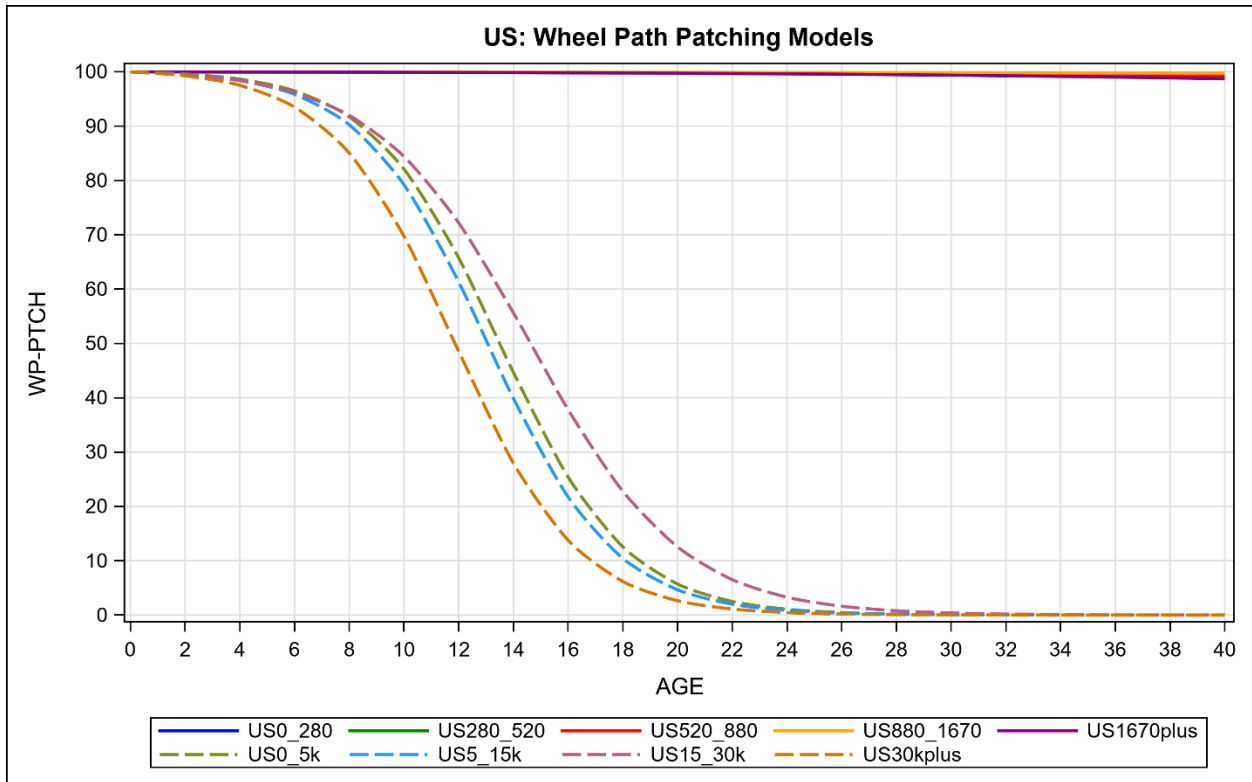


Figure C 16. US: Wheel Path Patching Models

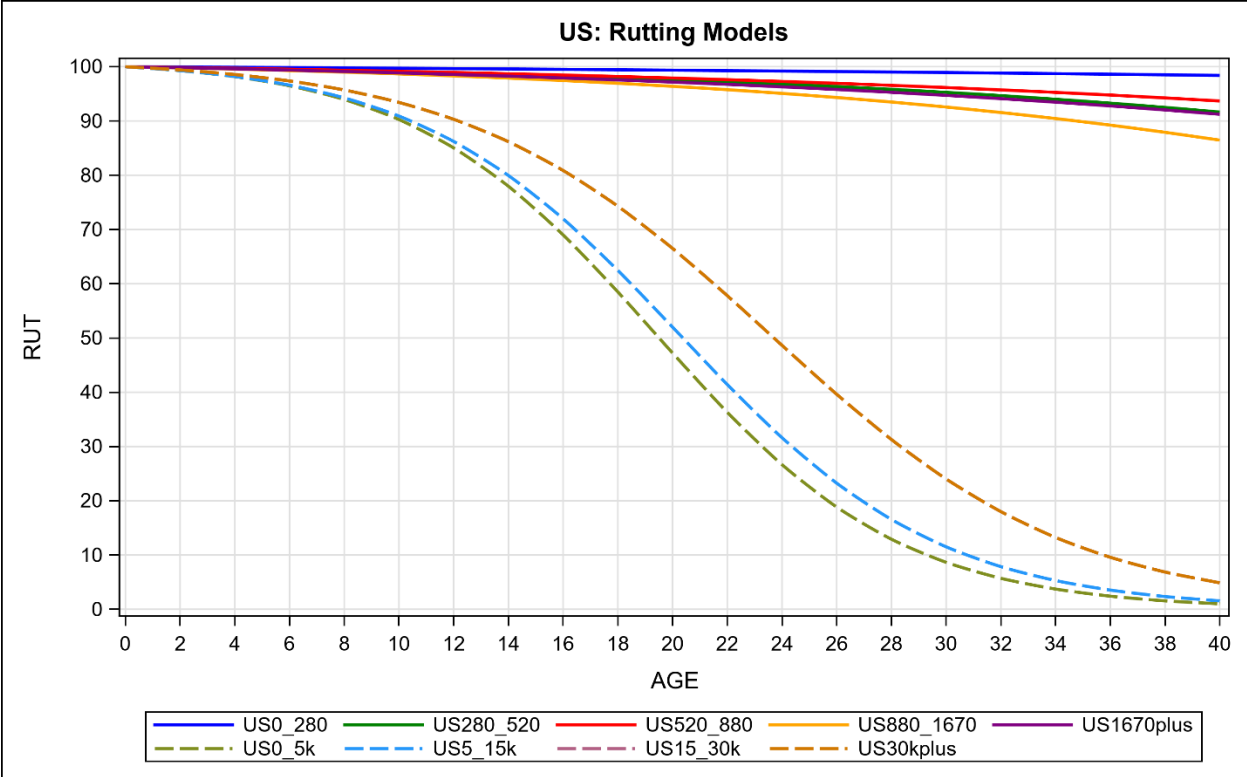


Figure C 17. US: Rutting Models

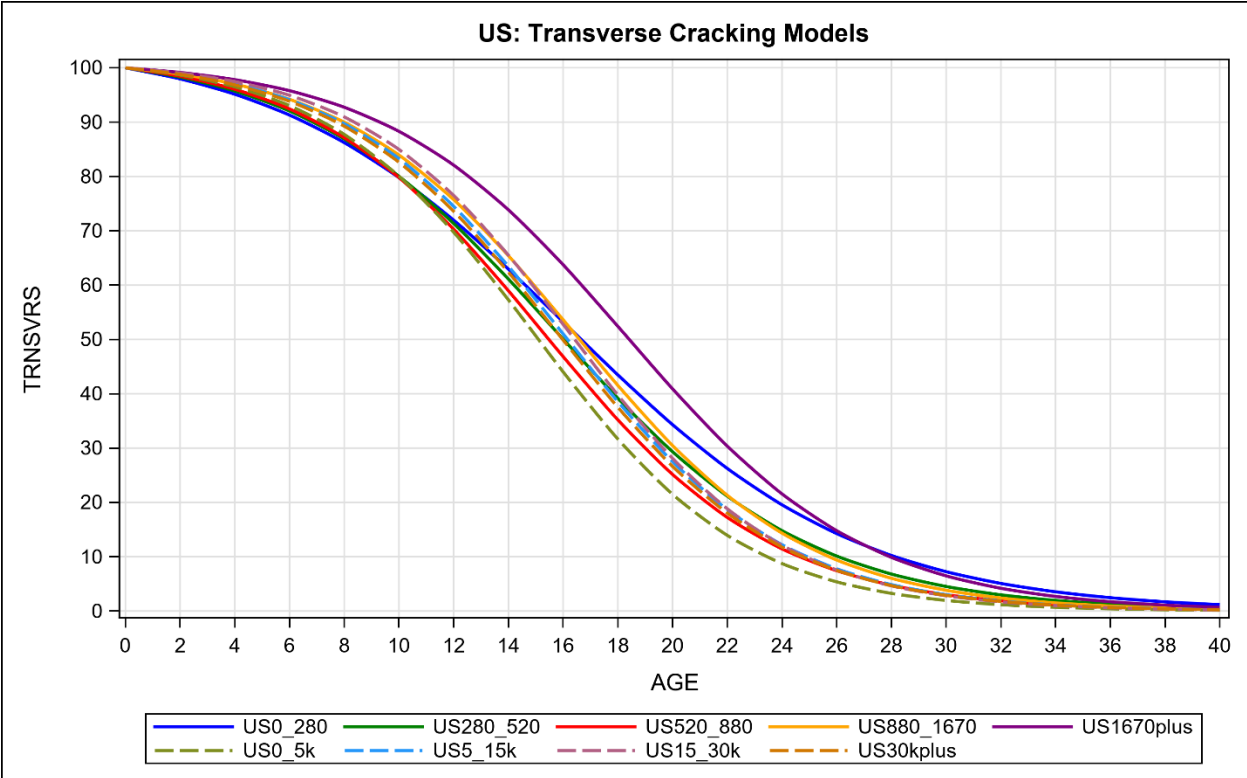


Figure C 18. US: Transverse Cracking Models

Appendix D. AADT vs. AADTT Performance Model Curves

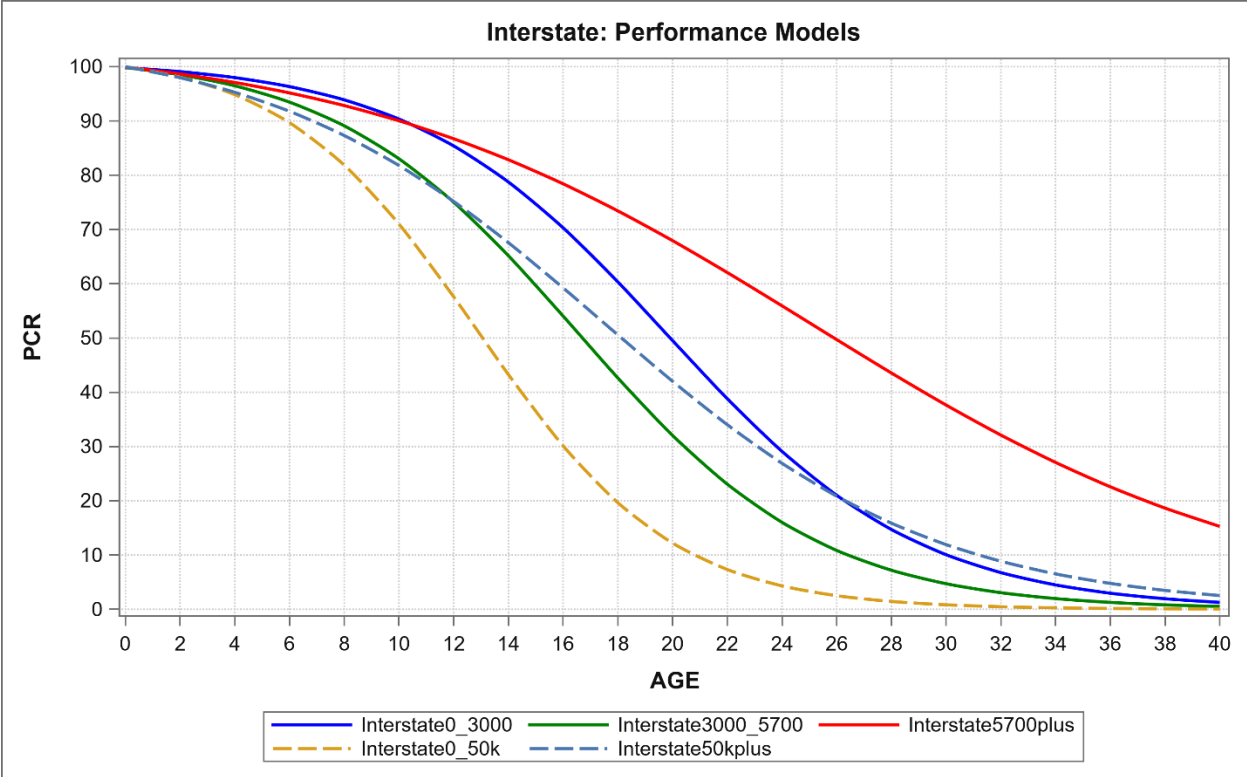


Figure D 1. Interstate: Performance Models

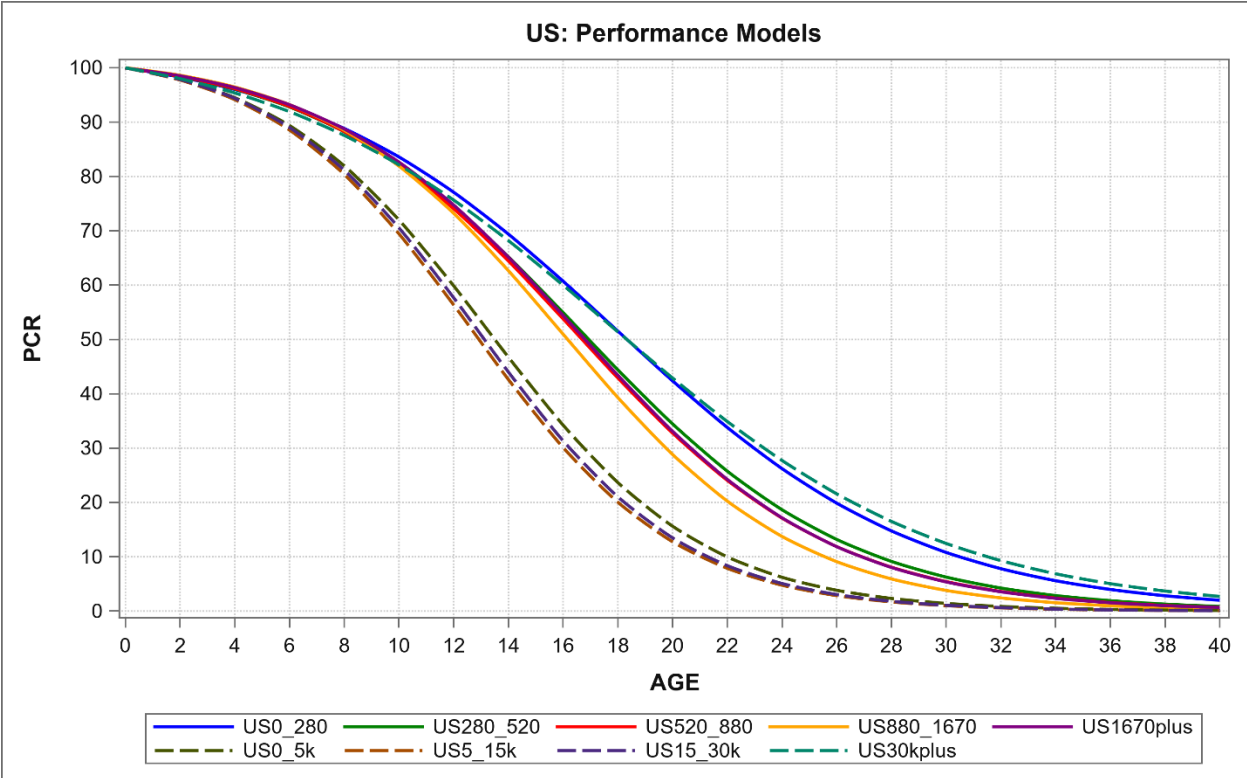


Figure D 2. US: Performance Models

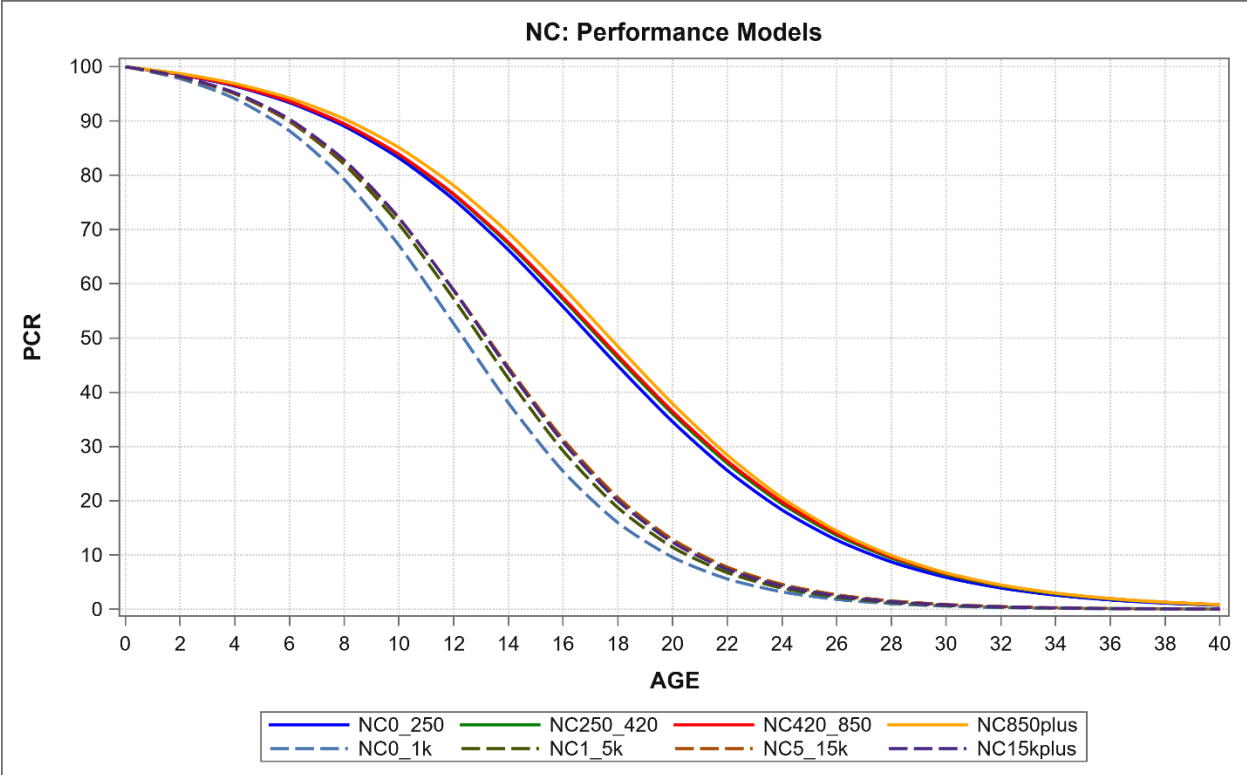


Figure D 3. NC: Performance Models

Appendix E. AADT vs. AADTT Roadway_Poor Performance Model Curves

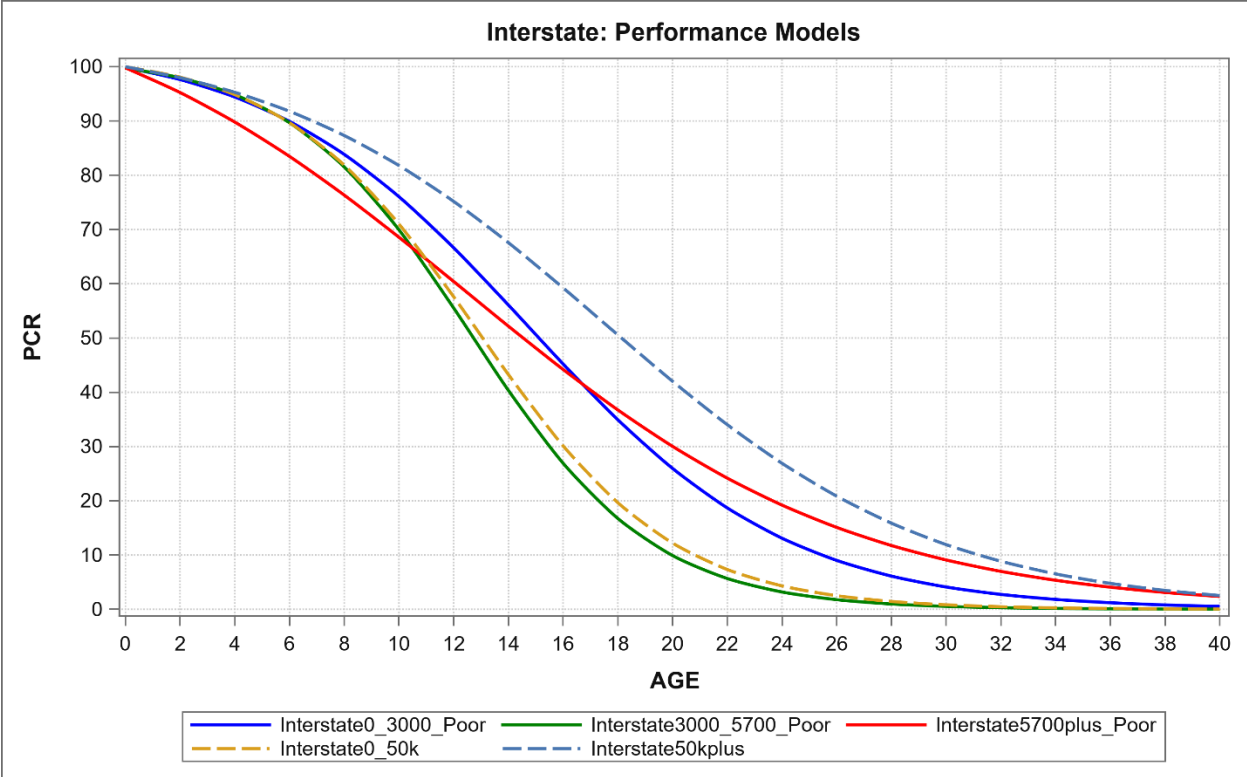


Figure E 1. Interstate Performance Models: AADT vs. AADTT Roadway_Poor

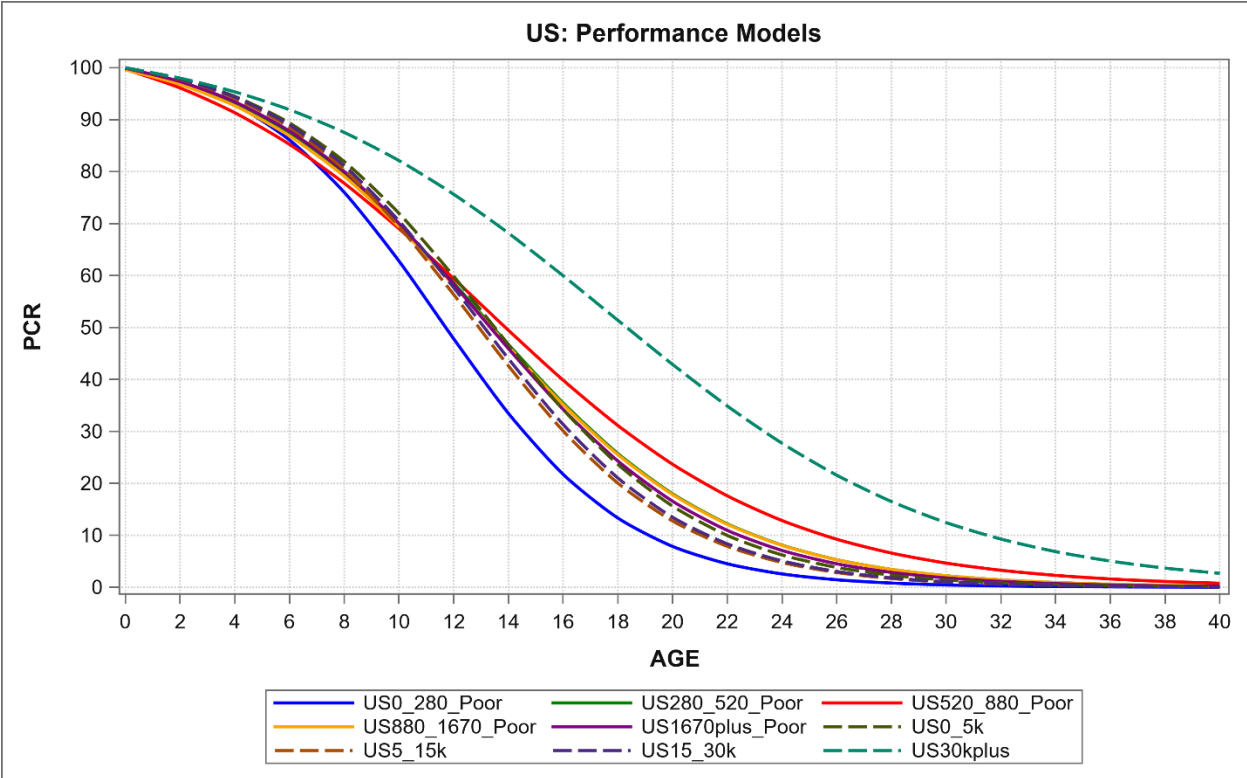


Figure E 2. US Performance Models: AADT vs. AADTT Roadway_Poor

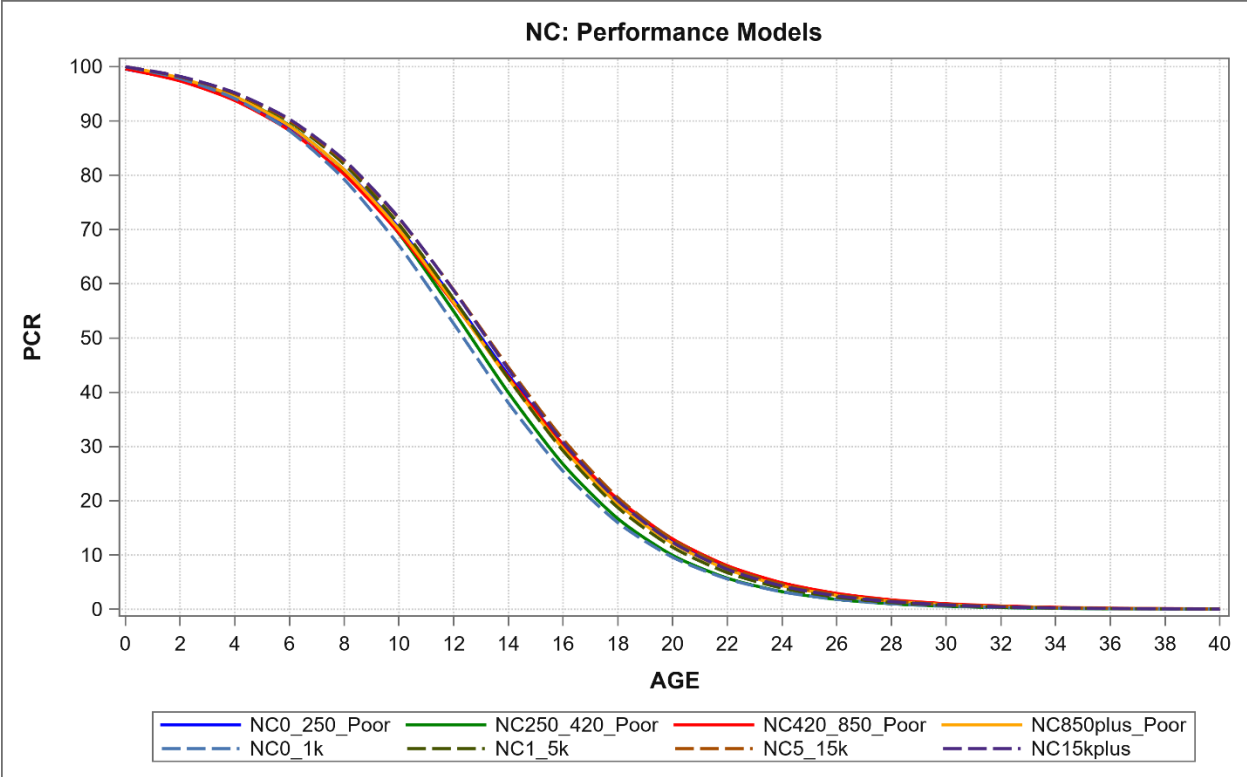


Figure E 3. NC Performance Models: AADT vs. AADTT Roadway_Poor

Appendix F. Distress Model Curves for Interstate Routes (ESAL)

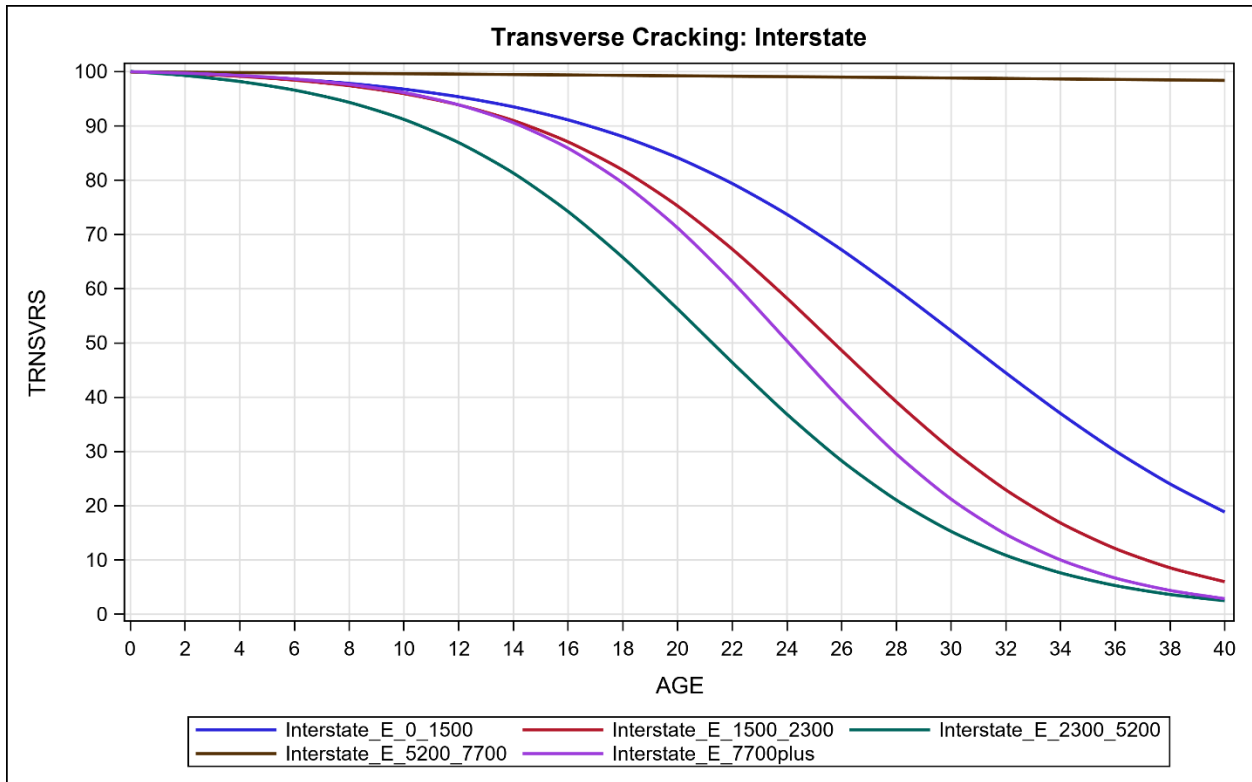


Figure F 1. Transverse Cracking: Interstate (ESAL)

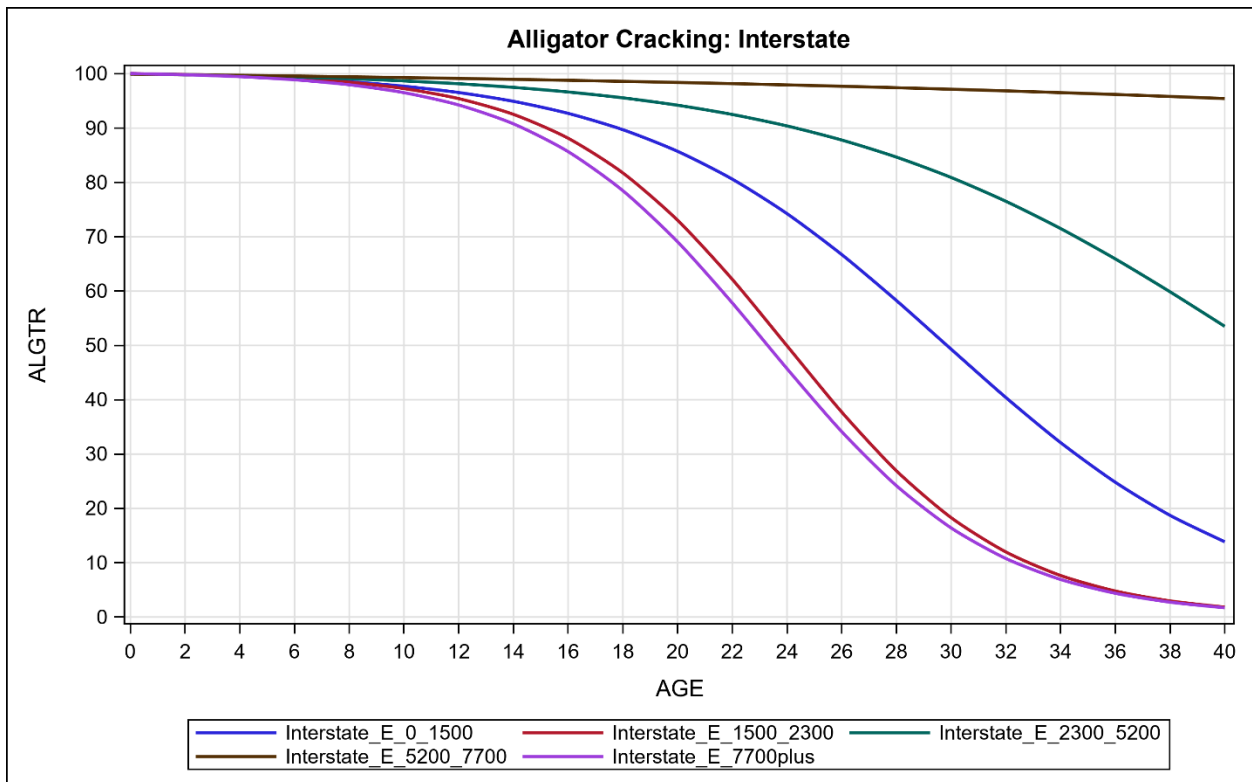


Figure F 2. Alligator Cracking: Interstate (ESAL)

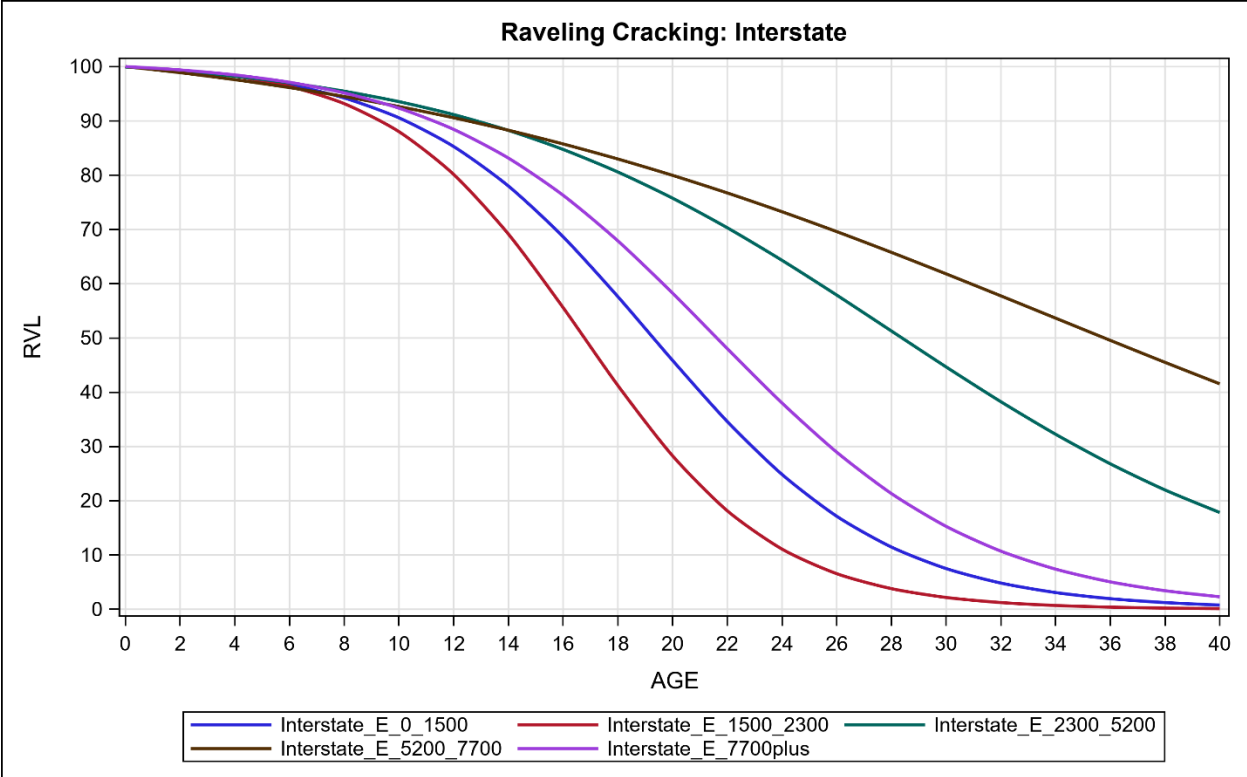


Figure F 3. Raveling: Interstate (ESAL)

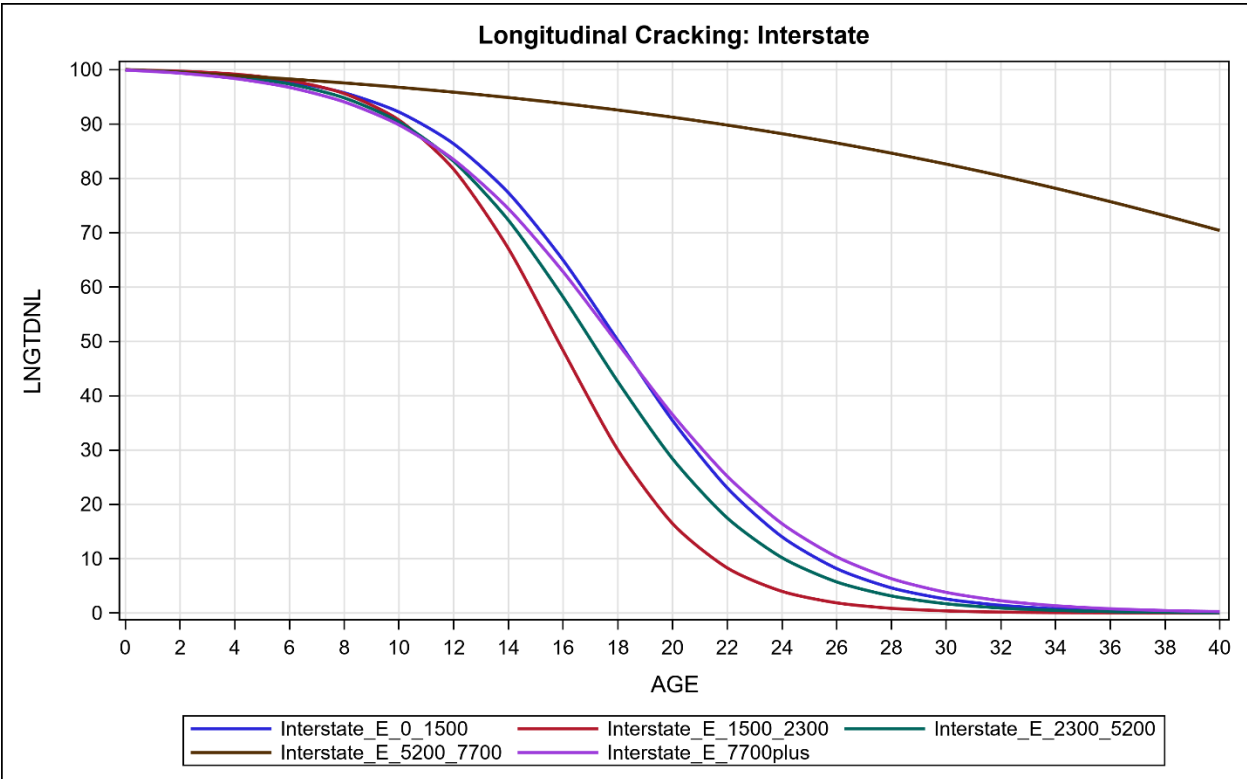


Figure F 4. Longitudinal Cracking: Interstate (ESAL)

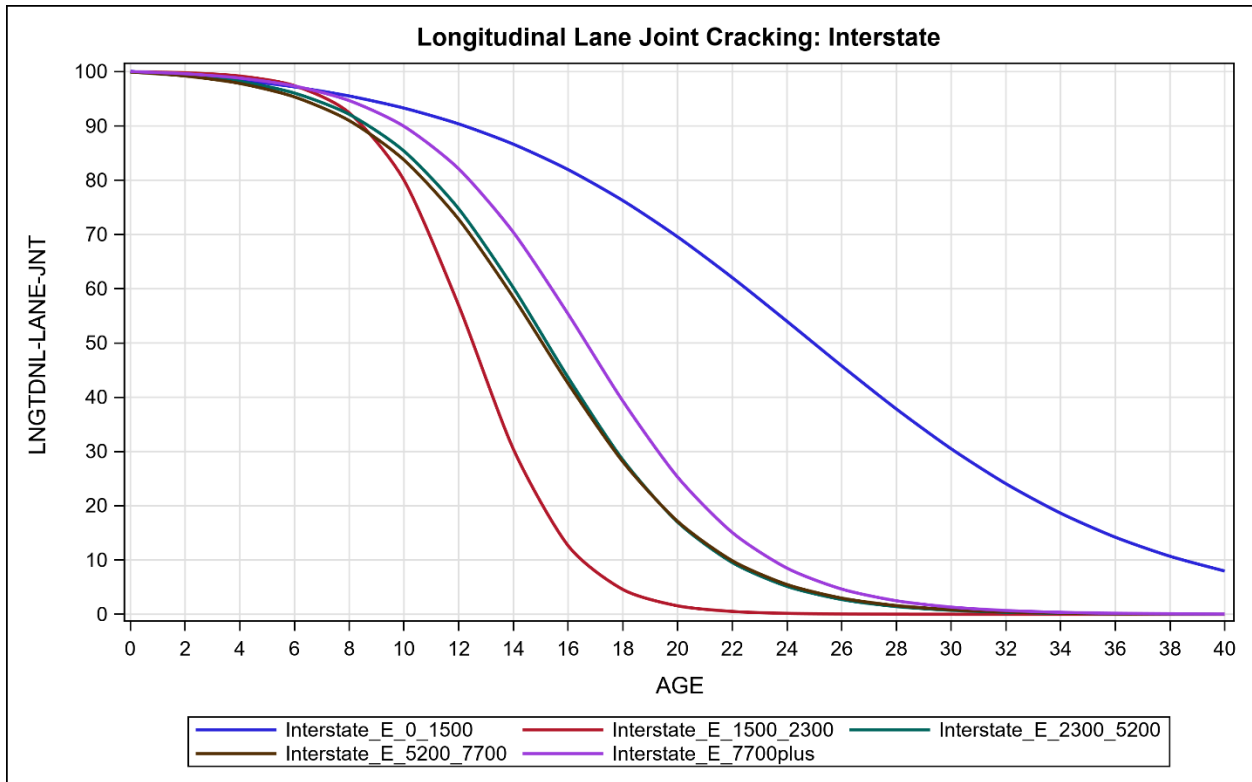


Figure F 5. Longitudinal Lane Joint Cracking: Interstate (ESAL)

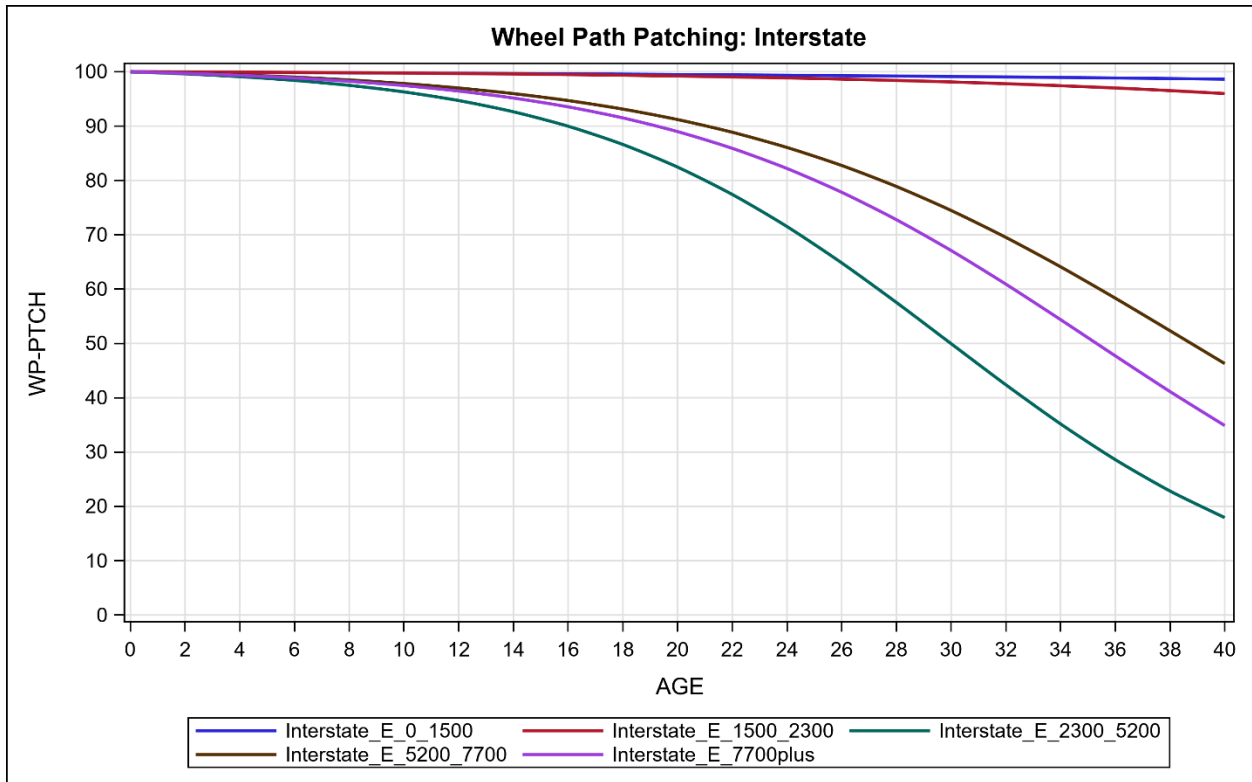


Figure F 6. Wheel Path Patching: Interstate (ESAL)

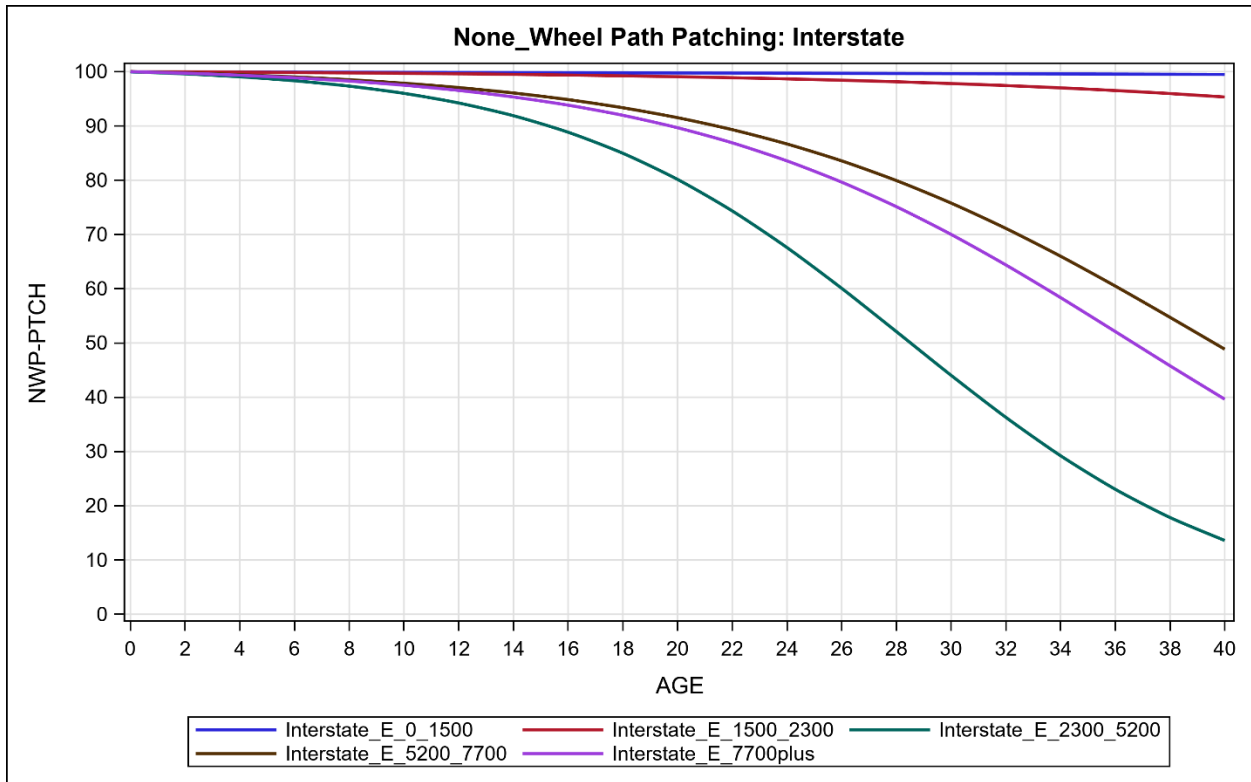


Figure F 7. Non-Wheel Path Patching: Interstate (ESAL)

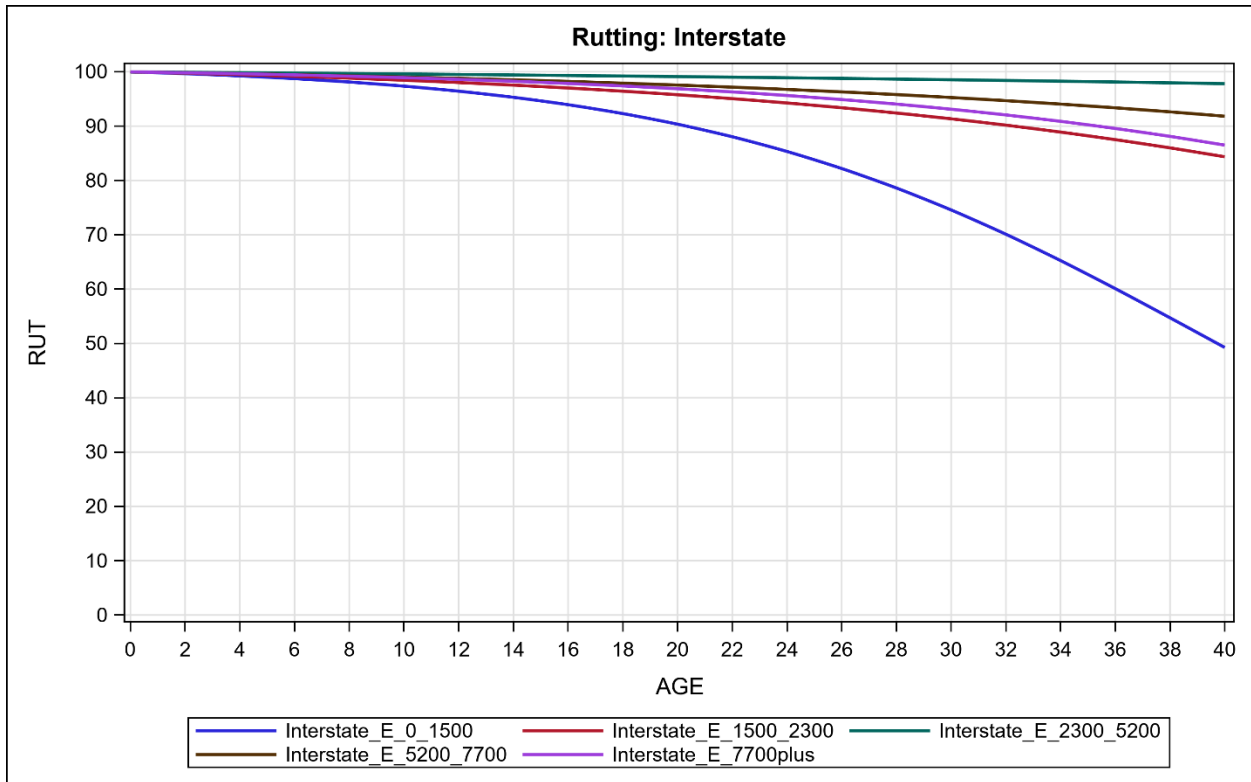


Figure F 8. Rutting: Interstate (ESAL)

Appendix G. Performance Model Curves for Interstate Routes (ESAL)

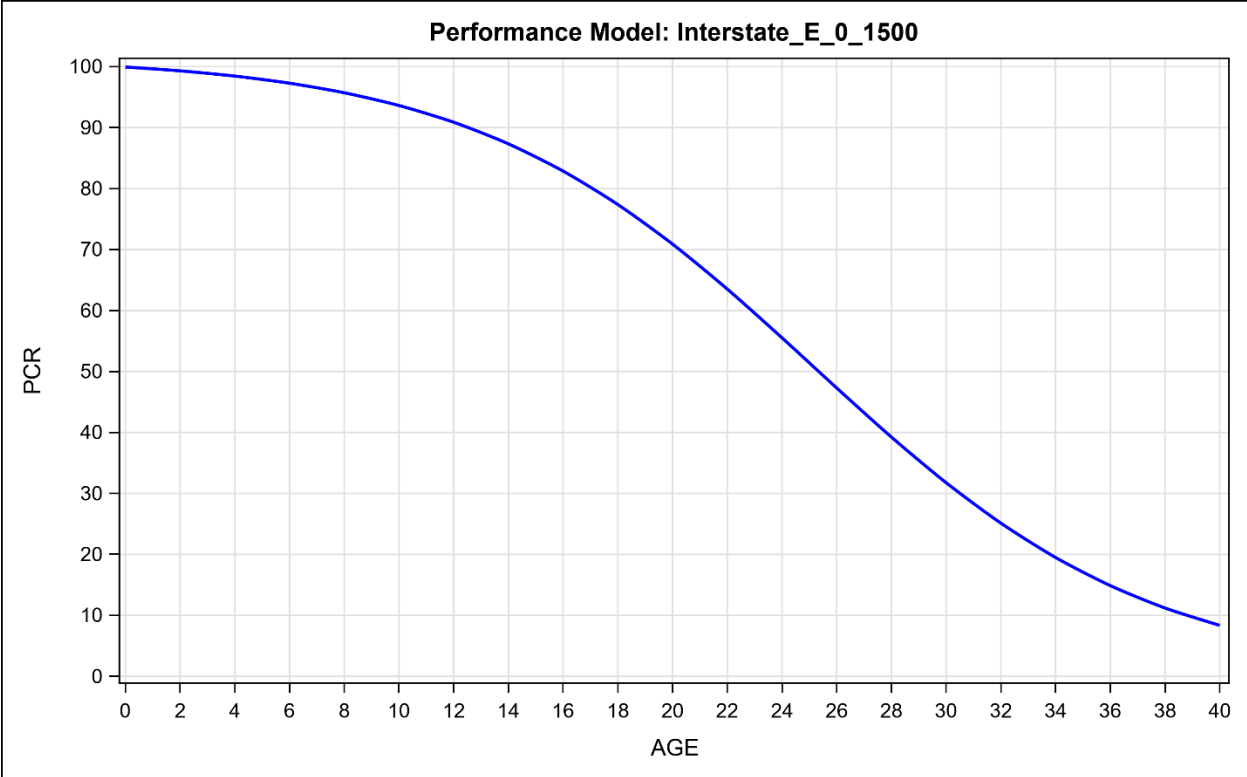


Figure G 1. Performance Model: Interstate0_1500 (ESAL)

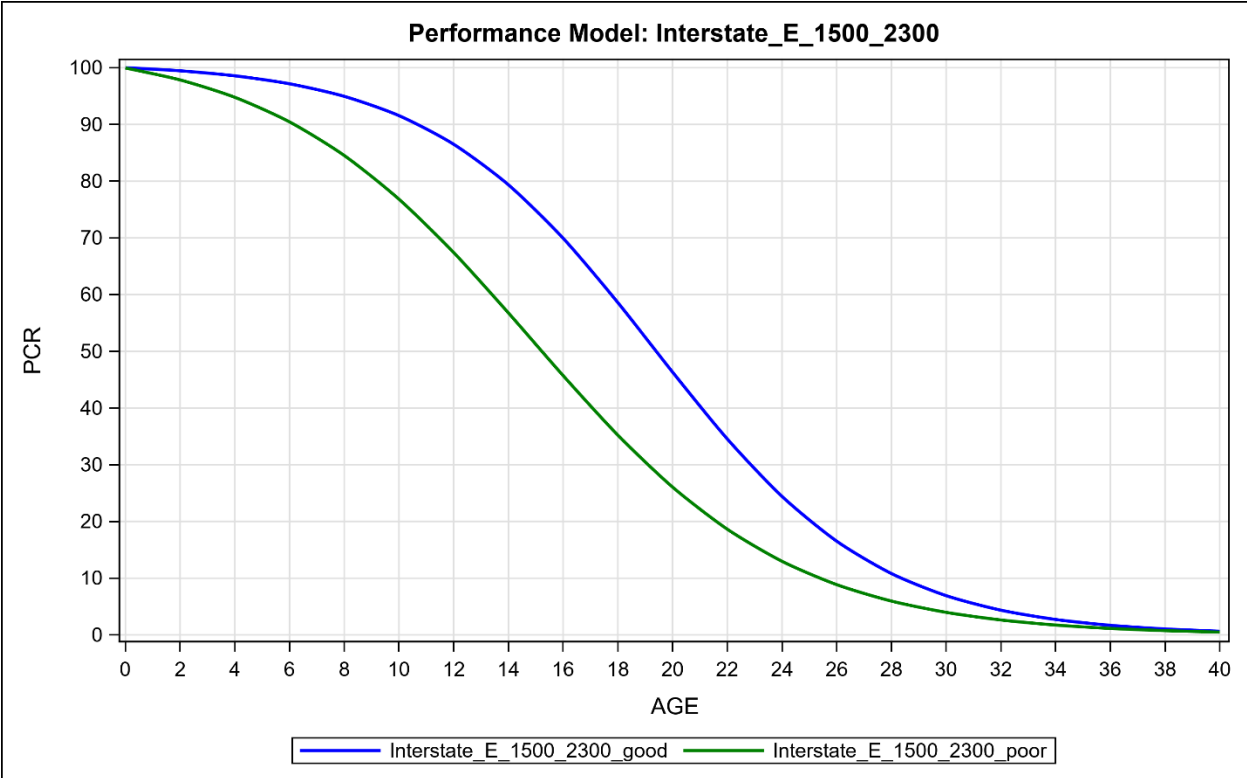


Figure G 2. Performance Model: Interstate1500_2300 (ESAL)

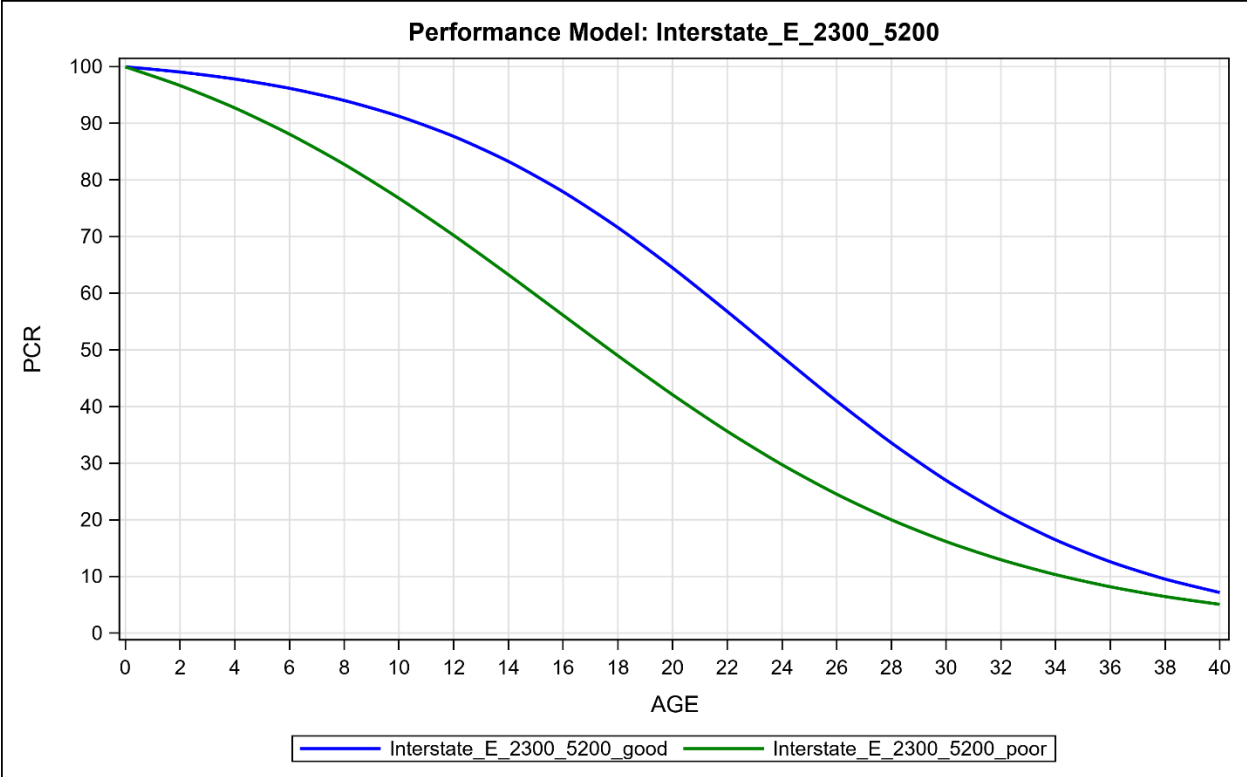


Figure G 3. Performance Model: Interstate2300_5200 (ESAL)

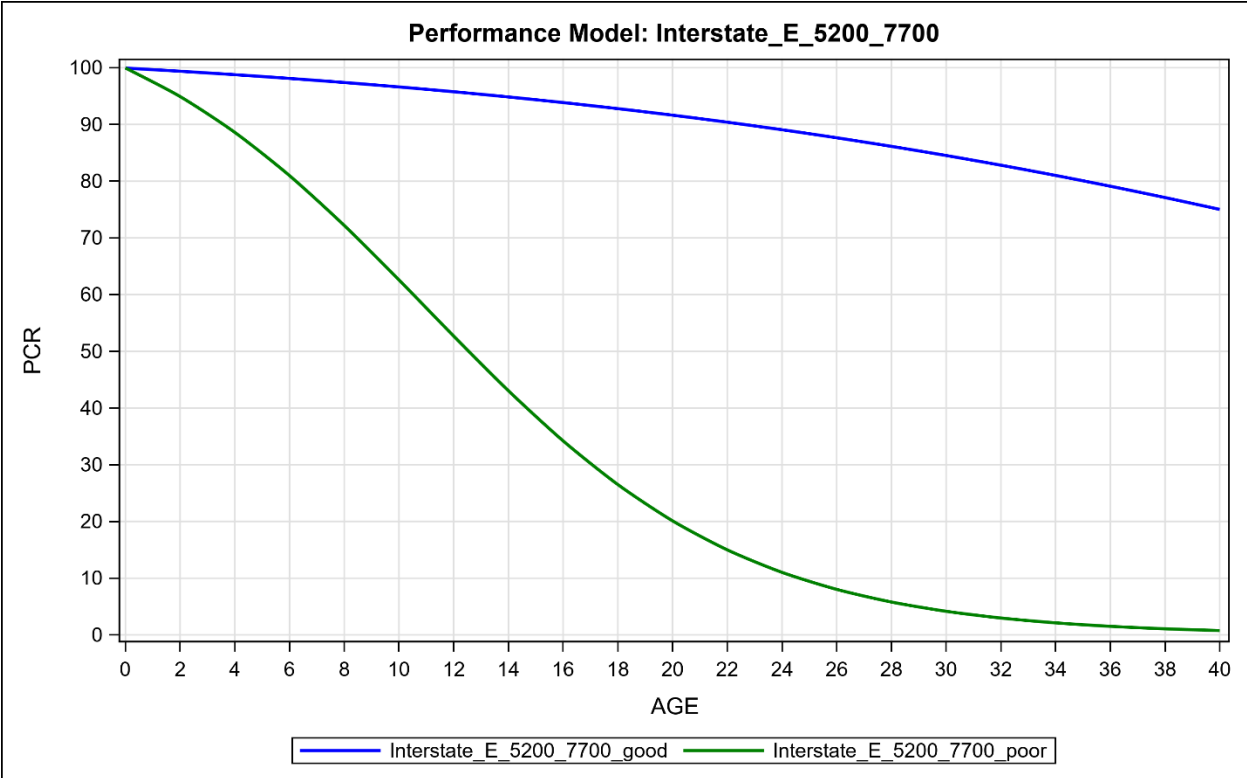


Figure G 4. Performance Model: Interstate5200_7700 (ESAL)

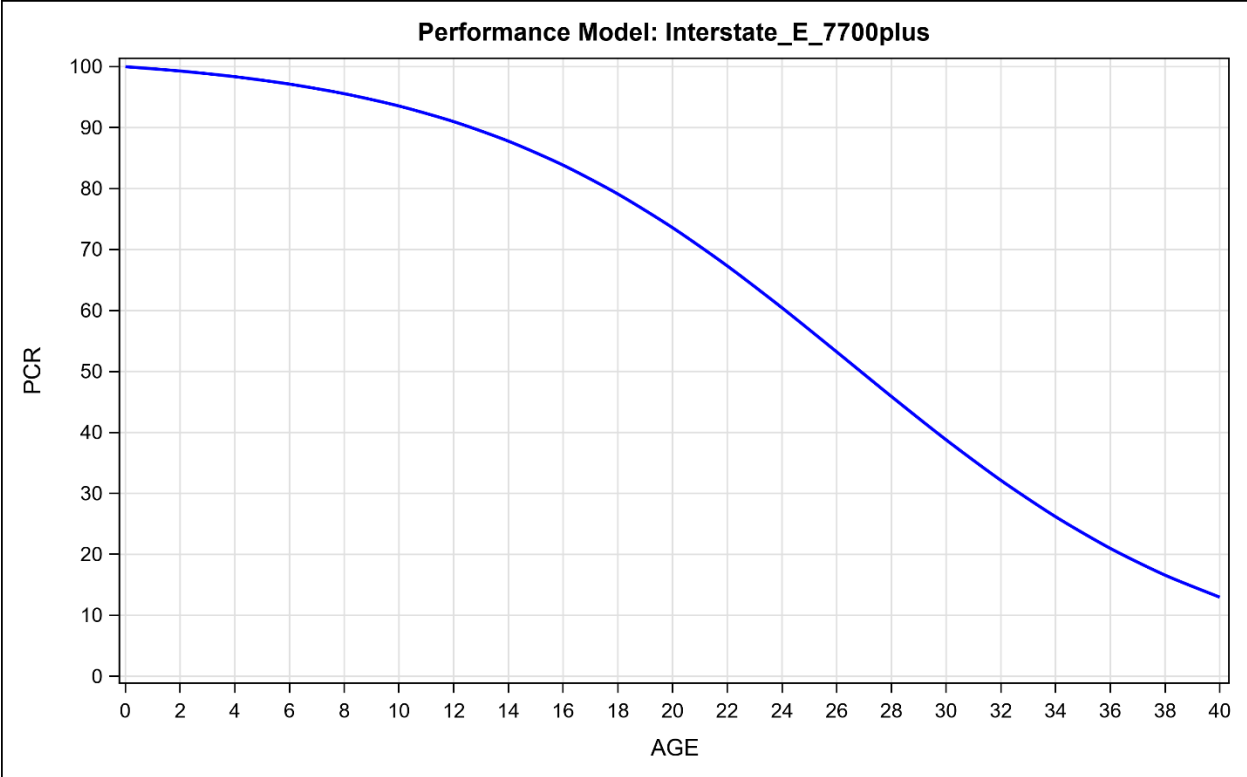


Figure G 5. Performance Model: Interstate7700plus (ESAL)